Université d'Ottawa · University of Ottawa

Université d'Ottawa • University of Ottawa

FACULTÉ DES ÉTUDES SUPÉRIEURES ET POSTDOCTORALES

FACULTY OF GRADUATE AND POSTDOCTORAL STUDIES

Tagenine ALLADIN

AUTEUR DE LA THÈSE - AUTHOR OF THESIS

M.Sc. (Chemistry)

GRADE - DEGREE

Department of Chemistry

FACULTÉ, ÉCOLE, DÉPARTEMENT - FACULTY, SCHOOL, DEPARTMENT

TITRE DE LA THÈSE - TITLE OF THE THESIS

Grafting and Thermolysis of Tetraneopentylzirconium on Silica

T. Durst

DIRECTEUR DE LA THÈSE - THESIS SUPERVISOR

S. Scott

CO-DIRECTEUR DE LA THÈSE - THESIS CO-SUPERVISOR

EXAMINATEURS DE LA THÈSE - THESIS EXAMINERS

A. Sayari

A. St-Amant

J.-M. De Koninck, Ph.D.

LE DOYEN DE LA FACULTÉ DES ÉTUDES SUPÉRIEURES ET POSTDOCTORALES

SIGNATURE

DEAN OF THE FACULTY OF GRADUATE AND POSTDOCTORAL STUDIES

Grafting and Thermolysis of Tetraneopentylzirconium on Silica

Tagenine Alladin

Thesis submitted to the School of Graduate Studies and Research

University of Ottawa

in partial fulfillment of the requirements for the degree of

Master of Science

in

Chemistry

in the Centre for Catalysis Research and Innovation,

Ottawa-Carleton Chemistry Institute

Department of Chemistry

University of Ottawa

Ottawa, ON

Canada

Tagenine Alladin

M.Sc. Candidate

Dr. Susannah L. Scott

Research Supervisor

Your file Votre référence
ISBN: 0-612-90021-5
Our file Notre référence
ISBN: 0-612-90021-5

Abstract

The gas-solid reaction of tetra(neopentyl)zirconium with the surface of Aerosil 200 pretreated thermally at 200 °C has been investigated. Consistent with previous investigations of a similar reaction involving deposition of tetra(neopentyl)zirconium from solution, a unique supported organometallic fragment is formed. It was characterized by IR, ^{13}C CP/MAS NMR, XAS and analytical techniques as $(\equiv SiO)_2Zr(CH_2C(CH_3)_3)_2$.

Thermolysis of silica-supported bis(neopentyl)zirconium(IV) at ca. 120°C results in the extrusion of one equiv. of neopentane. The nature of the remaining surface organometallic fragment was inferred, by its reactivity in olefin metathesis as well as by curve-fitting of its EXAFS spectrum, to be neopentylidenezirconium(IV), presumably formed by α-H abstraction. This result is analogous to previously established transformations of bis(alkyl) complexes of titanium, vanadium and chromium supported on silica, but was unexpected since earlier reports of the thermolysis of $Zr(CH_2C(CH_3)_3)_4$ supported γ-H abstraction and the formation of a zirconacyclobutane intermediate. The α-H abstraction occurs with pseudo-first-order kinetics and activation parameters $\Delta H^{\ddagger}$ = 24(5) kJ/mol and $\Delta S^{\ddagger}$ = -19(7) J/K•mol.

Both the bis(neopentyl)- and neopentylidenezirconium(IV) fragments were found to catalyze polymerization of ethylene, at room temperature without any added cocatalyst. The reactions are pseudo-first-order in $P(C_2H_4)$.

Acknowledgements

I would like express my heartfelt gratitude to my supervisor, Dr. Susannah Scott for her help, guidance and support during these two years. I have learned a lot under her supervision. A special thank also goes to Dr. Tony Durst for so generously accepting to be my 'formal supervisor'.

I would also like to thank Eric Deguns for all the EXAFS experiments and Dr. Glenn Facey for the NMR experiments.

Thanks also to all my friends from Dr. Scotts Group.

I would like to thank my family, especially my mum, and sister Nazeemah for all their support and for always believing in me.

Last, but not least, my thanks go to my husband, for his endless support, patience and love.

Table of Contents

Chapter 2. Experimental Techniques

Chapter 3. Grafting of Tetra(neopentyl)zirconium on Silica

List of Figures

Chapter 1

Chapter 2

Chapter 3

Chapter 4

Chapter 5

List of Schemes

Chapter 1

Chapter 4

Chapter 5

List of Tables

Chapter 1

Chapter 3

Chapter 4

Chapter 1

Introduction

1.1 Surface Organometallic Chemistry

Surface Organometallic Chemistry (SOMC) is a rapidly developing field driven by applications in the new areas of catalysis, separations (by molecular sieves) and chemical vapor deposition (CVD) of thin films.[1,2] The main objective of SOMC is understanding the chemisorption of organometallic complexes on oxide surfaces.[3] Catalysis is one of the most important chemical principles in the world; almost all industrial/chemical reactions involve a catalyst. In catalysis, interest in the grafting of organometallic compounds onto surfaces results from the exceptional reactivity of surface organometallic fragments.[4]

The grafting of organometallic complexes onto supports is also relevant to the mechanisms of heterogeneous catalysis, which are far from being understood.[5] Most heterogeneous catalysts are composed of at least two components: a solid support (e.g., silica, alumina) and an active phase (e.g., an organometallic fragment).[4] The advantages of heterogeneous catalysts over homogeneous ones include site isolation leading to reduced undesirable side reactions (especially intermolecular decomposition pathways), enhanced reactivity and easy separation and recovery of the catalyst.[5]

The controlled preparation of a supported catalyst is achieved only by taking into account the type and nature of the support as well as basic organometallic concepts that influence the surface species. In the early 1970s, Ballard and co-workers reported the grafting of zirconium(IV) alkyls onto silica and alumina (equation 1.1).[6]

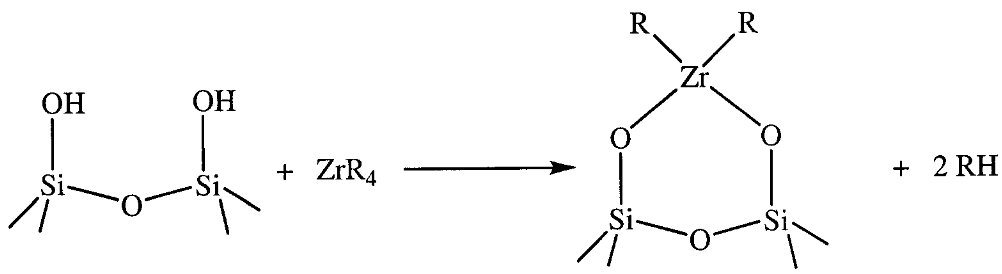

(1.1)

These surface organometallic complexes display enhanced reactivity in olefin polymerization,[6] isomerization[7] and hydrogenation[8] relative to their organometallic precursors ZrR_4. Subsequent investigations have shown their ability to catalyze such remarkable transformations as C-H activation and C-C cleavage.[5]

Film growth by organometallic chemical vapor deposition (OMCVD) has undergone tremendous development due to progress in analytical techniques that occurred in the 1980s, and which have allowed in-depth investigations of the physical and chemical properties of surfaces down to the nanoscale level.[9] Due to their refractory properties like high melting points, hardness and chemical stability, Group IV carbides are particularly interesting targets.[9] Organometallic complexes are now being used in OMCVD processes because of their greater volatility (subliming at temperatures of 75 to 100 °C at pressures of 10^{-3} Torr) compared to binary metal halides and because they are primary (single source) precursors to metal carbide films. Zirconium (IV) alkyls (e.g., tetra(neopentyl)Zr(IV)) are precursors for the deposition of zirconium carbide films.[10] The grafting of such complexes onto solid supports can provide insight into the metal carbide film growth mechanism, and may contribute to solving problems such as non-stoichiometric film growth and impurity incorporation.

1.2 Silica supports

Heterogeneous catalysis plays a key role in the chemical, petrochemical and environmental industries, and is responsible for the production of more than 85% of all bulk chemicals, intermediates and fine chemicals, and for the degradation of pollutants. Numerous solids are used as supports in catalysis, as listed in Table 1.1.

Silica is very extensively used as a support due to its relatively low cost, high thermal and chemical stability and also because it is available in many surface areas. The three types of silica that can be prepared are micro-, meso- and macroporous silica, with surface areas as high as 1000 $m^2\ g^{-1}$.[4]

In his early work on supported transition metal alkyl complexes, Ballard described the IR spectrum of fully hydrated silica, and that of silica partially dehydroxylated at 200 °C, shown in Figure 1.1. He attributed the band at 3740 cm^{-1} in the spectrum of the dried silica to residual OH groups, which he observed could be fully removed by calcining at 1200 °C.

Table 1.1: Common solid supports for catalysts

Type	Structure	Pore dimensions	Support
Amorphous			SiO_2, Al_2O_3, $SiO_2.Al_2O_3$, TiO_2, ZrO_2, MgO, La_2O_3, SnO_2 …
Crystalline	2-Dimensional		Clay minerals, layered double hydroxides…
	3-Dimensional	Microporous	Zeolites, aluminosilicates, silicates, metallophosphates…
		Mesoporous	Ordered mesoporous materials…

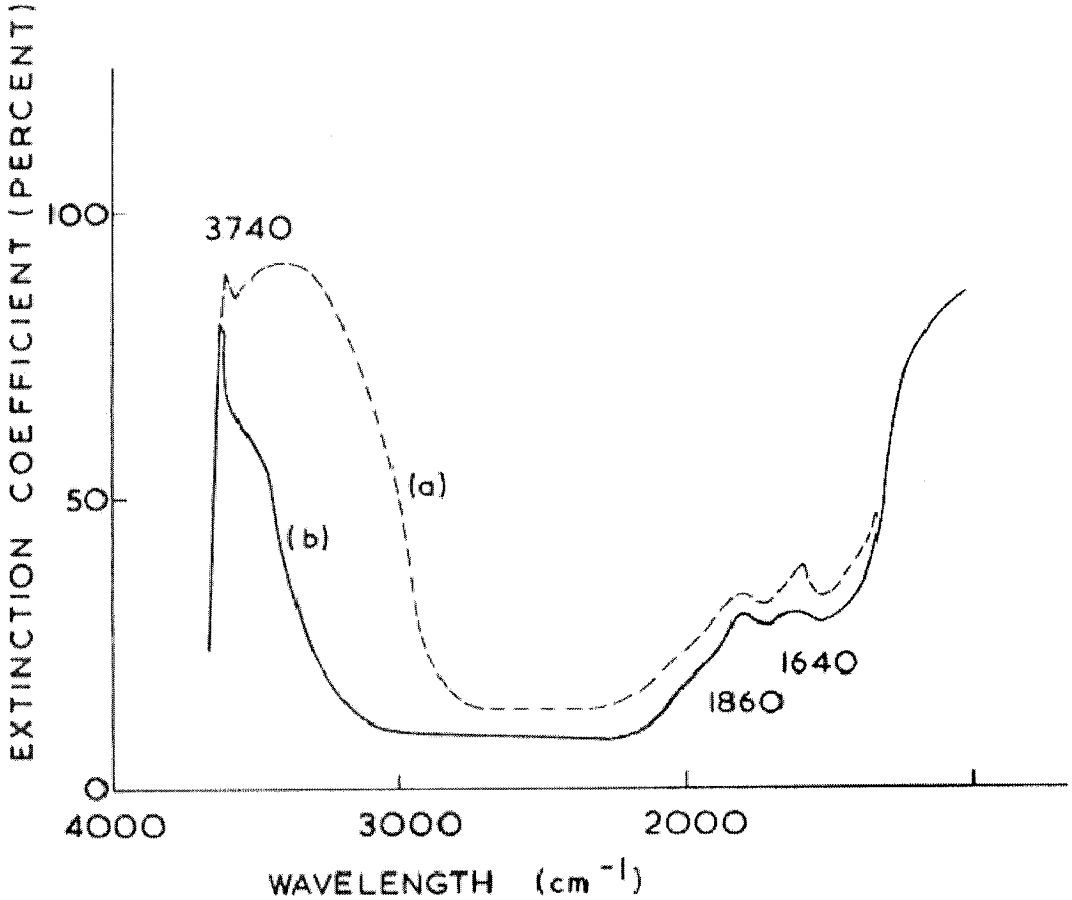

Figure 1.1: IR spectra of (a) fully hydrated silica, and (b) silica dehydroxylated at 200 °C for 3 hours.[6]

The number of OH groups on silica that are available for reaction was determined by treatment with methylmagnesium iodide, by measuring the amount of methane formed, equation 1.2.

$$\equiv SiOH \quad + \quad CH_3MgI \quad \rightarrow \quad \equiv SiOMgI \quad + \quad CH_4 \qquad (1.2)$$

The effect of pretreating silica at a specific temperature on the number and nature of the hydroxyl groups on the surface has been studied. Partial dehydroxylation occurs when silanol groups condense to siloxane bridges and water.[11] In all, four types of silanol groups have been identified: isolated, vicinal, geminal and hydrogen-bonded. These are shown in Figure 1.2.

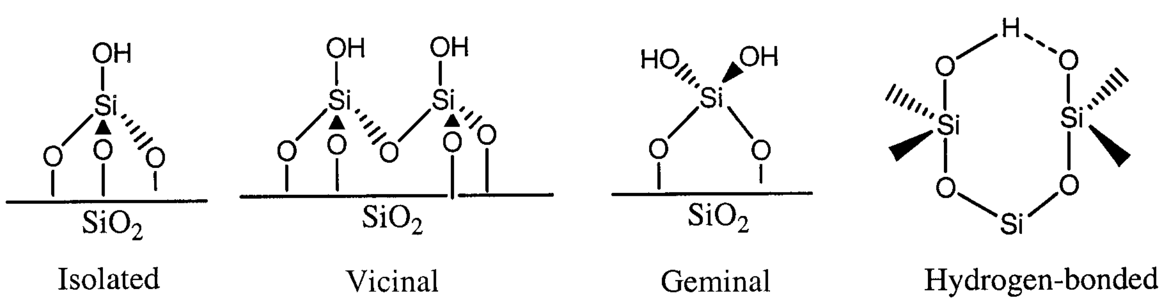

Figure 1.2: Schematic presentation of the four types of silanol groups present on silica.

Qualitative and quantitative data on the surface properties of silica have been obtained using a combination of vibrational spectroscopies and solid state NMR spectroscopy.[12]

1.2.1 Aerosil 200

Aerosils belong to a family of silicas made by Degussa AG (Frankfurt, FRG).[11] As with other amorphous silicas, the surface is made up of siloxane bridges (-SiOSi-) and silanol groups (-SiOH). Made by reacting $SiCl_4$ with O_2, these non-porous particles consist almost exclusively of silicon dioxide (> 99.8%). Aerosil 200 has a specific surface area in the range of 175-225 m^2 / g. When heated under vacuum at 200, 500 and 700 °C, the amount of accessible OH groups per nm^2 has been found to be 2.6, 1.2 and 0.7, respectively, that is a concentration of ca. 0.86, 0.42 and 0.23 mmol OH g^{-1} of silica, respectively.[11]

1.3 Supported Zirconium(IV) Alkyls in Catalysis

Before the discovery of alkylaluminum activators, the rate of olefin polymerization by molecular compounds (alkyl complexes of Ti, Zr, Hf and Th) was known to be very slow.[13] In contrast, oxide supported Zr(IV) alkyls were found to be highly active for the polymerization of α-olefins, even in the absence of cocatalyst.[6] High molecular weight linear polymers were obtained. Supported Zr(IV) complexes were more active than their Ti(IV) analogs, Table 1.2.

Polymerization of propylene in toluene at 65°C was also undertaken. A mixture of soluble and insoluble polypropylenes was obtained, Table 1.3. The insoluble polymer was crystalline with melting points ranging from 115-163°C. The polymer microstructure was determined from the characteristic spectral signatures of isotactic and syndiotactic polypropylene by ^1H NMR.

Zakharov and co-workers showed that the activity of the supported organoZr(IV) catalysts was affected by UV irradiation. This was explained by the partial reduction of the surface complexes to Zr(III). Replacement of an alkyl ligand by halide at the active centers also resulted in an increase in catalytic activity. These supported Zr(IV) alkyls were found to retain their catalytic activity at high temperatures (>200°C).

Polymerization of ethylene by supported Zr(IV) complexes is proposed to occur by the insertion of the olefin in the Zr-C bond, equation 1.3.

$$\text{(silica)ZrR} + C_2H_4 \longrightarrow \text{(silica)Zr-}CH_2CH_2R \tag{1.3}$$

An olefin complex is a likely intermediate, although the equilibrium constant for its formation is expected to be extremely low and it has not been detected.[14]

Candlin and Thomas investigated the ability of alumina-supported Zr(IV) complexes to catalyse the polymerization and disproportionation of olefins.[15] Though most of their work focused on π-allyl complexes, they studied the grafting of tetrabenzylZr(IV) on alumina treated thermally at different temperatures, and the catalytic properties of these materials in the polymerization of ethylene. At 80 °C in toluene, the activity was ca. 400 gram polyethylene/ mmol of catalyst/ hr/ atm of C_2H_4.

Table 1.2: C_2H_4 polymerization activities at 80°C [6]

Metal complex	**Support**	**Normalized polymerization activity** (g C_2H_4 / mmol M.hr.atm)
$Zr(CH_2C_6H_5)_4$	-	0.8
$Zr(CH_2C_6H_5)_4$	Al_2O_3 (500°C)	390
$Ti(CH_2C_6H_5)_4$	Al_2O_3 (500°C)	89
$Zr(CH_2SiMe_3)_4$	Al_2O_3 (650°C)	142
$Zr[CH_2OCH_3]_4$	Al_2O_3 (500°C)	107

Table 1.3: C_3H_6 polymerization activities and stereoisomer yields at 65°C [6]

Metal Complex	Activity g/mM^{-1} atm^{-1}hr^{-1}	Polymers soluble in toluene			Polymers insoluble in toluene		
		Yield %	Iso %	Syndio %	Yield %	Iso %	Syndio %
Zr(benzyl)$_4$	0.0007	100	68	21	0	-	-
Ti(benzyl)$_4$	0.004	98	75	23	2	-	-
Zr(benzyl)$_4$/ SiO_2 (200°)	5.8	30	40	60	70	80	20
Zr(benzyl)$_3$I /SiO_2 (200°)	1.03	52	47	53	48	71	29
Ti(benzyl)$_4$/ Al_2O_3	5.5	30	40	60	70	80	20

More recently, Collete *et al.* studied stereoisomerism in the polypropylene formed by the polymerization of C_3H_6 catalysed by $Zr(CH_2Ph)_4$, $Zr(CH_2CMe_3)_4$ and $Zr(CH_2C(CH_3)_2Ph)_4$ supported on a nonporous alumina with a particle size of 10-20 nm, a surface area > 100 m^2 / g and with a hydroxyl content of 0.4-0.8 mmol per g Al_2O_3.[15] The polymerization reaction was carried out in liquid propylene at 50°C and the isotacticity was measured by IR spectroscopy, using the ratio of intensities at 993 and 975 cm^{-1}. Stereoregularity was found to vary with the ligand and the loading of Zr, that is the Zr / Al ratio directly influenced the outcome. The higher this ratio, the more isotactic was polypropylene, and the lower the catalyst efficiency. Addition of a stoichiometric amount of alkylaluminum (Al^iBu_3 or Al^iBu_2H) resulted in lower activity.

Basset *et al.* investigated the insertion of carbon monoxide into the Zr-C bond of silica-supported cyclooctylzirconium (Scheme 1.1), synthesized by the reaction of the supported hydride with cyclooctane.[16]

Scheme 1.1: Insertion of CO into Zr-C bond

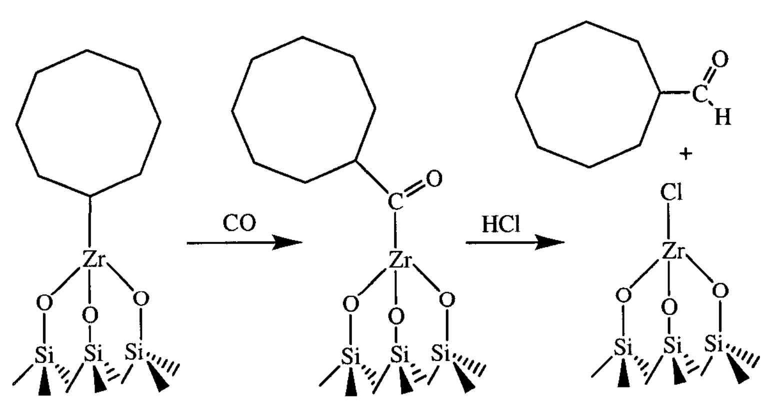

In 2002, Marks and co-workers reported the grafting of organozirconium complexes on sulfated zirconia, and the ability of these complexes to catalyze hydrogenation and polymerization reactions.[3] The zirconium complexes used were $Cp_2Zr(CH_3)_2$, $Cp^*Zr(CH_3)_3$, $Zr(CH_2{}^tBu)_4$, $Zr(CH_2TMS)_4$ and $Zr(CH_2Ph)_4$. Characterization of some of the supported complexes was facilitated by the use of $^{13}C_\alpha$-enriched precursors, e.g., $Cp_2Zr(^{13}CH_3)_2$, $Cp^*Zr(^{13}CH_3)_3$ and $Zr(^{13}CH_2{}^tBu)_4$. The supports used were zirconia (ZR) and sulfated zirconia ZRS300, ZRS400 and ZRS720 (the number represents the temperature at which the support was activated). The grafting reactions were monitored both by IR and ^{13}C NMR spectroscopy. One equivalent of alkane was formed during the grafting, indicating the overall reaction shown in equation 1.4.

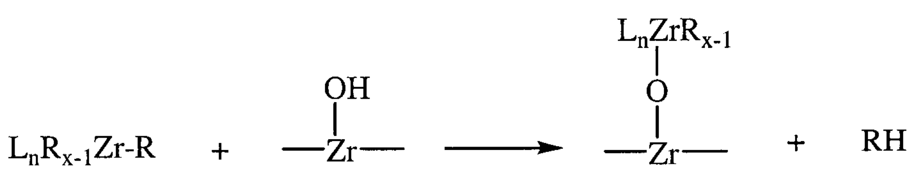

(1.4)

IR spectra provided compelling evidence of grafting, by the disappearance of ν(O-H) bands at 3650 and 3300 cm^{-1}, and appearance of new bands in the region 2890-2930 cm^{-1} for aliphatic ν(C-H). ^{13}C NMR spectra of the molecular precursors and the grafted complexes were recorded and compared. Figure 1.3 shows the spectra for $Zr(^{13}CH_2{}^tBu)_4$ before and after grafting.

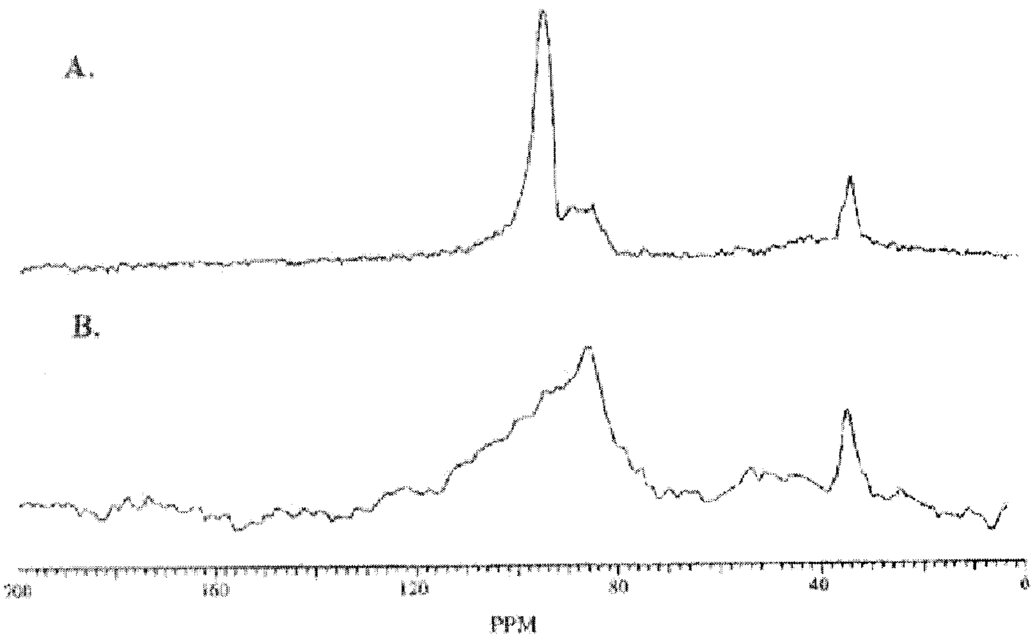

Figure 1.3: ^{13}C CP/MAS NMR spectra of (A) $Zr(^{13}CH_2{}^tBu)_4$, and (B) $Zr(^{13}CH_2{}^tBu)_4$ grafted on ZRS400.[3]

In spectrum A, the peaks at ca. 35.3 ppm and 94.7 ppm were assigned to the methyl and the α-methylene carbon atoms respectively. In the spectrum of the supported complex (B), the broad peak at ca.100 ppm was attributed to the labeled methylene carbons of $ZrOZrNp_3$ and $(ZrO)_2ZrNp_2$ species, as well as that of the cationic $[Zr(^{13}CH_2{}^tBu)_3]^+$ complex.

Hydrogenation of 1-hexene and benzene was carried using 50 mg of the catalyst. The activity depends both on the support and the catalyst. In the case of 1-hexene, $Cp^*Zr(CH_3)_3$ supported on ZRS400 was found to be much more active than $Cp_2Zr(CH_3)_2$ grafted on any of the supports. Significant activities were observed in all the systems for benzene hydrogenation. Furthermore, rate measurements showed that all the reactions were zero-order in substrate concentration over a broad range of benzene concentrations.

Polymerization of propylene and ethylene was also studied. The order of activity (total polymer / mole of Zr / hour) was $Zr(CH_2Ph)_4$ (2.5) > $Zr(CH_2TMS)_4$ (1.8) $Zr(CH_2{}^tBu)_4$ (1.2) > $Cp^*Zr(CH_3)_3$ (0.77). The polypropylene formed was found to be of ultrahigh molecular weights and predominantly atactic.

1.4 Supported Zr(IV) alkyls as potential precursors for supported alkylidenes

Olefin metathesis is an important reaction because it results in the formation of new C-C bonds, as shown in Scheme 1.2.

Scheme 1.2: Olefin metathesis by metal alkylidene complexes

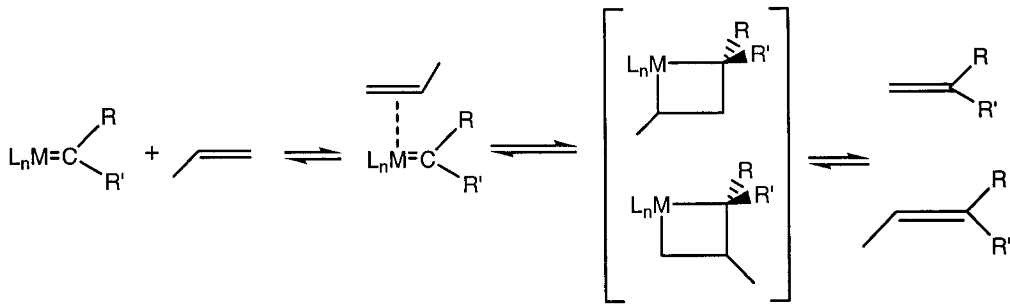

Alkylidene complexes of type $L_nM{=}CHR$ exhibit a very diverse chemistry as catalysts for olefin metathesis reactions and ring-opening metathesis polymerization (ROMP),[17] ring-opening metathesis (which is a common strategy for ring formation in organic synthesis),[18] in addition to be used stoichiometrically in "Wittig-type" reactions to give olefins from ketones and esters.[19]

Early transition metal alkylidene complexes have been the subject of many studies, because of their potential catalytic applications. The first such complex prepared was $(^tBuCH_2)_3Ta{=}CH^tBu$, equation 1.5, first synthesized in 1974 by Schrock.[20]

$$TaNp_5 \longrightarrow Np_3Ta{=}CHCMe_3 + NpH \qquad (1.5)$$

Since then, many alkylidene complexes of Group V and VI metals have been synthesized, fully characterized and their catalytic properties investigated.[18] By ^{13}C labeling experiments, the ^{13}C NMR chemical shift of the alkylidene carbon has been identified at about 250 ppm.[21] Amor Nait Ajjou and co-workers even reported the synthesis of a silica-supported Cr alkylidene, $(\equiv SiO)_2Cr{=}CH(CH_3)_3$.[22] However, only very few Group IV alkylidenes have been made. Most of them have been generated in situ and none has been grafted on any kind of support.[23,24]

One route to alkylidene complexes is by thermal or photochemical α-H abstraction from complexes containing α-hydrogen (equation 1.5). Girolami and coworkers compared α-H and γ-H abstraction pathways in $Ti(CH_2C(CH_3)_3)_4$, leading to an alkylidene and metallacyclobutane respectively.[25,26] Based on the results of these investigations, they concluded that the α-H pathway (that is, formation of the corresponding alkylidene) was more favorable in the thermolysis of $Ti(CH_2C(CH_3)_3)_4$ because the small size of the Ti atom favors the less crowded transition state. Attention then focused on the thermolytic pathways of Zr(IV) and Hf(IV) alkyl complexes. Xue and coworkers reported ab initio calculations on several Zr(IV) alkyls including neopentyl complexes.[27] They found that γ-H abstraction was more favorable than α-H abstraction in $Zr(CH_2C(CH_3)_3)_4$ by about 5.2 kcal/mol. Since the Zr-C bond is longer than the Ti-C bond, the metal can accommodate more readily the metallacyclobutane transition state, Scheme 1.3.

The formation of terminal alkylidenes may be favored by conducting the thermolysis of the Groups (IV) or (V) alkyl complexes in the presence of a tri(alkyl) phosphine, such as PMe_3.[28] The first attempts to make Zr(IV) alkylidene complexes by α-H abstraction were reported by Schrock and coworkers in 1981.[29] They synthesized several new neopentyl halide complexes $ZrNp_2X_2L_2$ and investigated their thermolysis and photolysis in the presence of phosphorus and nitrogen donor ligands (L= PMe_3, PMe_2Ph, NEt_3, ½ DMPE, ½ TMEDA).

Scheme 1.3: The formation of a zirconacyclobutane by γ-H abstraction in $Zr(CH_2C(CH_3)_3)_4$

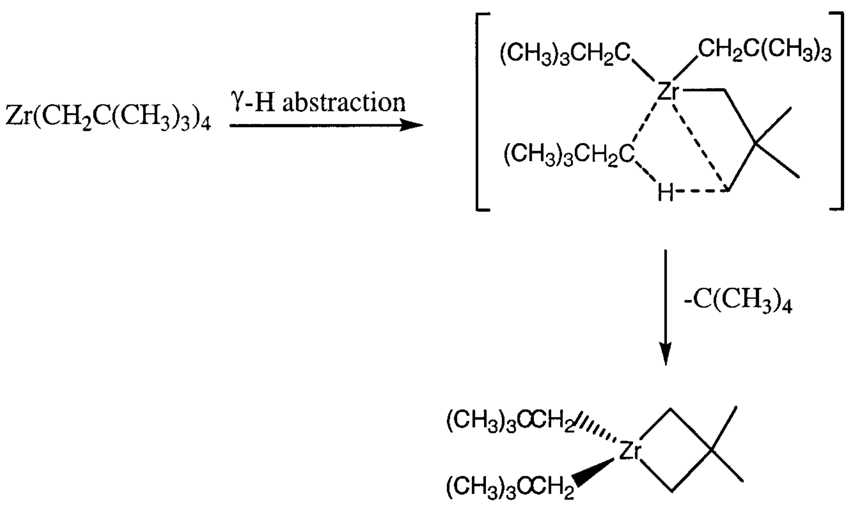

None of the complexes yielded stable alkylidenes upon thermolysis, though in some cases, the in situ formation of neopentylidene complexes could not be excluded.

It was only in 1993 that Fryzuk and co-workers synthesized and isolated the first stable Zr(IV) alkylidene.[17] $[\eta^5\text{-}C_3H_5\text{-}1,3\text{-}(SiMe_2CH_2PPr^i{}_2)_2]Zr{=}CHPh(Cl)$ was synthesized as shown in Scheme 1.4. The signal for the benzylidene proton was observed at 8.1 ppm in ^1H NMR spectrum, and the benzylidene carbon was responsible for the signal at 229.4 ppm in the coupled ^{13}C NMR spectrum. The structure of the alkylidene was further confirmed by X-ray data. Figure 1.4 shows an ORTEP view of the benzylidene complex.

Scheme 1.4: Synthesis of [η^5-C_3H_5-1,3-($SiMe_2CH_2PPr^i_2$)$_2$]Zr=CHPh(Cl)[17]

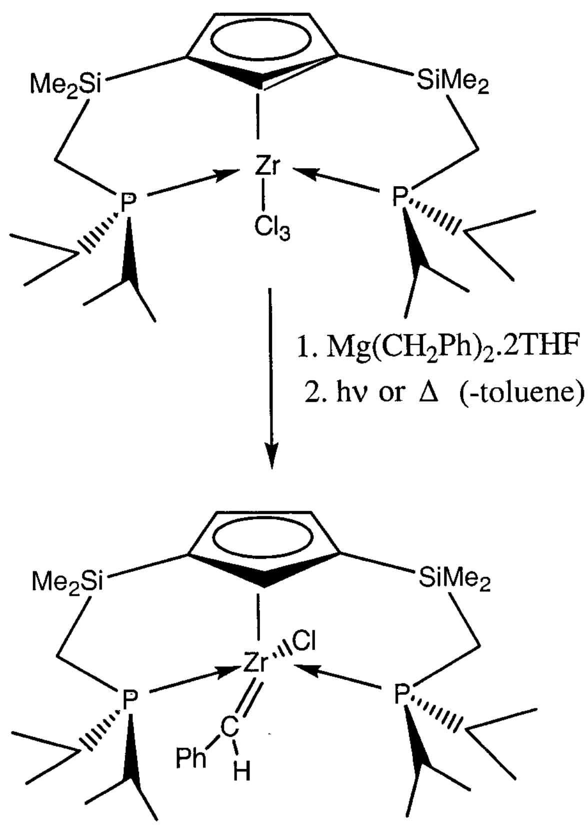

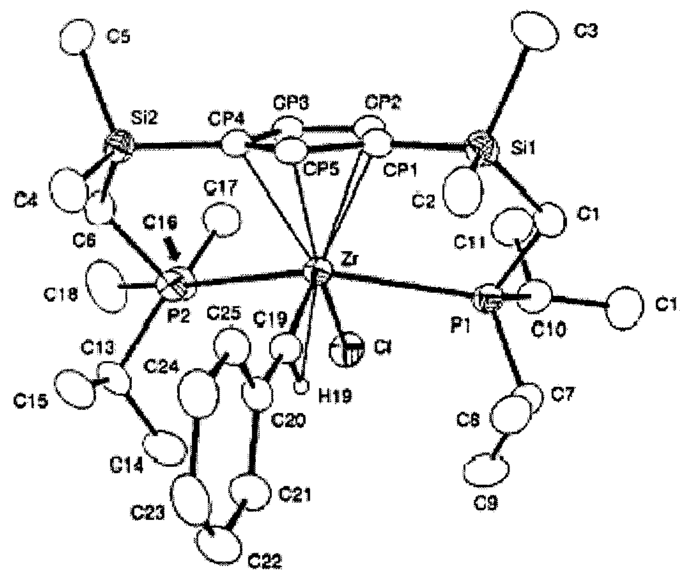

Figure 1.4: Labeled ORTEP view of $[\eta^5\text{-}C_3H_5\text{-}1,3\text{-}(SiMe_2CH_2P^iPr_2)_2]Zr{=}CHPh(Cl)$.[17]

The reactivity of this complex was studied.[23] With a stoichiometric amount of ethylene, there was a color change from orange to dark red and two isomeric forms of the ethylene complex were isolated, as shown in Scheme 1.5.

Scheme 1.5: Reaction of [η^5-C_3H_5-1,3-($SiMe_2CH_2P^iPr_2$)$_2$]Zr=CHPh(Cl) with ethylene

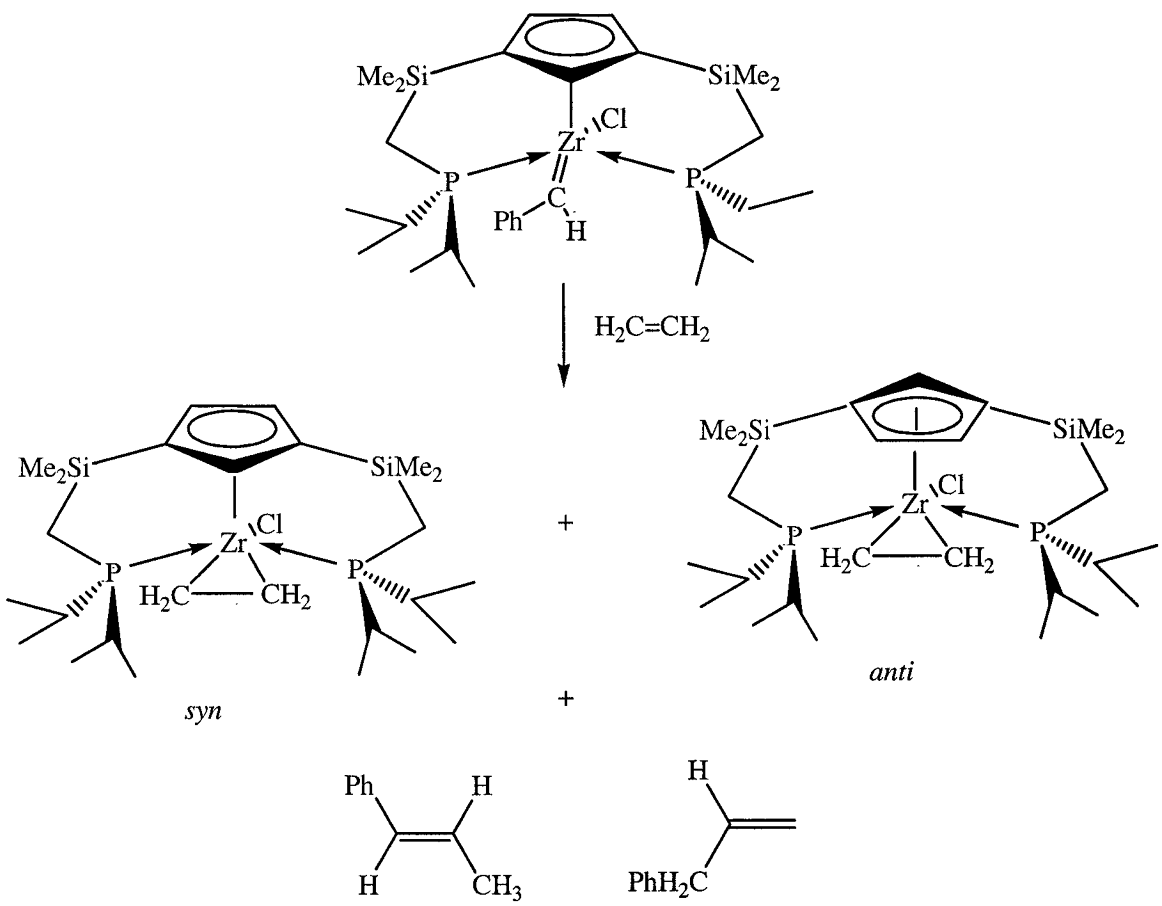

Other reactions of the alkylidene complex are shown in Scheme 1.6. The alkylidene complex underwent a pseudo-Wittig reaction with acetone, characteristic of early-metal alkylidene reactivity. The alkene $PhCH{=}C(CH_3)_2$ was identified by GC-MS. The Zr-containing product was not isolated, though the oxo structure shown below (Scheme 1.6) was proposed. With CN^{t}Bu, a ketenimine complex was formed, by insertion of the isocyanide into the Zr=C bond. This was the first example of such a reaction.

Scheme 1.6: Other reactions of $[\eta^5\text{-}C_3H_5\text{-}1,3\text{-}(SiMe_2CH_2P^iPr_2)_2]Zr{=}CHPh(Cl)$

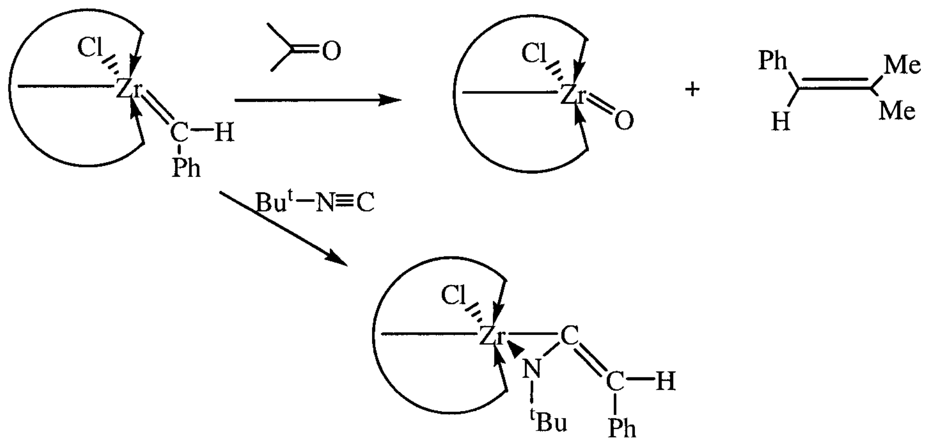

1.5 Supported Zr(IV) alkyls as precursors for other active sites

1.5.1 Supported Zr(IV) hydrides

Soon after the synthesis of the first supported Zr(IV) alkyls in the 1970s, Zakharov and Yermakov reported that heating these complexes with hydrogen induced an increase in catalytic activity towards the polymerization of olefins.[13] The catalytic properties were even retained after the removal of all organic ligands. They postulated the formation of surface hydrides that were immediate precursors of the propagation centers. The amount of hydride on the surface was determined by treatment with D_2O, whereby the amount of HD evolved was measured. One specific catalyst studied was $Zr(C_3H_5)_4$ supported on silica dehydroxylated at 450°C and treated with 200 Torr of hydrogen at 120°C for 30 minutes. The formation of the hydride was confirmed by IR spectroscopy by appearance of Zr-H band at 1625 cm^{-1}.[30] This catalyst polymerized ethylene more readily than the precursor allyl complex.

Since then, a number of studies have been carried out on the synthesis and catalytic activities of supported Zr(IV) hydrides, including the application of grafted Zr(IV) hydrides as isomerization and hydrogenation catalysts for long-chain olefins.[8] Scheme 1.7 summarizes the procedure used to make the hydride.

Scheme 1.7: Synthesis of silica-grafted Zr(IV) hydride.

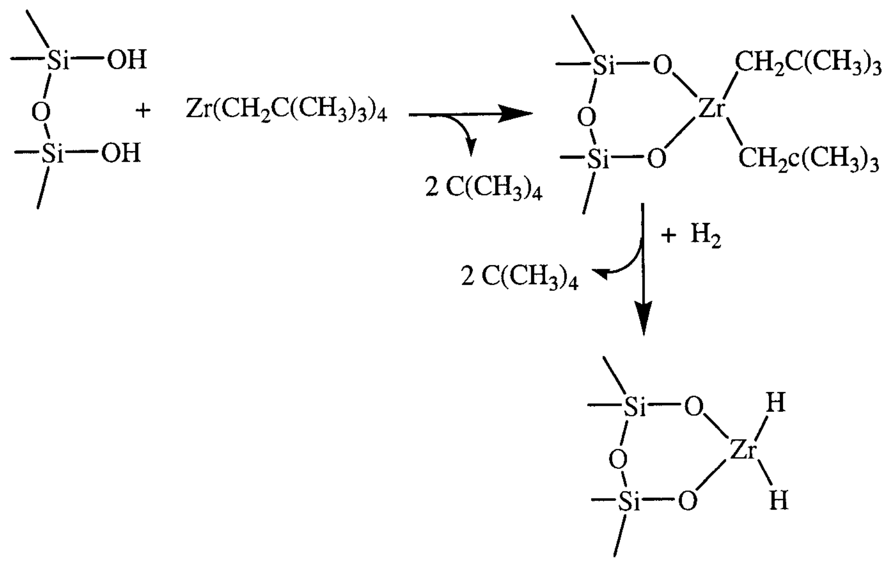

While its precursor was found to catalyze the isomerization of olefins very inefficiently, the supported hydride showed significant activity. The most impressive result was obtained with 1-butene, with total conversion of a twentyfold molar excess achieved in two hours at 20 °C.[8] Isomerization was slower in the case of 1-hexene, allylbenzene and methylenecyclohexane.

The activation and functionalization of alkanes is another major challenge in catalysis, and supported Zr(IV) hydrides have been found to be potential catalysts for these types of reactions.[1,16,11] As stated earlier, $(\equiv SiO)_3ZrH$ is known to react with cyclooctane [16] and methane [31] to form the corresponding alkyl complexes, equations 1.6-1.7.

$$(\equiv SiO)_3\text{-}Zr\text{-}H \quad + \quad cyclo\text{-}C_8H_{16} \rightarrow (\equiv SiO)_3\text{-}Zr\text{-}cyclo\text{-}C_8H_{15} + H_2 \qquad (1.6)$$

$$(\equiv SiO)_3\text{-}Zr\text{-}H \quad + \quad CH_4 \rightarrow (\equiv SiO)_3\text{-}Zr\text{-}CH_3 + H_2 \qquad (1.7)$$

Evidence for these reactions was provided by the fact that ν(Zr-H) decreased considerably in intensity in the IR spectrum, molecular hydrogen was formed and reaction of the product with D_2O gave the expected deuterated alkane, e.g. CH_3D from the methyl complex.

$(\equiv SiO)_3ZrH$ also catalyses the hydrogenolysis of neopentane producing a 3:1 ratio of methane and ethane, which indicates β-methyl transfer as a key step in C-C bond cleavage.[11] Further confirmation for this mechanism was obtained by the low-temperature hydrogenolysis of n-alkanes, wherein no ethane was produced. Scheme 1.8 shows the mechanism of the hydrogenolysis reaction for propane.

Scheme 1.8: Catalytic hydrogenolysis of alkanes by supported Zr(IV) hydride[11]

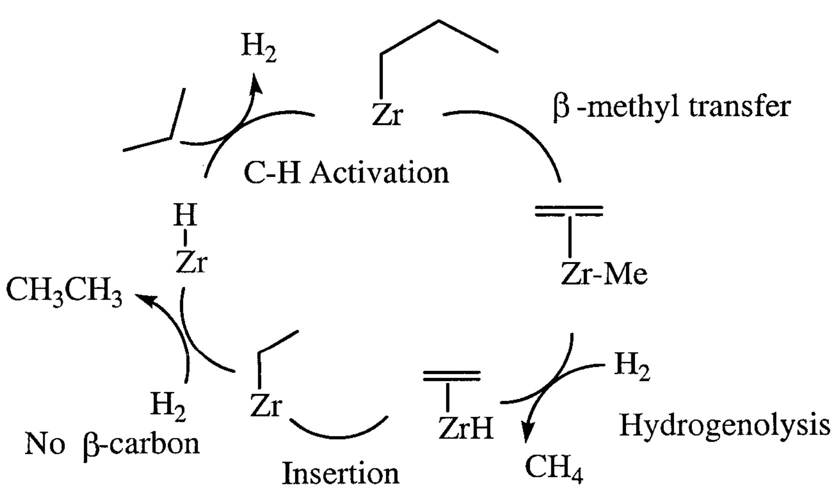

1.5.2 Other supported Zr(IV) catalysts

Supported Zr(IV) alkyls complexes have also been used to make supported alkoxy complexes, equation 1.8.[32,33]

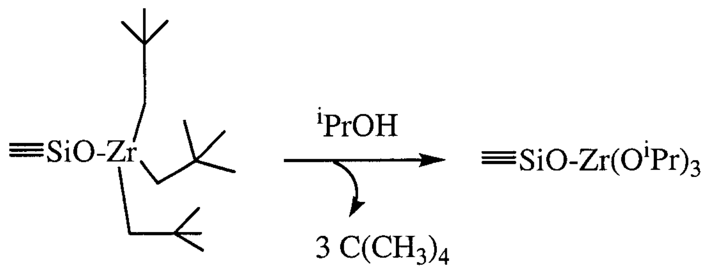

(1.8)

$(\equiv SiO)Zr(O^iPr)_3$ is active as a catalyst for both Meerwein-Ponndorf (hydrogen transfer) and Oppenauer reactions (inclucing reduction / oxidation by hydrogen transfer). Table 1.4 shows some results of these catalytic reactions.

One interesting point to note here is that the silica-supported Zr catalyst obtained by directly grafting $Zr(O^iPr)_4$ on silica is much less active than the one obtained from $(\equiv SiO)ZrNp_3$.

Two other catalysts that were made from $(\equiv SiO)ZrNp_3$, namely $(\equiv SiO)Zr(OH)_3$ and $(\equiv SiO)_3ZrOH$.[32] They were synthesized according to Scheme 1.9.

Table 1.4: Transfer of hydrogen catalyzed by $(\equiv SiO)Zr(O^iPr)_3$

Substrate	Reductant (oxidant)	[Substrate] / [Zr]	T (K)	% Conv.
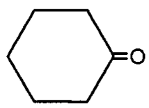	^{i}PrOH[a]	72	353	75[c]
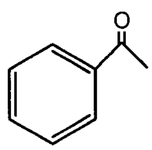	^{i}PrOH[a]	50	353	38[c]
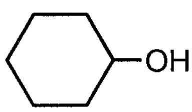	PhC(O)Me	40	383	49[b]
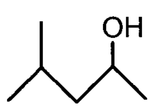	PhC(O)Me	40	383	55[d]
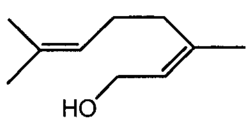	PhCHO	72	383	49[b]

[a] solvent; [b] after 6 h, solvent: toluene; [c] after 20h; [d] solvent : octane

Scheme 1.9: Two other catalysts made derived from (≡SiO)$ZrNp_3$[32]

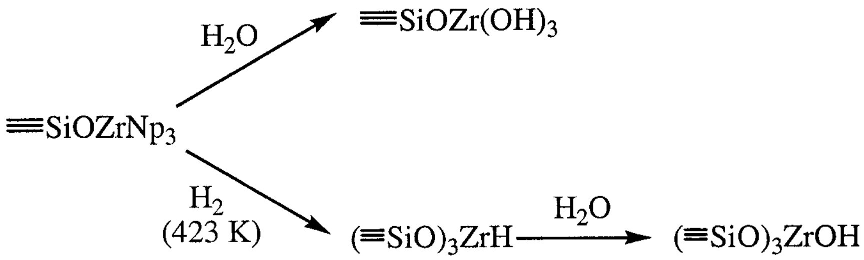

Both supported complexes effectively catalyzed the epoxidation of cyclohexene in the presence of H_2O_2. They also exhibited significant catalytic activity in the hydroxylation of phenol with H_2O_2, as shown in Table 1.5.

Table 1.5: Hydroxylation of phenol with H_2O_2 by $(\equiv SiO)Zr(OH)_3$ and $(\equiv SiO)_3ZrOH$

Catalyst	Zr (% wt)	Conv. H_2O_2	$S_{\text{dihydroxybenzenes}}$ (%)
$(\equiv SiO)Zr(OH)_3$	0.93	98	31
$(\equiv SiO)_3ZrOH$	0.67	90	24

1.6 References

(1) Scott, S. L.; Basset, J.-M. *J. Mol. Catal* **1994**, *86*, 5-22.

(2) Quignard, F.; Lecuyer, C.; Bougault, C.; Lefebvre, F.; Choplin, A.; Olivier, D.; Basser, J.-M. *Inorg. Chem.* **1992**, *31*, 928-930.

(3) Ahn, H.; Nicholas, C. P.; Marks, T. J. *Organometallics* **2002**, *21*, 1788-1806.

(4) Serp, P.; Kalck, P. *Chem. Rev.* **2002**, *102*, 3085.

5) Corker, J.; Lefebvre, F.; Lecuyer, C.; Dufaud, V.; Quignard, F.; Choplin, A.; Evans, J.; Basset, J.-M. *Science* **1996**, *271*, 966-969.

(6) Ballard, D. G. H. *Adv. Catal.* **1973**, *23*, 263-325.

(7) Yermakov, Y.; Zakharov, V. *Adv. Catal.* **1975**, *24*, 173-243.

(8) Schwartz, J.; Ward, M. D. *J. Mol. Catal* **1980**, *8*, 465-469.

(9) Smith, D. C.; Rubiano, R. R.; Healy, M. D.; Springer, R. W. In *Proc. 11th Int. Conf. Chemical Vapor Deposition*; 5th ed.; Jensen, K. F., Cullin, G. W., Eds.: NJ, 1993, p 417.

(10) Parmeter, J. E.; Smith, D. C.; Healy, M. D. *J. Vac. Sci. Technol. A* **1994**, *12*, 2107.

(11) Coperet, C.; Chabanas, M.; Saint-Arroman, R. P.; Basset, J.-M. *Angew. Chem. Int. Ed.* **2003**, *42*, 156-181.

(12) Dijkstra, T. W.; Duchateau, R.; Santen, R. A.; Meetsma, A.; Yap, G. P. A. *J. Am. Chem. Soc.* **2002**, *124*, 9853.

(13) Zakharov, V. A.; Yermakov, Y. *Catal. Rev.-Sci. Eng.* **1979**, *19*, 67.

(14) Ballard, D. G. H.; Burnham, D. R.; Twose, D. L. *J. Catal.* **1976**, *44*, 116.

(15) Candlin, J. P.; H., T. *Adv.Chem. Ser.* **1974**, *132*, 212-239.

(16) Quignard, F.; Choplin, A.; Basset, J.-M. *J. Chem. Soc., Chem. Commun.*, **1991**, 1589-1590.

(17) Fryzuk, M. D.; Mao, S. S. H. *J. Am. Chem. Soc.* **1993**, *115*, 5336-5337.

(18) Wu, Y.-D.; Peng, Z.-H. *J. Am. Chem. Soc.* **1997**, *119*, 8043.

(19) Diminie, J. B.; Blanton, J. R.; Quisenberry, K. T.; Xue, Z. *Organometallics* **2001**, *20*, 1504.

(20) Schrock, R. R. *J. Am. Chem. Soc.* **1974**, *96*, 6796.

(21) Marks, T. J.; Ahn, H. *J. Am. Chem. Soc.* **2002**, *124*, 7103.

(22) Amor Nait Ajjou, J.; Rice, G. L.; Scott, S. L. *J. Am. Chem. Soc.* **1998**, *120*, 13436.

(23) Fryzuk, M. D.; Duval, P. B.; Mao, S. S. H.; Zaworotko, M. J.; MacGillivray, L. R. *J. Am. Chem. Soc.* **1999**, *121*, 2478-2487.

(24) Fryzuk, M. D.; Duval, P. B.; Mao, S. S. H.; Rettig, S. J.; Zaworotko, M. J.; MacGillivray, L. R. *J. Am. Chem. Soc.* **1999**, *121*, 1707.

(25) Cheon, J.; Dubois, L. H.; Girolami, G. S. *J. Am. Chem. Soc.* **1997**, *119*, 6814.

(26) Cheon, J.; Rogers, D. M.; Girolami, G. S. *J. Am. Chem. Soc.* **1997**, *119*, 6804.

(27) Wu, Y.-D.; Peng, Z.-H.; Chan, K. W. K.; Liu, X.; Tuinman, A. A.; Xue, Z. *Organometallics* **1999**, *18*, 2081.

(28) Wang, S.-Y. S.; Vanderlende, D. D.; Abboud, K. A.; Boncella, J. M. *Organometallics* **1998**, *17*, 2628.

(29) Wengrovius, J. H.; Schrock, R. R. *J. Organomet. Chem.* **1980**, *205*, 319.

(30) Zakharov, V. A.; Dudchenko, V. K.; Paukshtis, E. A.; Karakchiev, L. G.; Yermakov, Y. *J. Mol. Catal* **1977**, *2*, 421.

(31) Quignard, F.; Lecuyer, C.; Choplin, A.; Olivier, D.; Basset, J.-M. *J. Mol. Catal.* **1992**, *74*, 353-363.

(32) Quignard, F.; Graziani, O.; Teissier, R. *Appl. Catal.* **1999**, *182*, 29.

(33) Quignard, F.; Choplin, A.; Teissier, R. *J. Mol. Catal* **1997**, *120*, L27.

Chapter 2

Experimental Techniques

2.1 Materials

2.1.1 Silica

The silica used in all experiments is Aerosil 200, manufactured by Degussa Corporation AG (Frankfurt). It is an amorphous silica with a surface area of 175-225 m^2 / g, manufactured by the flame hydrolysis of $SiCl_4$:

$$SiCl_4 + O_2 \rightarrow SiO_2 + 2Cl_2 \qquad (2.1)$$

$$2\,H_2O + 2\,Cl_2 \rightarrow 4\,HCl + O_2 \qquad (2.2)$$

2.1.2 Reagents and solvents

Reagents and solvents were purchased from Aldrich and used as received, except as noted. Mg was stored in an oven at 120°C for 24 hours prior to use. *Tert*-butanol was dried by stirring over CaH_2, followed by distillation under N_2. It was stored under N_2 in a high vacuum reactor containing 3 Å molecular sieves. Neopentyl bromide (98%) and neohexene (95%) were used as received. Styrene was stored in a glass reactor under N_2 after being distilled under reduced pressure from CaH_2.

Solvents (hexanes, diethyl ether, toluene, *etc*) were dried by passage through a column purification prior to use.

2.1.3 Gases

Neopentane (96%, Air products) was transferred from a lecture bottle into a glass bulb. Ethylene (99.9%, Matheson) was purified by passing it through a trap containing BTS Deoxo catalyst (Fluka) and 4 Å molecular sieves to remove oxygen and moisture, respectively, during its transfer from the cylinder to a glass bulb. The trap was activated by first heating under a flow of H_2 at 325°C for 4 hours, followed by heating at the same temperature under vacuum for 4 hours. It was then stored under 3 Å molecular sieves in a gas bulb.

2.2 Synthesis of $Zr(CH_2C(CH_3)_3)_4$

All glassware used in this synthesis was pre-dried overnight in an oven at 120°C. A round-bottom three-necked flask equipped with a condenser and containing oven-dried magnesium (1.2 g, 50 mmol) was connected via one neck to a Schlenk line and filled with a nitrogen atmosphere. A dropping funnel was inserted into the second neck of the flask. Through a septum located at the third neck, dry diethyl ether (30 mL) was added via cannula. $(CH_3)_3CCH_2Br$ (5.0 g, 33 mmol) was introduced into the flask drop-wise through the dropping funnel, which was then removed.

No immediate reaction was observed, however upon stirring at room temperature for about 15 minutes, a greyish color appeared. The mixture was then refluxed overnight in an oil bath, when the final color of the mixture was yellowish-green. This indicated the successful formation of $(CH_3)_3CCH_2MgBr$. The Grignard solution was transferred via cannula to a Schlenk tube under nitrogen atmosphere.

Its concentration was determined by back-titration. 1 mL $(CH_3)_3CCH_2MgBr$ was neutralized with 20 mL 0.14 M HCl. A few drops of phenolphthalein solution were added and the solution was titrated with 0.1 M NaOH. 14.7 mL of the latter was needed to reach the end-point. The concentration of $(CH_3)_3CCH_2MgBr$ was hence calculated to be 0.44 M, and its yield was determined to be 95%.

$ZrCl_4$ (0.65 g, 2.8 mmol) was added to an oven-dried, two-necked round bottom flask inside the glove-box. The flask was stoppered and brought out to a Schlenk line, where diethyl ether (25 mL) was added under a nitrogen atmosphere. The solution was then cooled to 0°C using an ice bath. To the cold, stirred solution of $ZrCl_4$, $(CH_3)_3CCH_2MgBr$ (25 mL, 11 mmol) was added dropwise by syringe, through a septum. A cream-coloured slurry was observed. The reaction mixture was allowed to warm slowly to room temperature. A yellow solution and a white precipitate were observed, indicating the successful preparation of $Zr(CH_2C(CH_3)_3)_4$:

$$4\,(CH_3)_3CCH_2MgBr + ZrCl_4 \rightarrow Zr(CH_2C(CH_3)_3)_4 + 4\,MgBrCl \qquad (2.3)$$

Because the white precipitate of MgBrCl adhered to the walls of the flask, the yellow solution of $Zr(CH_2C(CH_3)_3)_4$ was easily transferred via cannula to a Schlenk tube under nitrogen. The diethyl ether was removed *in vacuo*, leaving behind a yellow-brown solid of crude $Zr(CH_2C(CH_3)_3)_4$. The pure product was obtained by sublimation at 50°C through a U-tube wrapped with heating tape to a second Schlenk tube under a high vacuum. Sublimation required a period of 1-2 days. $Zr(CH_2C(CH_3)_3)_4$ is extremely air and light sensitive, and was stored under nitrogen in a freezer.

2.3 Preparation of silica-supported Zr(IV)

2.3.1 Preparation of silica

Aerosil 200 belongs to a family of fumed silicas made by Degussa AG (Frankfurt, FRG) and has a specific surface area in the range 175-225 m^2 / g. When heated under vacuum at 200, 500 and 700 °C, the number of accessible OH groups per nm^2 is 2.6, 1.2 and 0.7 respectively, that is, a concentration of approximately 0.86, 0.42 and 0.23 mmol OH per gram of silica, respectively.

Aerosil 200 was used either in the form of a pellet or as powder. To make the pellet, the desired amount of silica (10-40 mg) was pressed in a stainless steel die at 125 kg/m^2 into a self-supporting disk with diameter 1.6 cm. The disk was transferred to a glass or quartz sample holder, which was then carefully inserted into an IR cell. For reactions requiring powdered samples (*e.g.*, NMR experiments), the silica was first pressed into thick pellets which were then ground in a mortar. This powder was then transferred into the reactor.

The silica was dehydroxylated at 200°C under dynamic vacuum (< 10^{-4} Torr) for at least four hours. This thermal treatment ensures that adsorbed moisture is removed, and that the surface hydroxyl density is reproducible.

2.3.2 Sublimation grafting

A small amount of $Zr(CH_2C(CH_3)_3)_4$ was transferred under nitrogen via a U-tube to a breakseal reactor. The breakseal reactor consists of a glass tube containing a breakseal and equipped with a high vacuum stopcock. The tube, containing the Zr reagent, was sealed off under vacuum at a pre-made restriction. The breakseal was kept wrapped in Al foil to prevent photolytic decomposition during subsequent reactions. A "hammer" (generally a 2 cm long nail sealed inside a glass tube) was introduced into the tube, and held in place near the breakseal by a magnet taped to the outside of the tube. A second restriction was made on the open side of the tube to facilitate sealing of the breakseal tube after grafting. The open end of the breakseal tube was then welded at right angles onto the body of the reactor.

The silica (either in powder form or as a pellet) was introduced into the IR cell (Figure 2.1), and the silica was heated to 200°C. Once thermal treatment was complete, the "hammer" was used to break the breakseal under vacuum and the silica pellet was displaced inside the IR cell to the region immediately above the breakseal.

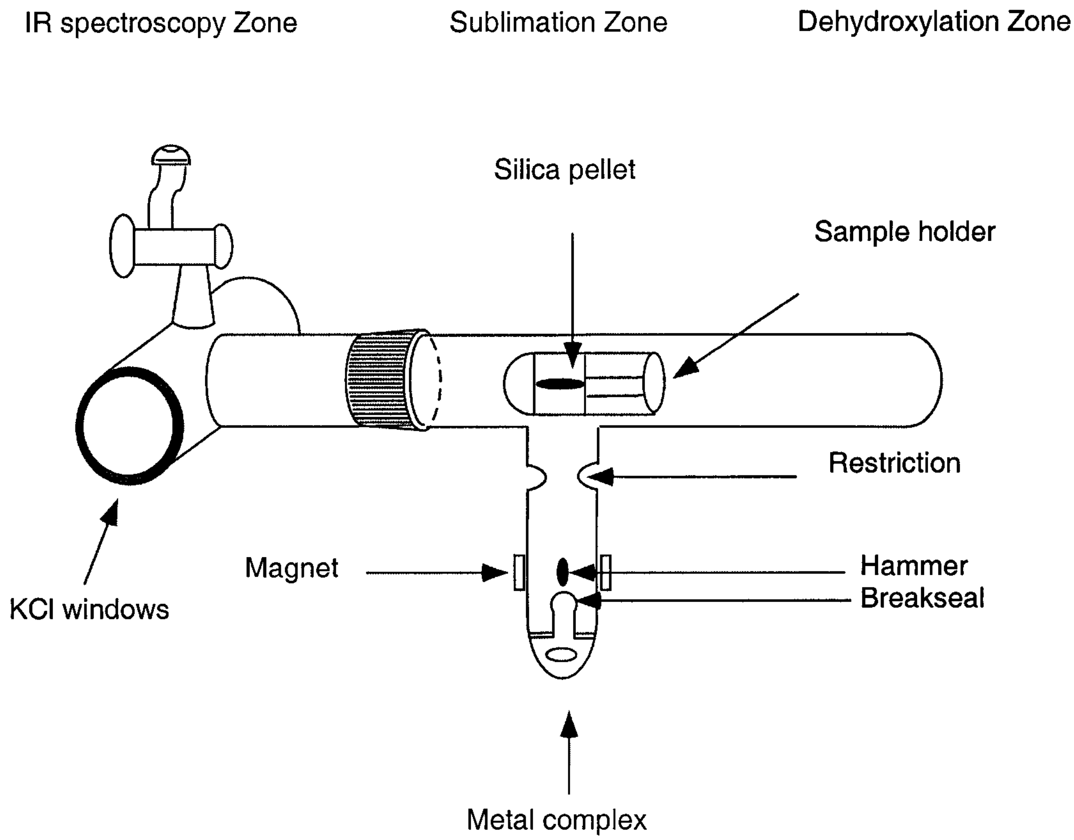

Figure 2.1: Schematic of an IR cell

Sublimation of the zirconium alkyl was undertaken for at least 3 hours at 50°C, by wrapping heating tape around the breakseal. If powdered silica was used, the heating tape was also wrapped around the body of the IR cell up to the region where the silica was located.

After sublimation, unreacted (physisorbed) material was removed from the silica and the IR reactor by heating the the silica at 50°C using heating tape, while submerging the breakseal in liquid nitrogen. The breakseal tube was then flame-sealed at the pre-made restriction.

2.3.3 Solution grafting

Solution grafting was accomplished in the dry-box. About 300 mg of silica powder was weighed in a Schlenk tube equipped with a high vacuum stop-cock which was then connected to a high vacuum line. Thermal treatment was performed as usual. After cooling to room temperature, the Schlenk tube was brought into the dry-box. $Zr(CH_2C(CH_3)_3)_4$ (ca. 0.5 g) and a few drops of toluene were added to make a slurry, which was stirred at room temperature for about 1 hour. Hexane (10 mL) was then added, and the stirring continued for another 30 minutes. No color change of the white silica was observed. The silica was allowed to settle and the solvent was decanted and separated using a Pasteur pipette. The silica was then washed with five 10 mL portions of fresh hexane, in order to remove unreacted $Zr(CH_2C(CH_3)_3)_4$.

After the last portion of hexane was removed, the Schlenk tube was stoppered and removed from the glove-box. The solid was dried, first on a Schlenk line, then on a high vacuum line. The modified silica was then brought back into the glove-box, where weighed portions were transferred to other reactors for further study, or to rotors for NMR analysis.

2.4 Characterization of silica-supported Zr(IV) complexes

2.4.1 Infrared spectroscopy

The IR cell is equipped with KCl windows through which the beam passes during IR data acquisition. Spectra were recorded under static vacuum. The IR cell is capable of holding a vacuum of 10^{-4} Torr for a few days.

Infrared spectra were recorded on either a Mattson Research series FTIR or a Thermo Nicolet Nexus 670 FT-IR. Both instruments were equipped with a DTGS detector and were purged with CO_2-free dry air. Spectra of the background (usually taken after the thermal threatment of the silica) and of silica pellets were taken by co-adding 32 scans at a resolution of 2 cm^{-1}. Gas phase IR spectra were taken at a resolution of 0.75 cm^{-1}.

To obtain transmission IR spectra of silica pellets, the pellet holder was carefully moved to the top of the IR cell, where the KCl windows are located, such that the beam passed through the windows and the thin silica disk. To obtain spectra of gaseous products, the pellet holder was displaced from the IR window zone.

2.4.2 Solid state NMR spectroscopy

^{1}H and ^{13}C CP/MAS NMR spectra were recorded on Bruker Avance 500 MHz and Bruker AMX-200 spectrometers. Samples were either packed directly in 7 mm zirconia rotors (100 mg) or sealed off at 30 mm lengths under vacuum in 5 mm pyrex NMR tubes (35 mg) that were then placed in the zirconia rotors. ^{1}H NMR spectra of solid samples directly packed in 7 mm rotors were recorded at a frequency of 500 MHz with a relaxation delay of 10 seconds. ^{13}C spectra of such samples were run on the same instrument at 125 MHz, with a relaxation delay of 2 seconds. ^{13}C spectra of samples packed in glass tubes were run at either 37 or 125 MHz.

2.4.3 XAS Spectroscopy

Experiments were performed at the Stanford Synchrotron Research Laboratory (SSRL) on beamline BL2-3 (Bend) which operates at 3.0 GeV with a current between 2-3 mA. Square, 2mm thick, polished aluminum plates with sample compartments of 35mm × 5mm had 6.0μm gauge polypropylene film (Chemplex #425) as sample windows affixed with double-sided tape to each side of the plate. Powdered samples, previously sealed under vacuum in glass ampules, were loaded under N_2 in a glove box (<3ppm O_2) at SSRL and adequately taped, trapping an inert environment to prevent hydrolysis and exposure to air. Fresh samples appeared dull orange-brown, but rapidly turned white once exposed to atmosphere.

Synchrotron x-rays were monochromatized via reflections from a pair of parallel Si(111) crystals through an entrance slit of ~1mm. The subsequent beam was detuned 20 to 30% to eliminate harmonics. The fundamental reflection intensity was measured by an initial ion chamber detector (I_o) and then passed though the sample, mounted at a 45 degree angle to the beam. Transmitted x-rays were detected by a second ion detector (I_1) and subsequently passed through a zirconium calibration foil into a final detector (I_2). In addition, fluorescence emissions were recorded from the sample via an argon purged Lytle detector, optimized by removing the detector's Soller slits to facilitate collecting a greater number of fluorescence photoelectrons. Data at SSRL was acquired on a Sun Workstation using the program XASCollect, and subsequently exported as ASCII files. All samples were examined at room temperature immediately after loading in the glove box.

XAS Analysis. Extended X-ray Absorption Fine Structure (EXAFS) and X-ray Near Edge Structure (XANES) data were generated from no less than three separate ASCII files averaged and analyzed using WinXAS (version 2.3). The spectra were normalized to the Zr calibration foil, as well as background corrected for baseline normalization. Pre-edge and K-edge positions and intensities were measured by fitting XANES spectra with Lorentian and ArcTangent functions using WinXAS's least-squares feature. EXAFS spectra were generated from the data by application of a 20% Hanning window prior to Fourier transformations. Values of E_o were assigned to the first inflection point in the data set. Initial models of the surface species were approximated using CambrigeSoft's ChemDraw and Chem3D 2002 with X/Y coordinates exported to

FEFF 8.2. Parameters for the initial models were based on crystal structure data in the literature and are described in Chapter 3. The models were then fit to the data using WinXAS' EXAFS Fit feature, which employs a least squares analysis. The parameters of coordination number *CN*, path length *R*, Debye-Waller factor (σ^2), and initial state energy E_o were optimized for each path. Columns of parameters (*i.e.*, all σ^2 values) in the EXAFS fitting were allowed to vary independently while other parameters were held fixed. This procedure was necessary in order to ensure accurate fitting since first-shell parameters were highly correlated to each other.

2.5 Analysis of Volatiles

2.5.1 Infrared spectroscopy

Neopentane formed during the grafting of $Zr(CH_2C(CH_3)_3)_4$ on silica and thermolysis of the grafted material was qualitatively and quantitatively analyzed by IR spectroscopy. The evolution of neopentane was followed by integrating the region from 2800 to 3000 cm^{-1}, and or using peak height at 1369 cm^{-1}, by comparison to an infrared calibration curve prepared using neopentane with pressures in the range 1-3 and 1-10 Torr, respectively.

2.5.2 GC and GC/MS analysis

Mixtures of gaseous products of surface reactions were separated by injection at 50 °C in an HP 6890A GC equipped with an HP-5 column (30 m long x 0.320 mm i.d.). Identification was achieved with an FID detector (whereby the identities of the gases were determined by comparison to the retention times of standards), or with a Mass Selective detector (where retention times and mass spectra of the tested gas were compared with those of standards).

2.6 Kinetics experiments

Thermolysis of silica-supported tetraneopentylzirconium and ethylene polymerization were monitored by IR spectroscopy of volatiles. For thermolysis experiments, the modified reactor containing the silica pellet or powder was heated in situ at a temperature between 113 to 130 °C in a preheated oven. IR spectra of neopentane in the gas-phase were recorded at regular intervals until no significant changes were noted in consecutive spectra. From the peak height at 1369 cm^{-1}, the amount of neopentane evolved was calculated. From the integration of the ν(CH) spectral region (2800 to 3000 cm^{-1}), the relative amount of neopentane was evaluated, and hence the absorbance values (A_t) were found. Non-linear least square fits with the three variables A_0, A_∞ and k were then performed to obtain the first-order integrated rate equation:

$$A_t = A_0 + (A\infty - A_0)(e^{-kt})$$

Activation parameters were extracted from the line as fit of ln(k/T) versus 1/T. According to the Eyring equation, the slope and intercept correspond to $-\Delta H^{\ddagger}/R$ and $[\ln(R/Nh) + \Delta S^{\ddagger}/R]$, respectively.

$$\ln(k/T) = \ln(R/Nh) + \Delta S^{\ddagger}/R - \Delta H^{\ddagger}/RT$$

Kinetic studies of ethylene polymerization were undertaken in situ. After completion of sample preparation, if a pellet was being used, the cell was evacuated, and IR spectra of both the silica disk and gas phase were recorded. A known pressure of ethylene (e.g., 100 Torr) was admitted to the cell, which was then quickly aligned in the spectrometer. The progress of the polymerization was followed either on the disk (formation of polyethylene) or in the gas phase (consumption of C_2H_4). After the reaction was complete, the pellet was removed from the reactor and weighed.

In the case of polymerization by powder samples of grafted silica, after making the grafted product, the cell was brought into the glove-box, where a known amount of the silica was introduced into a cell which equipped with a side-arm. The powder as well as a small magnetic stirrer was carefully moved to the bottom of the sidearm. Once out of the box, a known amount of ethylene was introduced into the cell, which was then quickly aligned in the IR spectrometer with the beam passing through the gasphase. The side-arm was immersed in a beaker of water whose temperature had been allowed to equilibrate with room temperature. The powder was stirred. The consumption of C_2H_4

was followed by taking spectra of the gas phase at regular intervals. The integration of the region 800 to 1200 cm^{-1} was used to find A_t, and a non-linear least square fit of the data was performed.

Chapter 3

Grafting of Tetra(neopentyl)zirconium on Silica

3.1 Introduction

It was first demonstrated in the early 1970s that silica surfaces, after thermal treatment, can act as either a monodentate or bidentate ligand to organometallic fragments.[1] When silica dried at 200 °C reacts with a solution of $Zr(CH_2C_6H_5)_4$ or $Zr(CH_2Si(CH_3)_3)_4$, the supported organometallic complexes $(\equiv SiO)_2Zr(CH_2C_6H_5)_2$ or $(\equiv SiO)_2Zr(CH_2Si(CH_3)_3)_2$, respectively, were obtained, equation 3.1.

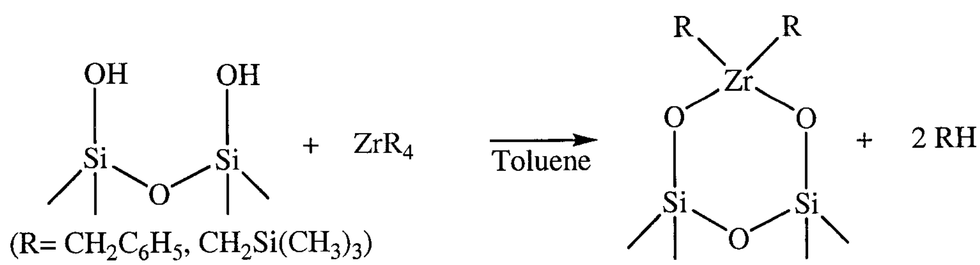
(3.1)

The stoichiometry of the reaction was confirmed by exposing the grafted complexes to excess ^nBuOH, whereupon two equivalents of $CH_3C_6H_5$ and $Si(CH_3)_4$ were formed, respectively, equation 3.2.[1]

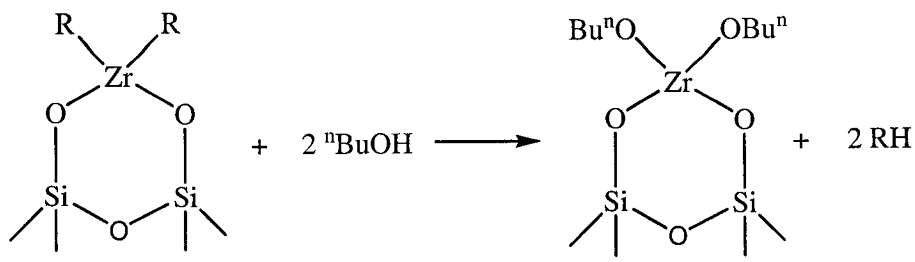

(3.2)

(R= $CH_2C_6H_5$, $CH_2Si(CH_3)_3$)

In 1979, Schwartz and co-workers synthesized $(\equiv SiO)_2Zr(CH_2C(CH_3)_3)_2$ by reaction of silica (Aerosil, 300 m^2/g) pretreated at 200 °C with a solution of $Zr(CH_2C(CH_3)_3)_4$ in toluene at room temperature.[2] Grafting occurred with the stoichiometry shown in equation 3.3, based on the yield of $C(CH_3)_4$ and the amount of Zr grafted.

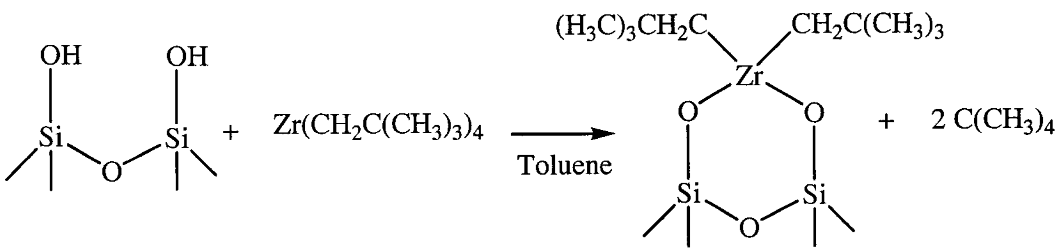

(3.3)

Basset and coworkers demonstrated that grafting could also be achieved by subliming $Zr(CH_2C(CH_3))_4$ at 75 °C onto silica under static vacuum.[3,4] The silica was Aerosil-200 partially dehydroxylated at 500 °C, and a different grafting stoichiometry was achieved, equation 3.4.

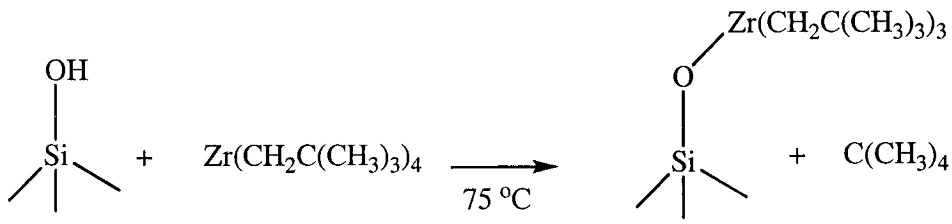

(3.4)

The presence of neopentyl groups on the surface was demonstrated by IR spectroscopy, with ν(C-H), $\delta(CH_2)$ and $\delta(CH_3)$ vibrational modes at 2953, 2864, 1464 and 1369 cm^{-1}. As expected, $(\equiv SiO)Zr(CH_2C(CH_3)_3)_3$ reacted with water to form 3.0 equiv. of neopentane gas.

The surface hydroxyls were identified as the exclusive grafting sites in an experiment using deuterated silica, in which ca. one mole of $C(CH_3)_3(CH_2D)$ was liberated per mole of grafted Zr.[5] IR spectroscopy confirmed that the appearance of vibrational bands characteristic of neopentyl ligands is accompanied by disappearance of the ν(OH) band at 3747 cm^{-1}.

Silica-supported alkylzirconium(IV) fragments have also been characterized by solid state NMR and X-ray absorption spectroscopy.[4,6] The ^{13}C CP/MAS NMR spectrum of $(\equiv SiO)Zr(CH_2C(CH_3)_3)_3$ was initially reported to show only one signal at 33.9 ppm, assigned to the neopentyl methyl group, Figure 3.1.[4] A more recent attempt also identified the methylene signal at 96 ppm.[7]

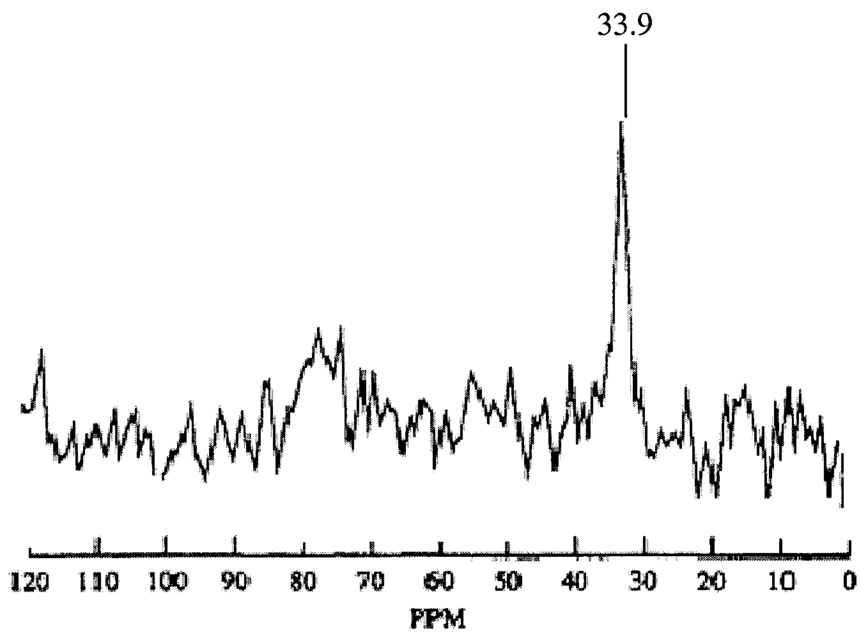

Figure 3.1: ^{13}C CP/MAS NMR spectrum of $(\equiv SiO)Zr(CH_2C(CH_3)_3)_3$.[4]

Structural parameters for $\equiv SiOZr(CH_2C(CH_3)_3)_3$ were derived from the Zr K-edge EXAFS.[8] The first coordination sphere was found to consist of 1.1(1) O atoms at 1.96 Å and 3.2(1) C atoms at 2.22 Å. A second C shell at 3.42 Å was tentatively ascribed to the three quaternary neopentyl C atoms. These results are in accordance with the presence of discrete $\equiv SiOZr(CH_2C(CH_3)_3)_3$ complexes on the silica surface.

3.2 Grafting of $Zr(CH_2C(CH_3)_3)_4$ on Aerosil-200

3.2.1 Stoichiometry

In this work, the grafting stoichiometry, or the ratio of $ZrNp_4$ grafted per surface hydroxyl on Aerosil-200 pretreated at 200 °C, was evaluated by measuring the uptake of Zr and the yield of neopentane. The latter was verified by GC/MS to be the sole volatile product of grafting, and was quantified in situ by the intensity of its gas phase IR spectrum. The results of nine independent experiments are shown in Table 3.1. The amount of neopentane formed corresponds to (1.0 ± 0.1) per surface hydroxyl. The zirconium loading was measured in only two experiments. The maximum Zr content observed is 0.5 Zr per surface hydroxyl. Therefore grafting is suggested to occur with the stoichiometry shown in equations 3.1-3.2, as previously reported by both Ballard and Schwartz.[1,2]

Table 3.1. Stoichiometry of grafting $Zr(CH_2C(CH_3)_3)_4$ on Aerosil 200 silica pretreated at 200°C

Mass of silica (mg)	OH[a] (μmol)	Zr (μmol)	Zr / OH	NpH (μmol)	NpH / OH
17.0	14.6			13.5	0.92
20.0	17.2	8.8	0.51	18.5	1.07
20.3	17.5	6.3	0.36	15.9	0.91
32.0	27.5			29.5	1.07
32.3	27.8			31.1	1.12
33.9	29.0			31.0	1.07
35.2	30.3			32.9	1.09
35.3	30.4			26.4	0.87
37.1	31.8			28.6	0.90
					Avg 1.01 ± 0.09

[a] The initial number of hydroxyl groups present is calculated from the known hydroxyl content of Aerosil-200 treated at this temperature (0.86 mmol OH / g silica).[9]

The stoichiometry of the grafting reaction was confirmed by protonolysis. Upon treatment of a 17.0 mg sample of $(\equiv SiO)_2Zr(CH_2C(CH_3)_2)_2$ with tert-butanol, 11.9 μmol of $C(CH_3)_4$ was liberated, compared with 13.5 μmol liberated during grafting. This reaction is shown in equation 3.3.

$$(\equiv SiO)_2Zr(CH_2C(CH_3)_3)_2 + 2\,{}^tBuOH \longrightarrow (\equiv SiO)_2Zr(O^tBu)_2 + 2\,C(CH_3)_4 \qquad (3.3)$$

3.2.2 IR characterization

The IR spectrum of the unmodified silica contains a band at 3747 cm^{-1} assigned to non-hydrogen bonded OH groups, Figure 3.2a. Hydroxyl groups perturbed by hydrogen-bonding are responsible for the shoulder at 3675 cm^{-1}. These are inaccessible to chemical reagents.[10] Reaction with $Zr(CH_2C(CH_3)_2)_4$ resulted in the irreversible disappearance of the sharp band at 3747 cm^{-1}, Figure 3.2b. Only a slight change was observed in the broad shoulder at 3675 cm^{-1}, confirming that these hydrogen-bonded hydroxyls are mostly inaccessible to chemical reagents.[11] The presence of chemisorbed neopentyl ligands is shown by the appearance of C-H stretching bands in the region 3000-2800 cm^{-1}, as well as methyl and methylene deformation modes in the region of 1500-1300 cm^{-1}.

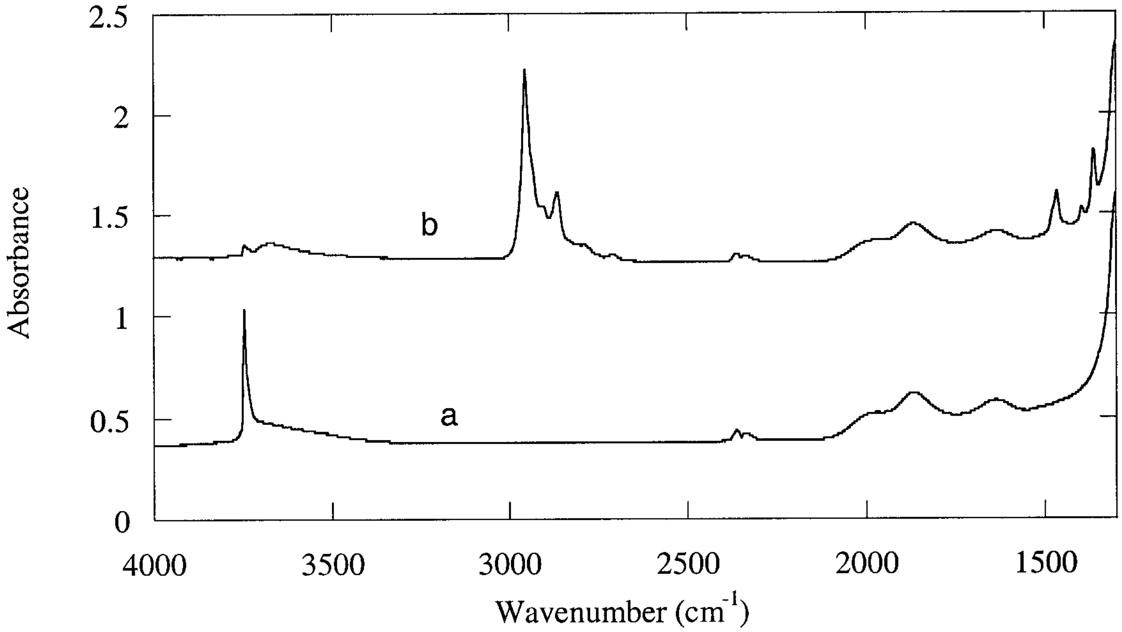

Figure 3.2: IR spectrum of (a) a self-supporting disk of Aerosil 200 partially dehydroxylated at 200 °C; (b) after reaction with excess $ZrNp_4$ followed by desorption of unreacted material.

3.2.3 ^{13}C CP/MAS NMR Spectroscopy

The ^{13}C CP/MAS NMR spectrum of $(\equiv SiO)_2Zr(CH_2C(CH_3)_3)_2$ is shown in Figure 3.3. The peak at 34.1 ppm is assigned to the methyl carbons of the neopentyl ligands, by comparison to the methyl signal of $Zr(CH_2C(CH_3)_3)_4$ (C_6D_6) at 35.1 ppm. The quaternary carbon was not detected, though it was seen at 35.8 ppm in the solution ^{13}C NMR spectrum of $Zr(CH_2C(CH_3)_3)_4$, Figure 3.4. In contrast, signals for both the methyl C and the quaternary C were observed at 35 and 32 ppm, respectively, in the ^{13}C CP/MAS spectrum of $(\equiv SiO)_2Ti(CH_2C(CH_3)_3)_2$.[12]

The broad peak at 95 ppm is attributed to the methylene carbon by comparison to the methylene signal of $Zr(CH_2C(CH_3)_3)_4$ at 103 ppm. Its greater linewidth is ascribed to its greater proximity to the surface and consequent lack of mobility. The shift in the methylene signal from 103 ppm in $ZrNp_4$ to 95 ppm in the silica-supported complex can be explained by the fact that bonding of the Zr atom to the two oxygen atoms of the silica results in a change in the electronic environment of the methylene C atoms.

Figure 3.3 also shows two weak bands at ca. 25 and 85 ppm. In a previous study, a band at 25 ppm was assigned to the methyl carbons of the neopentoxy ligand arising from the insertion of adventitious O_2.[4] Addition of excess O_2 led to the spectrum shown in Figure 3.5, attributed to $(\equiv SiO)Zr(OCH_2C(CH_3)_3)_3$. The signals at 24, 32 and 82 ppm were assigned to the methyl, quaternary and methylene carbons, respectively, by comparison to the spectrum of $Zr(OCH_2C(CH_3)_3)_4$.[13]

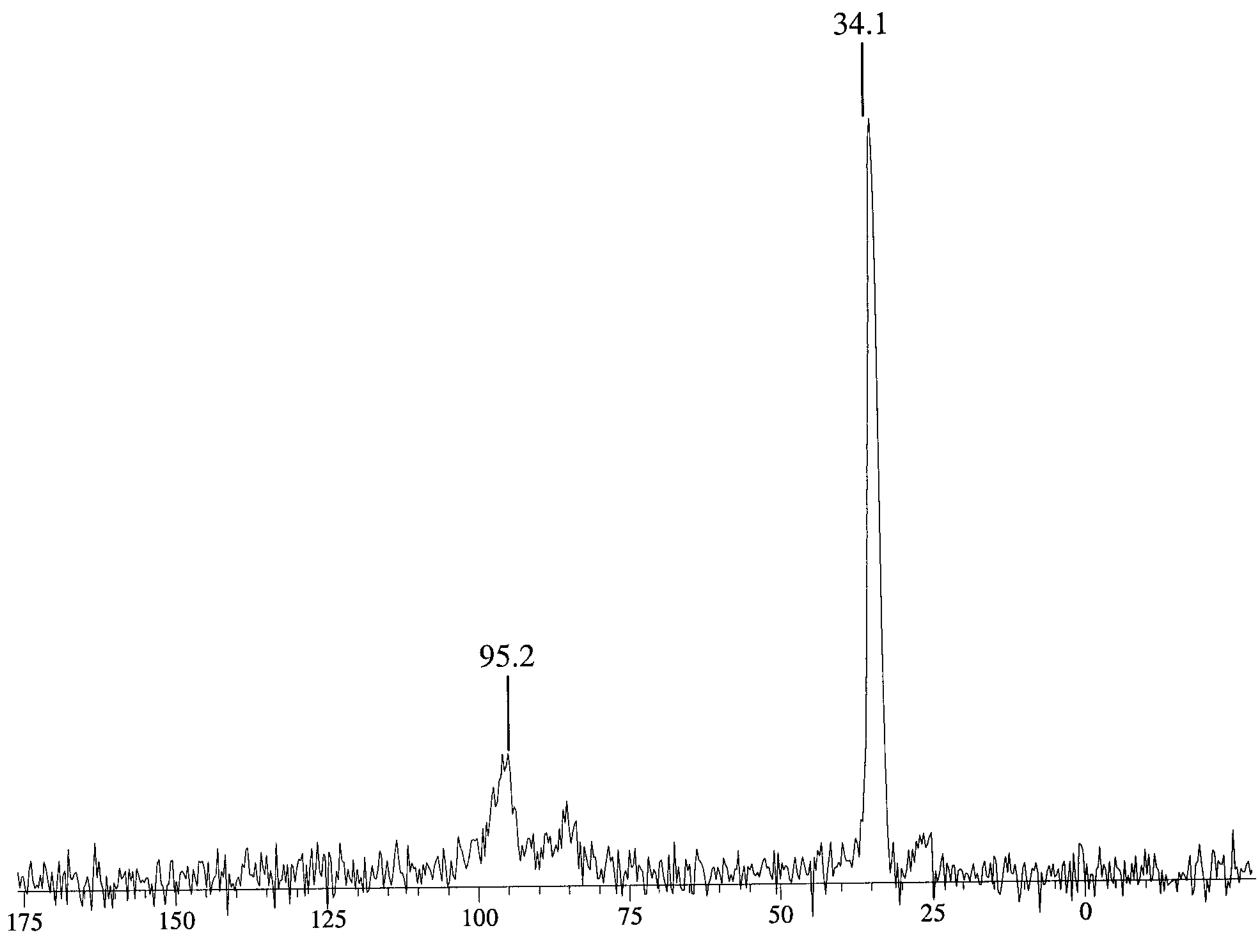

Figure 3.3: ^{13}C CP/MAS NMR spectrum of $(\equiv SiO)_2Zr(CH_2C(CH_3)_3)_2$.

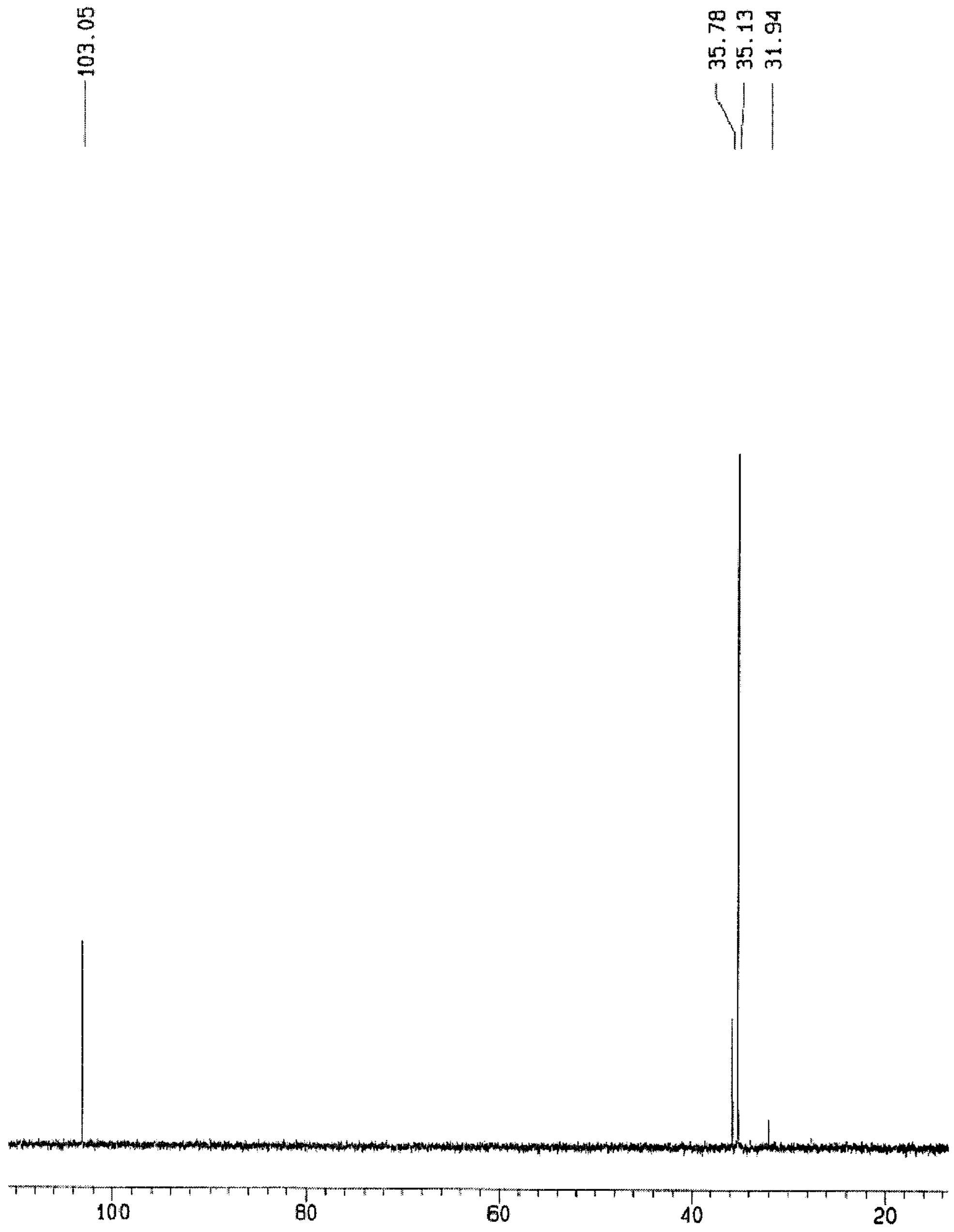

Figure 3.4: ^{13}C NMR spectrum of $Zr(CH_2C(CH_3)_3)_4$ in C_6D_6.

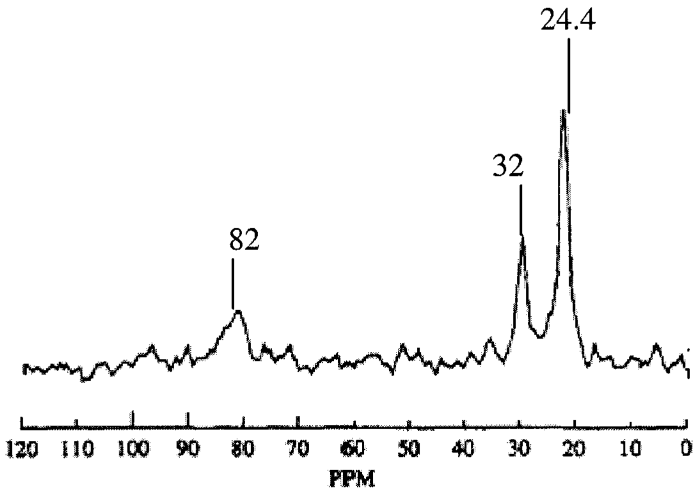

Figure 3.5: ^{13}C CP/MAS NMR spectrum of $(\equiv SiO)Zr(OCH_2C(CH_3)_3)_2)_3$.[4]

3.2.4 X-ray absorption spectroscopy

The XAS spectrum of $(\equiv SiO)_2Zr(CH_2C(CH_3)_3)_2$ is shown in Figure 3.6. In the XANES region, a difference of ca.18 eV was recorded between the K-edge (that is, the transition that causes ejection of the innermost 1s electron)[14] of $(\equiv SiO)_2Zr(CH_2C(CH_3)_3)_2$ and that of a Zr foil (used as reference, with a K-edge energy of 17,997.6 eV). This shift is indicative of a +IV oxidation state of Zr, as shown by studies of the authentic Zr(IV) solids ZrO_2, $Zr(SO_4)_2.4H_2O$ and $ZrSiO_2$, all of which were shown to have a K-edge of ca. 18 eV.[15,16]

The Fourier transformed EXAFS region is shown in Figure 3.7. The simulated EXAFS spectrum of $(\equiv SiO)_2Zr(CH_2C(CH_3)_3)_2$ is superimposed. Structural parameters obtained from a single scatterer curve fit are shown in Table 3.2. The fit is consistent with a first coordination sphere consisting of two O neighbors at 1.94 Å and two C neighbors at 2.24 Å. The latter distance is within the range of typical Zr-C bonds and is comparable to the Zr-C distances in $Zr(CH_2Ph)_4$, (2.23, 2.26, 2.28 and 2.29 Å).[17] The Zr-O distance of 1.94 Å is similar to previously reported values for siloxyzirconium complexes (e.g., 1.91 Å in $(DME)ZrCl_2(OSiPh_3)_2)$[18] and hydroxyl complexes (1.95 Å in $Cp^*{}_2Zr(OH)Cl$).[19] The EXAFS study of $(\equiv SiO)Zr(CH_2C(CH_3)_3)_3$ described above found one O neighbor at 1.96 Å and three C neighbors at 2.22 Å.[8]

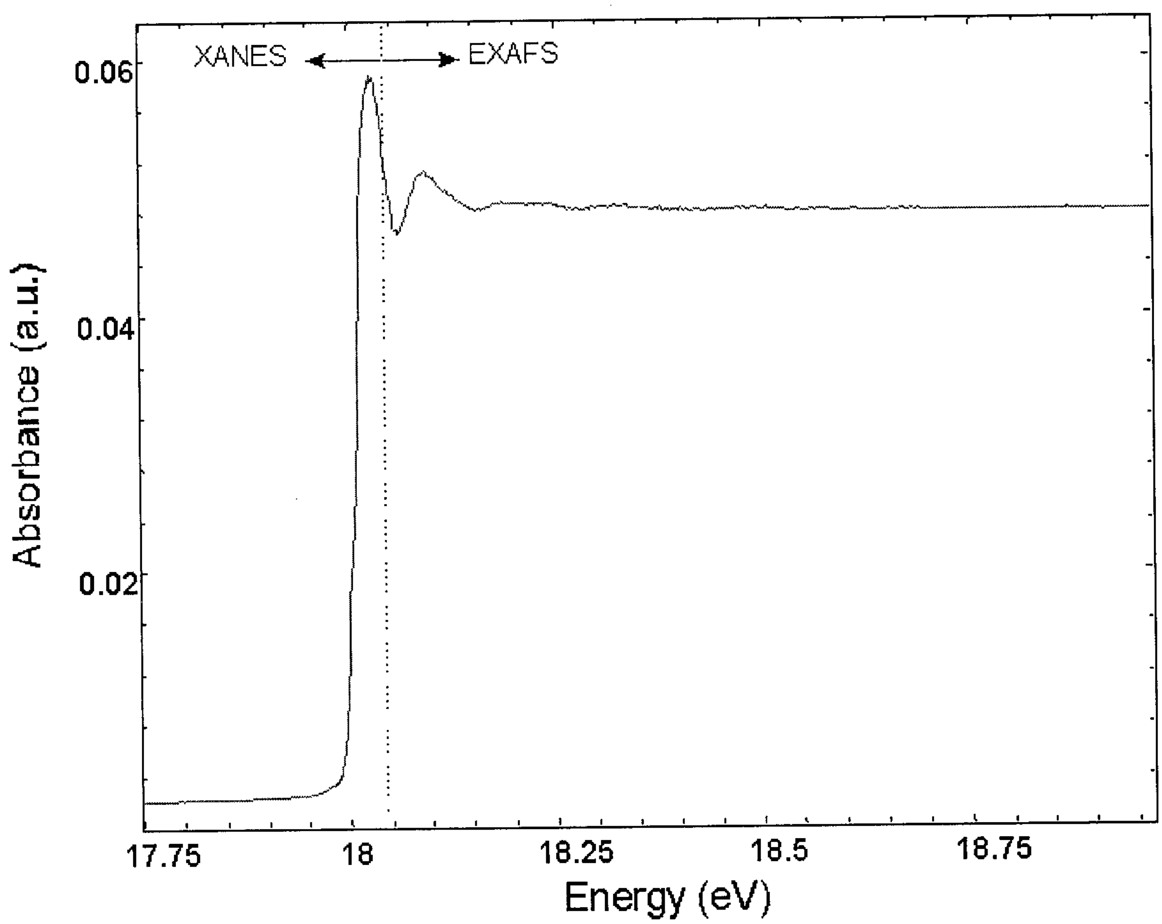

Figure 3.6: K-edge X-ray absorption spectrum of $(\equiv SiO)_2Zr(CH_2C(CH_3)_3)_2$.

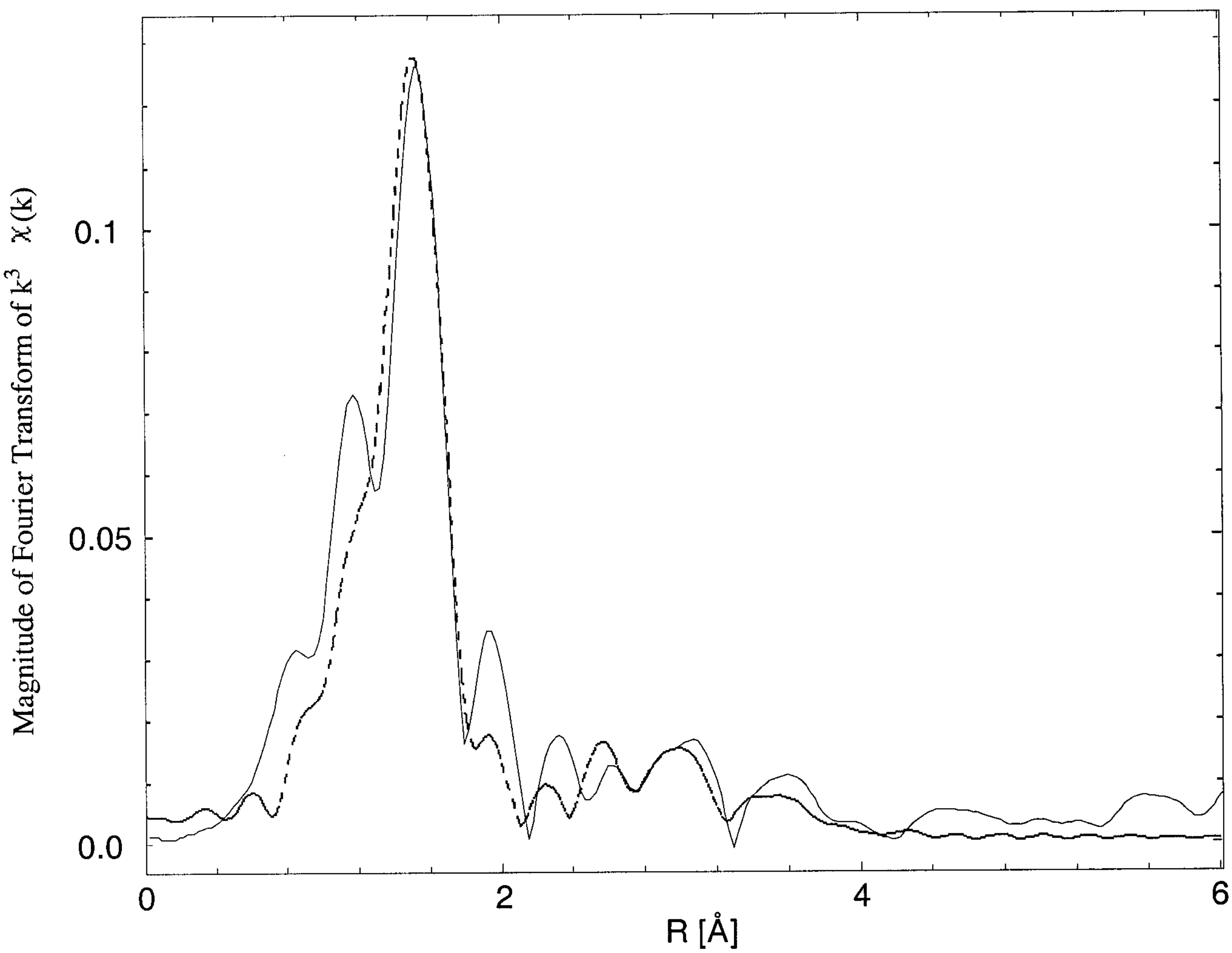

Figure 3.7: Fourier transformed EXAFS of $(\equiv SiO)_2Zr(CH_2C(CH_3)_3)_2$ (solid line) and simulated EXAFS spectrum (dashed line).

Table 3.2. Structural parameters of $(\equiv SiO)_2(ZrCH_2C(CH_3)_3)_2$ from EXAFS fit

Shell	Coordination number	Distance (Å)	σ^2
Zr-O	2	1.94	0.00024
Zr-C	2	2.24	0.00454
Zr-Si	2	3.12	0.0087
Zr-O	1	3.43	0.00932
Zr-C	2	3.32	0.01

The second coordination sphere was also refined. Two quaternary C atoms were fitted at 3.32 Å, compared to 3.42 Å in $(\equiv SiO)Zr(CH_2C(CH_3)_3)_3$. Two silicon neighbors at 3.12 Å were found, corresponding to the siloxide silicons. Finally, a second shell O was fitted at 3.43 Å. This may be the siloxane oxygen in the surface directly beneath Zr. All these findings are consistent with the structure shown below.

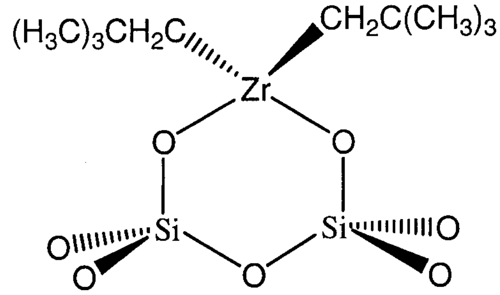

3.3 Discussion

When $Zr(CH_2C(CH_3)_3)_4$ is grafted on Aerosil 200 pretreated at 200°C by sublimation (this work) or from solution,[2] $(\equiv SiO)_2Zr(CH_2C(CH_3)_3)_2$ is formed. The 2:1 stoichiometry of reaction with surface hydroxyl groups was established by analysis of the maximum Zr loading as well as the ratio of neopentane formed in grafting and in the subsequent protonolysis reaction with tert-butanol. IR spectroscopy was a very useful tool in monitoring the grafting reaction, both for measuring the amount of neopentane formed in the gas phase and following the disappearance of the OH band at 3747 cm^{-1}, and the appearance of ν(C-H) bands in the region of 2800-3000 cm^{-1}. ^{13}C CP/MAS NMR spectroscopy confirmed the formation of organozirconium surface fragments, as well as the purity of the grafted complex, since formation of neopentoxy groups was easily detected in the ^{13}C spectrum, with bands at ca. 25, 32 and 84 ppm. The EXAFS fit supports the proposed formulation, with a first shell consisting of two O atoms and two C atoms, and a second shell of two quaternary C and two Si atoms.

Our results also provide evidence that there is no transfer of the neopentyl groups to the silica surface via the cleavage of the siloxane bonds, as shown in equations 3.5 and 3.6.

$$\equiv SiOSi\equiv + Zr(CH_2C(CH_3)_3)_4 \longrightarrow \equiv SiOZr(CH_2C(CH_3)_3)_3 + \equiv SiCH_2C(CH_3)_3 \quad (3.5)$$

$$\equiv SiOSi\equiv + \equiv SiOZr(CH_2C(CH_3)_3)_3 \longrightarrow (\equiv SiO)_2Zr(CH_2C(CH_3)_3)_2 + \equiv SiCH_2C(CH_3)_3 \quad (3.6)$$

In the next chapters, the thermal stability of $(\equiv SiO)_2Zr(CH_2C(CH_3)_3)_2$ will be discussed, as well as its reactivity towards olefin polymerization.

3.4 References

(1) Ballard, D. G. H. *Adv. Catal.* **1973**, *23*, 263-325.

(2) Schwartz, J.; Ward, M. D. *J. Mol. Catal* **1979**, *12*, 465-469.

(3) Quignard, F.; Choplin, A.; Basset, J.-M. *J. Chem. Soc., Chem. Commun.*, **1991**, 1589-1590.

(4) Quignard, F.; Lecuyer, C.; Bougault, C.; Lefebvre, F.; Choplin, A.; Olivier, D.; Basser, J.-M. *Inorg. Chem.* **1992**, *31*, 928-930.

(5) Quignard, F.; Lecuyer, C.; Choplin, A.; Olivier, D.; Basset, J.-M. *J. Mol. Catal* **1992**, *74*, 353-363.

(6) Marks, T. J.; Ahn, H. *J. Am. Chem. Soc.* **2002**, *124*, 7103.

(7) Coperet, C.; Chabanas, M.; Saint-Arroman, R. P.; Basset, J.-M. *Angew. Chem. Int. Ed.* **2003**, *42*, 156-181.

(8) Corker, J.; Lefebvre, F.; Lecuyer, C.; Dufaud, V.; Quignard, F.; Choplin, A.; Evans, J.; Basset, J.-M. *Science* **1996**, *271*, 966-969.

(9) Rice, G. L.; Scott, S. L. *Langmuir* **1997**, *13*, 1545.

(10) Amor Nait Ajjou, J.; Scott, S. L. *Organometallics* **1997**, *16*, 86-92.

(11) Morrow, B. A. *Stud. Surf. Sci. Catal.* **1990**, *57A*, 161-224.

(12) Beaudoin, M. C.; Womiloju, O.; Fu, A.; Amor Nait Ajjou, J.; Rice, G. L.; Scott, S. L. *J. Mol. Catal.* **2002**, *190*, 159-169.

(13) Davidson, P. J.; Lappert, M. F.; Pearce, R. *J. Organomet. Chem.* **1973**, *57*, 269-277.

(14) Rehr, J. J.; Albers, R. C. *Rev. Mod. Phy.* **2000**, *3*, 621.

(15) Greegor, R. B.; Blohowiak, K. Y.; Osborne, J. H.; Krienke, K. A.; Cherian, J. T. *J. Sol-Gel Sci. Tech.* **2001**, *20*, 35-50.

(16) Gavin, M.; Pickup, D.; Anderson, R.; Wallidge, G. W.; Holland, M. A.; Newport, R. J.; Smith, M. E. *Phys. Chem. Chem. Phys* **2000**, *2*, 2455-2460.

(17) Davies, G. R.; Jarvis, J. A. J.; Kilbourn, B. T.; Pioli, A. J. P. *J. Chem. Soc.,Chem. Comm.* **1971**, 677.

(18) Babaian, E. A.; Hancir, D. C.; Bott, S. G.; Atwood, J. L. *Inorg. Chem.* **1986**, *25*, 4818.

(19) Bartolin, R.; Patel, V.; Munday, I.; Taylor, N. J.; Carty, A. J. *J. Chem. Soc., Chem. Comm.* **1985**, 456.

Chapter 4

Thermolysis of silica-supported bis(neopentyl)zirconium (IV)

4.1 Introduction

Transition metal alkylidene complexes continue to generate huge interest as active sites in catalysts for reactions such as alkene metathesis, ring-opening metathesis polymerization, ring closing metathesis, and so on.[1] Many alkylidene complexes of Group V and VI metals have been fully characterized.[1] The first high oxidation state transition metal complex with a metal-carbon multiple bond to be synthesized was the alkylidene $(Me_3CCH_2)_3Ta{=}CHCMe_3$, reported in 1974.[2] Since then, numerous Ta alkylidene complexes as well as other Groups V and VI alkylidene complexes have been synthesized and characterized. Ta and Nb alkylidene complexes are very effective in Wittig-like reactions.[3] Because of the predominance of α-H abstraction processes in Groups V and VI, many alkylidene complexes of these metals have been synthesized using this method.[4]

Alkylidene complexes of Group IV metals are still comparatively rare, though they have been detected as short-lived intermediates in many reactions.[5,6] In many cases, phosphine ligands have been used to trap the alkylidenes.[7] The failure to isolate alkylidene complexes involving Group IV metals has been attributed to intramolecular processes such as C-H activation that take place after their formation, as shown in the example below (equation 4.1).

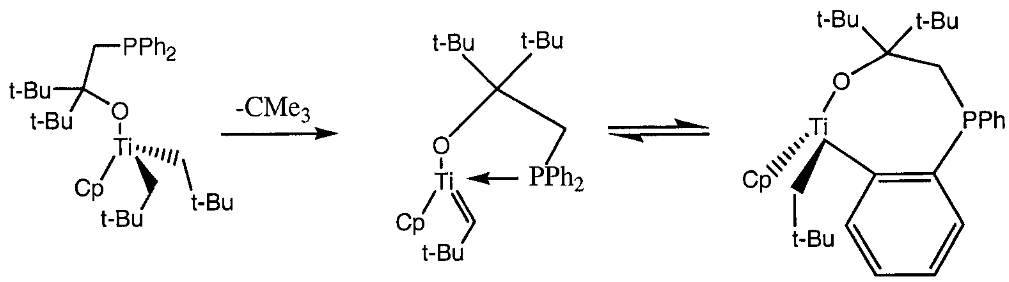

(4.1)

Though attempts to isolate a zirconium alkylidene complex via α-H abstraction started in the 1970s,[8] it was only in 1993 that Fryzuk and coworkers synthesized the first Zr(IV) alkylidene, [η^5-C_3H_5-1,3-($SiMe_2CH_2P^iPr_2$)$_2$]Zr=CHPh(Cl), by this route.[6] This benzylidene complex was characterized by X-ray crystallography, which revealed a Zr-C distance of 2.024(4) Å. The generality of the reaction was then extended towards the synthesis of other alkylidenes such as [P_2Cp]Zr=$CHEMe_3$(Cl) (E = C, Si) and [P_2Cp]Zr=CHPh(Cl).[9,10] The alkylidene C is characterized by a triplet at 225 ppm in the $^{13}C\{^1H\}$ NMR spectrum. These alkylidenes have also been studied for their reactivity towards reagents like C_2H_4, CO and CN^tBu.

Several well-defined supported metal alkylidene complexes have been characterized on thermally treated silica.[11] (≡SiO)Ta(=CHC(CH_3)$_3$)($CH_2C(CH_3)_3$)$_2$ and (≡SiO)$_2$Ta(=CHC(CH_3)$_3$)($CH_2C(CH_3)_3$) were reported in a 1:1 ratio when Ta(=CHC(CH_3)$_3$)($CH_2C(CH_3)_3$)$_3$ was grafted by sublimation onto silica partially dehydroxylated at 500 °C .[12,13] The supported complexes were characterized using a combination of elemental analyses, IR, ^1H and ^{13}C CP/MAS spectroscopy. However, the alkylidene C was not detected in the ^{13}C NMR spectrum. Marks and co-workers later located the alkylidene carbon signal at 247 ppm in the ^{13}C CP/MAS NMR spectrum, by grafting Ta(^{13}CHC(CH_3)$_3$)$_3$($^{13}CH_2C(CH_3)_3$)$_3$ on silica.[14]

Amor Nait Ajjou and coworkers synthesized $(\equiv SiO)_2Cr{=}CHC(CH_3)_3$ by thermally-induced α-H elimination, equation 4.2.[15]

$$(\blacksquare SiO)_2Cr(CH_2C(CH_3)_3)_2 \xrightarrow{69\ ^{o}C} (\blacksquare SiO)_2Cr{=}CHC(CH_3)_3 + C(CH_3)_4 \qquad (4.2)$$

Formation of the alkylidene complex was confirmed by a selective D-labelling experiment. Thermolysis of $(\equiv SiO)_2Cr(CD_2C(CH_3)_3)_2$ resulted in the formation of $C(CH_3)_3(CD_3)$ and a kinetic isotope effect k_H/k_D of 2.8. Further evidence for the presence of $(\equiv SiO)_2Cr{=}CHC(CH_3)_3$ was provided by its reactions with styrene, bromine and acetone. $(\equiv SiO)_2Cr{=}CHC(CH_3)_3$ reacts with styrene via metathesis to form neohexene, equation 4.3.

$$(\equiv SiO)_2Cr{=}CHC(CH_3)_3 + PhCH{=}CH_2 \rightarrow (\equiv SiO)_2Cr{=}CHPh + CH_2{=}CHC(CH_3)_3 \qquad (4.3)$$

Electrophilic cleavage of the neopentylidene ligand with bromine resulted in the formation of $C(CH_3)_3(CBr_2H)$, equation 4.4.

$$(\equiv SiO)_2Cr{=}CHC(CH_3)_3 + Br_2 \rightarrow C(CH_3)_3(CHBr_2) + (\equiv SiO)_2CrBr_2 \qquad (4.4)$$

With acetone, $(CH_3)_2C{=}CH(CH_3)_3$ was formed by a pseudo-Wittig reaction, equation 4.5.

$$(\equiv SiO)_2Cr{=}CHC(CH_3)_3 + (CH_3)_2C{=}O \rightarrow \text{“}(\equiv SiO)_2Cr{=}O\text{”} + (CH_3)_2C{=}CHC(CH_3)_3 \qquad (4.5)$$

Similar α-H abstraction chemistry was also observed for $(\equiv SiO)_2Cr(CH_2Si(CH_3)_3)_2$,[15] $(\equiv SiO)_2Ti(CH_2C(CH_3)_3)_2$[11] and $(\equiv SiO)_2V(CH_2Si(CH_3)_3)_2$.[15]

A possible competing reaction to α-H elimination is γ-hydrogen elimination, which results in the formation of a metallacyclobutane, Scheme 4.1.

Scheme 4.1: Competing C-H activation reactions in bis(alkyl) metal complexes

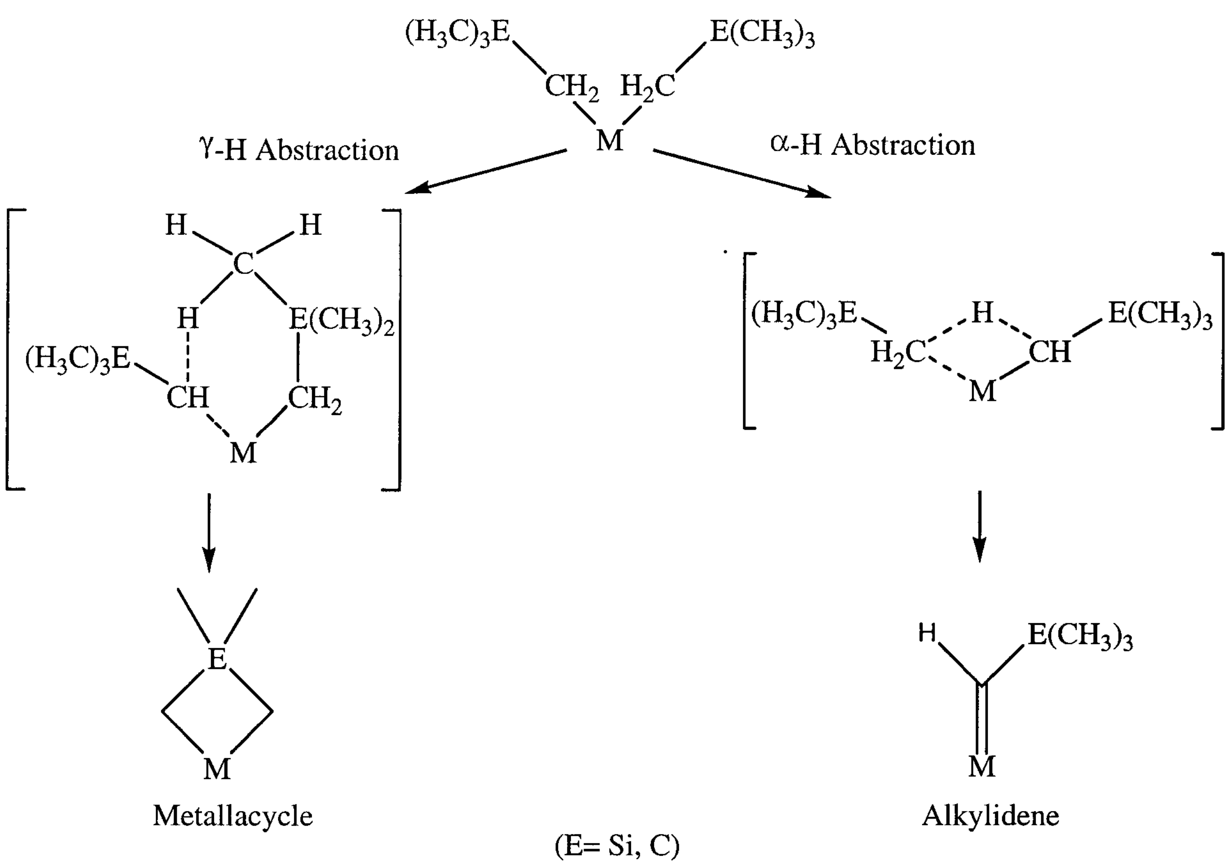

Thermolysis of homoleptic metal alkyls is also of interest because of its potential application in the chemical vapor deposition (CVD) of metal carbide films.[16,17] The use of metal alkyls as precursors has been found to overcome many of the shortcomings of binary metal halides such as halide impurities in the final material and low vapor pressures of some of the halides. Deposition of ZrC on a variety of surfaces using $Zr(CH_2C(CH_3)_3)_4$ has been found to occur at temperatures above 500 °C and pressures as low as 10^{-4} Torr. The morphology of the films was determined to be crystalline by X-ray diffraction, while x-ray photoelectron spectra of the films correspond to standard zirconium carbide spectra.

Girolami and co-workers investigated CVD of TiC from $Ti(CH_2C(CH_3)_3)_4$.[18] They showed that the α-H elimination pathway is favored over γ-H abstraction since it is easier for the small Ti(IV) centre to achieve the former transition state.[18,19] Xue and co-workers examined the pathway for thermolysis of $ZrNp_4$ using a combination of computational and experimental studies.[20] Since the Zr-C bond is longer than the Ti-C bond, the metal centre is less crowded. The energies of the transition states for α-H and γ-H abstraction were compared; the latter was favored by 5.2 kcal/mol. Experimental evidence for the preference for γ-H abstraction was provided by chemical vapor deposition (CVD) of $Zr(CH_2C(CH_3)_3)_4$ and $Zr(CD_2C(CH_3)_3)_4$ at temperatures from 400-500 °C, and base pressures of ca. 10^{-4}-10^{-5} Torr. When the volatile reaction products were analyzed, it was found $ZrNp_4$-d_8 gave predominantly $C_5H_{10}D_2$ (59%), indicative of a γ-H abstraction pathway, since α-H abstraction should have resulted in the formation of a large amount of $C_5H_9D_3$.

This chapter will describe the thermolysis of $(\equiv SiO)_2Zr(CH_2C(CH_3)_3)_2$ and the characterization of its product.

4.2 Thermolysis of $(\equiv SiO)_2Zr(CH_2C(CH_3)_3)_2$

When silica-supported bis(neopentyl)zirconium(IV) was thermolyzed at 120 ^{o}C using a preheated oven, a color change from white to orange was observed and neopentane was liberated into the gas phase. The progress of the reaction was monitored in situ by gas phase IR spectroscopy. Spectra of the neopentane product were recorded at regular intervals until no further changes were obtained. IR spectra of the Zr-modified silica recorded at room temperature before and after thermolysis were also compared.

In all experiments, the amount of neopentane formed during thermolysis of $(\equiv SiO)_2Zr(CH_2C(CH_3)_3)_2$ was (0.49 ± 0.02) of the amount formed during grafting of $Zr(CH_2C(CH_3)_3)_4$ on silica (Table 4.1). Neopentane was furthermore confirmed to be the only volatile product of thermolysis by GC/MS. The IR spectrum of $(\equiv SiO)_2Zr(CH_2C(CH_3)_3)_2$ underwent a change in the region 2800-3000 cm^{-1}, corresponding to the ν(CH) modes. (50.9 ± 1.1) of the integrated ν(CH) intensity was lost (Figure 4.1), although the general shapes of the peaks remained unchanged.

^{13}C CP/MAS NMR spectroscopic analysis of $(\equiv SiO)_2Zr{=}CHC(CH_3)_3$ was attempted. No alkylidene C was detected. However this is not unexpected. Beaudoin and co-workers did not observe the alkylidene C of $(\equiv SiO)_2Ti(CH_2C(CH_3)_3)_2$ in its natural abundance ^{13}C CP/MAS NMR spectrum.[11] This was attributed to its low cross-polarization efficiency and rigidity. The same was observed with Basset's $(\equiv SiO)_2Ta(=CHC(CH_3)_3)(CH_2C(CH_3)_3)$.[12,13] It was only by using a ^{13}C enriched sample, $(\equiv SiO)_2Ta(^{13}CHC(CH_3)_3)(^{13}CH_2C(CH_3)_3)_3$, that Marks and coworkers were successful in locating the alkylidene carbon signal at 247 ppm.[11]

4.3 Kinetics of thermolysis

A kinetic study of neopentane extrusion was undertaken at 125 °C. A plot of the integrated absorbance of the ν(C-H) region (2800-3000 cm^{-1}) vs time is shown in Figure 4.2 for a 35.2 mg pellet of $(\equiv SiO)_2Zr(CH_2C(CH_3)_3)_2$. The solid line shows the fit to the first-order integrated rate equation with k= (0.00191 ±0.00004) min^{-1}. Figure 4.3 shows the kinetic data recorded for the thermolysis performed at 121 °C with a 32.0 mg pellet.

First order rate constants were determined at temperatures from 113-125 °C. In all cases, first order behavior was observed. The rate constants are tabulated in Table 4.2. This data was used to construct the Eyring plot shown in Figure 4.4. It is linear over this temperature range with slope = (-10714 ± 330) and y-intercept = (10.48 ± 0.84)

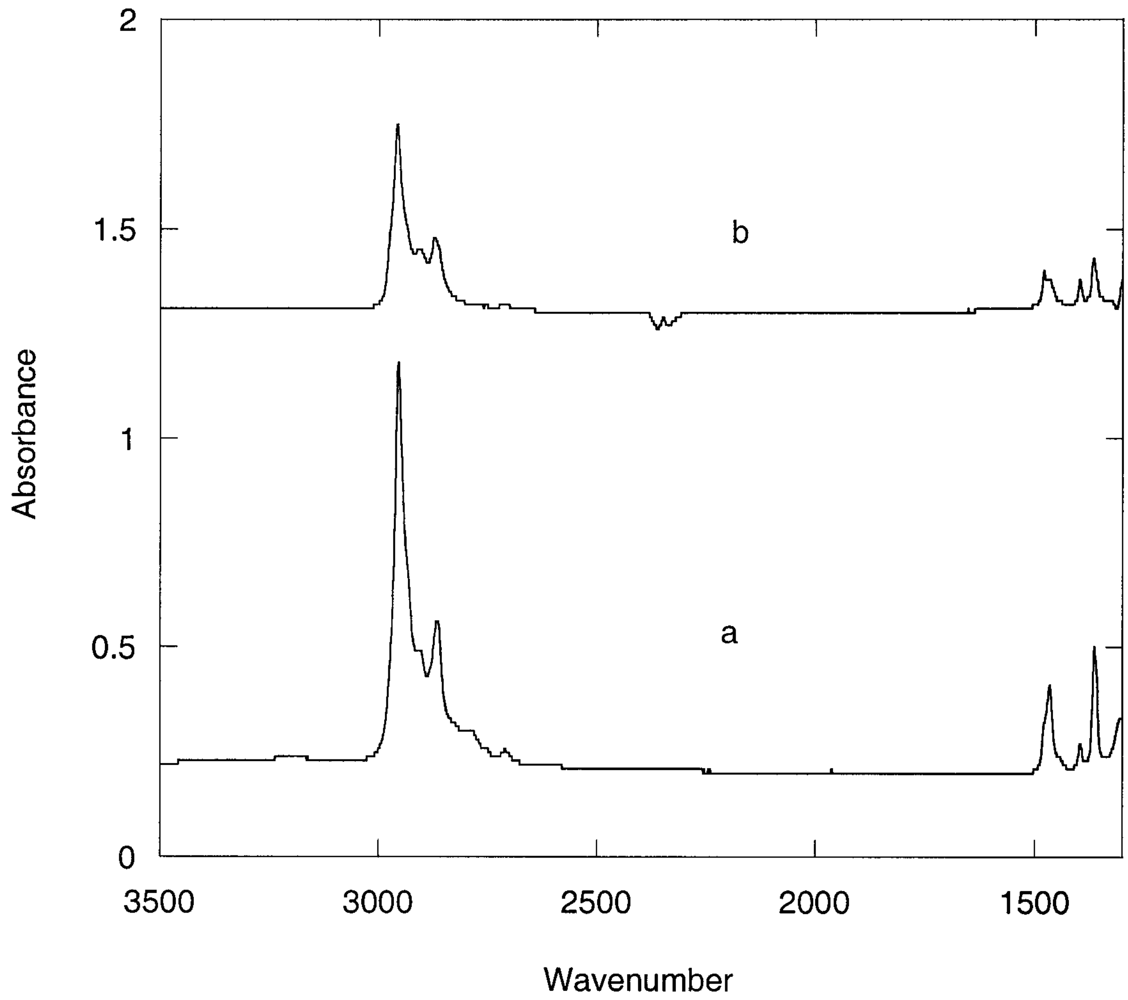

Figure 4.1: Difference spectra of $(\equiv SiO)_2Zr(CH_2C(CH_3)_3)_2$ (a) before and (b) after thermolysis at 125 °C for 25 hrs. The IR spectrum of the silica support was removed by spectral subtraction and the spectra offset.

Table 4.1: Quantitative analysis of the loss in integrated ν(CH) intensity and yield of NpH formed during the thermolysis of $(\equiv SiO)_2Zr(CH_2C(CH_3)_3)_2$.

Mass of silica (mg)	NpH formed in grafting (μmol)	% loss of surface ν(CH)	NpH formed in thermolysis (μmol)	Ratio of NpH thermolysis / grafting
20.3	15.9	49.9	7.4	0.46
32.0	29.5	52.5	15.3	0.51
32.3	31.1	51.2	15.7	0.50
33.9	31.0	50.3	14.9	0.48
35.2	32.9	48.9	16.5	0.51
35.3	26.4	52.9	12.8	0.49
37.1	28.6	50.6	13.6	0.47
		Average 50.9 ± 1.1		Average 0.49 ± 0.02

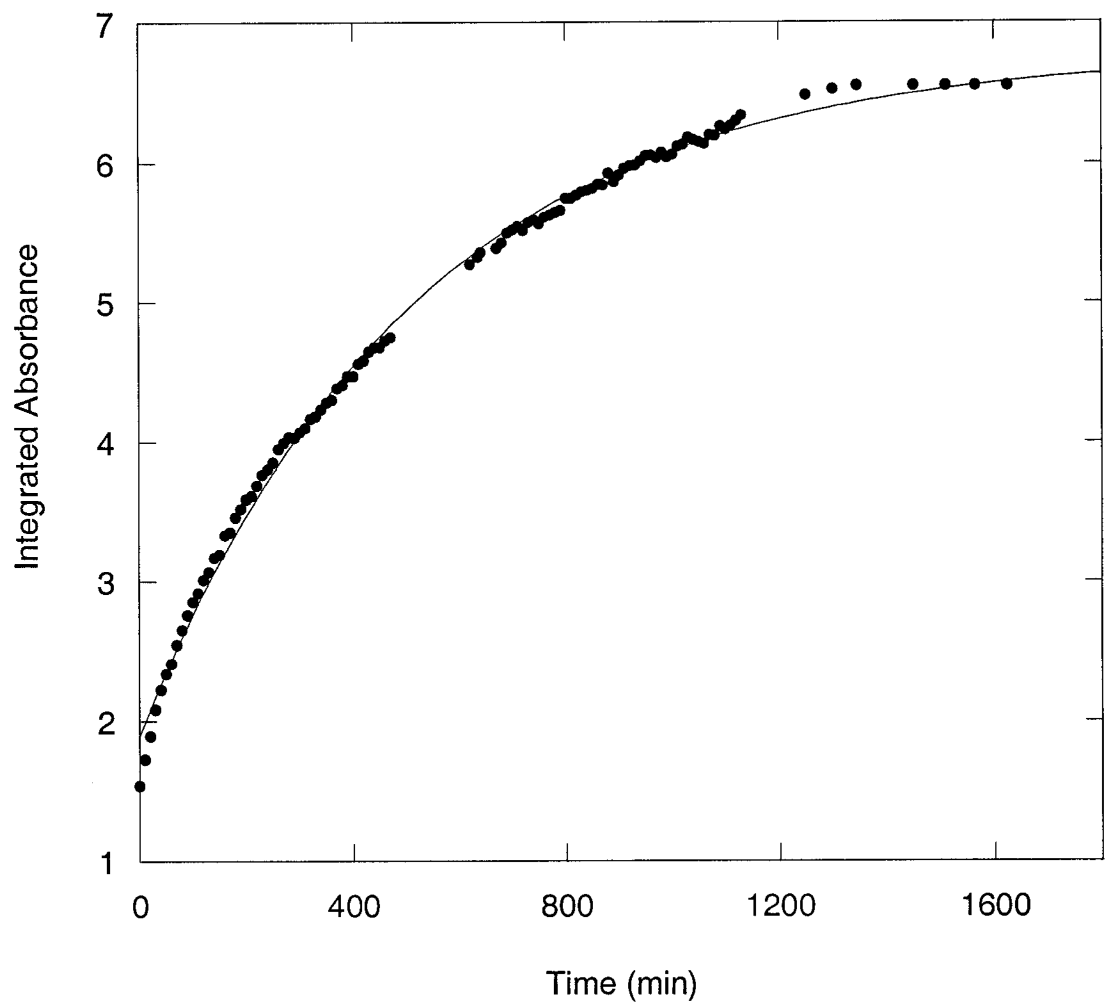

$A_t = A_\infty + (A_0 - A_\infty)\exp(-k_{app}t)$		
	Value	Error
A_∞	6.79	0.04
A_o	1.89	0.03
k_{app}	0.00191	0.00004
R	0.998	NA

Figure 4.2: Time-resolved evolution of $C(CH_3)_4$ from $(\equiv SiO)_2Zr(CH_2C(CH_3)_3)_2$ at 125 °C, monitored as the integrated absorbance of the in situ gas phase IR spectrum in the ν(C-H) region (2800-3000 cm^{-1}).

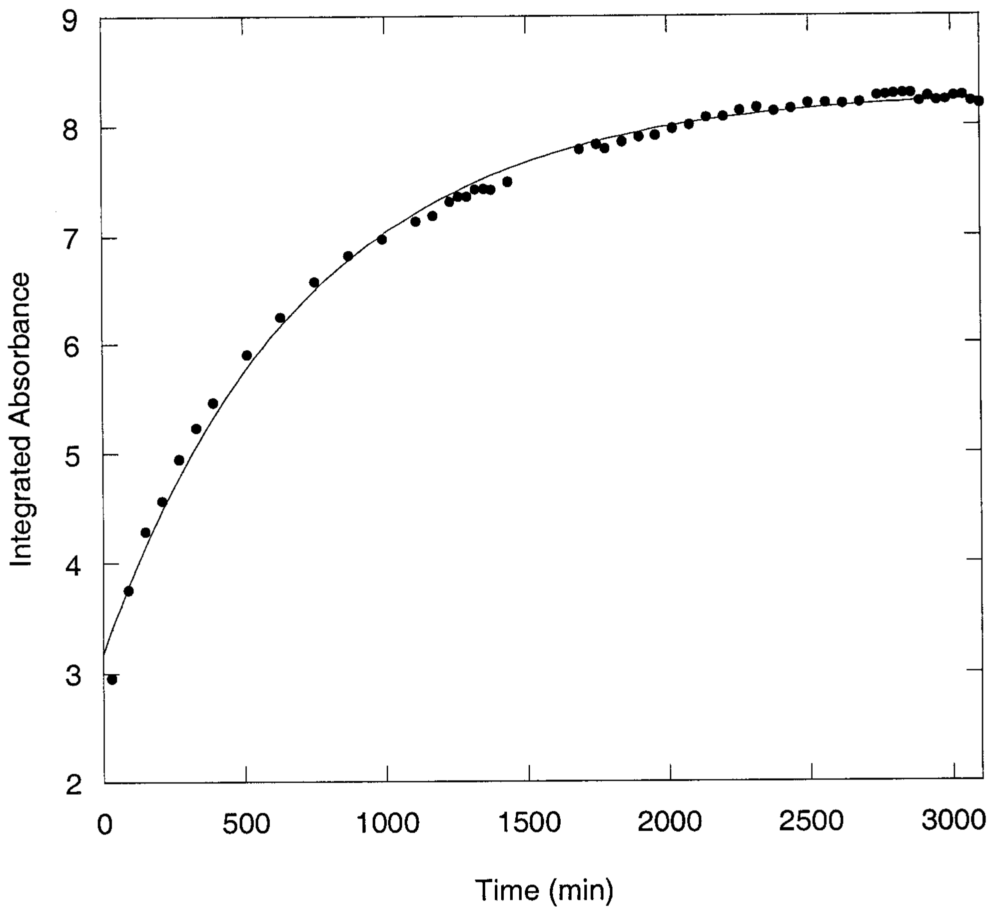

$A_t = A_\infty + (A_0 - A_\infty)\exp(-k_{app}t)$		
	Value	Error
A_∞	8.31	0.03
A_o	3.18	0.06
k_{app}	0.00126	0.00005
R	0.997	NA

Figure 4.3: Time-resolved evolution of $C(CH_3)_4$ from $(\equiv SiO)_2Zr(CH_2C(CH_3)_3)_2$ at 121 °C, monitored as the integrated absorbance of the in situ gas phase IR spectrum in the ν(C-H) region (2800-3000 cm^{-1}).

Table 4.2: Rate constants (k) for the thermolysis of $(\equiv SiO)_2Zr(CH_2C(CH_3)_3)_2$ at different temperatures.

Temperature (°C)	10^3 k (min^{-1})
125	1.91
121	1.26
113	0.66

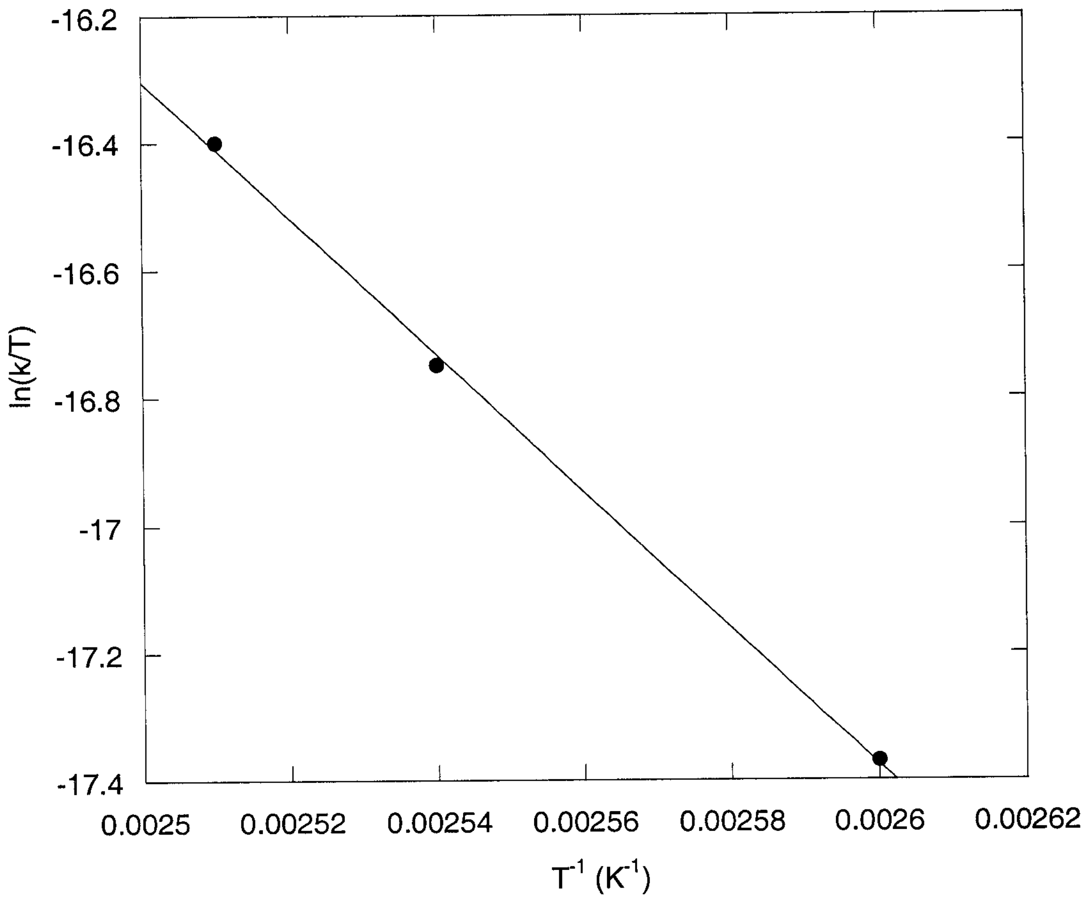

Figure 4.4: Eyring plot for the thermolysis of $(\equiv SiO)_2Zr(CH_2C(CH_3)_3)_2$

4.4 X-Ray absorption spectroscopy

The XANES spectrum of $(\equiv SiO)_2Zr{=}CHCMe_3$ is shown in Figure 4.5. The K-edge is shifted 17 eV from the foil edge, consistent with the presence of Zr(IV). Therefore we conclude that reduction of Zr during thermolysis of $(\equiv SiO)_2Zr(CH_2CMe_3)_2$ is unlikely. A Zr(III) site would be expected to show an edge shift closer to 14 eV.[21] The pre-edge structure and intensity are comparable to that of $(\equiv SiO)_2Zr(CH_2CMe_3)_2$, suggesting a similar site symmetry. No other discernable features were apparent in the XANES region.

The Fourier transformed EXAFS of $(\equiv SiO)_2Zr{=}CHCMe_3$ is shown in Figure 4.6. Comparison to the EXAFS of $(\equiv SiO)_2Zr(CH_2CMe_3)_2$ (Figure 3.7) reveals subtle differences. There are slight radial distribution shifts for the prominent peaks around 2 Å and intensity variations in the paths longer than 2 Å.

Fitting the spectra with an electronic model of $(\equiv SiO)_2Zr{=}CHCMe_3$ gave reasonable results. The model was first constructed as a trigonal planar species and fitted with one alkylidene carbon at 2.05 Å and two siloxide oxygens at 1.90 Å.

A second model of $(\equiv SiO)_2Zr{=}CHC(CH_3)_3$ was constructed with a siloxane oxygen coordinated to the zirconium centre. Amor Nait Ajjou *et al.* previously suggested that surface siloxane sites participate and promote alkylidene formation.[15] Calculations confirm that alkylidene sites on silica surfaces are stabilized by siloxane interactions.[22] Figure 4.7 shows the coordinated siloxane model fit to the data. The siloxane oxygen is fit at 2.14 Å. This model has a much better refinement to the data, with smaller associated Debye-Waller factors (Table 4.3).

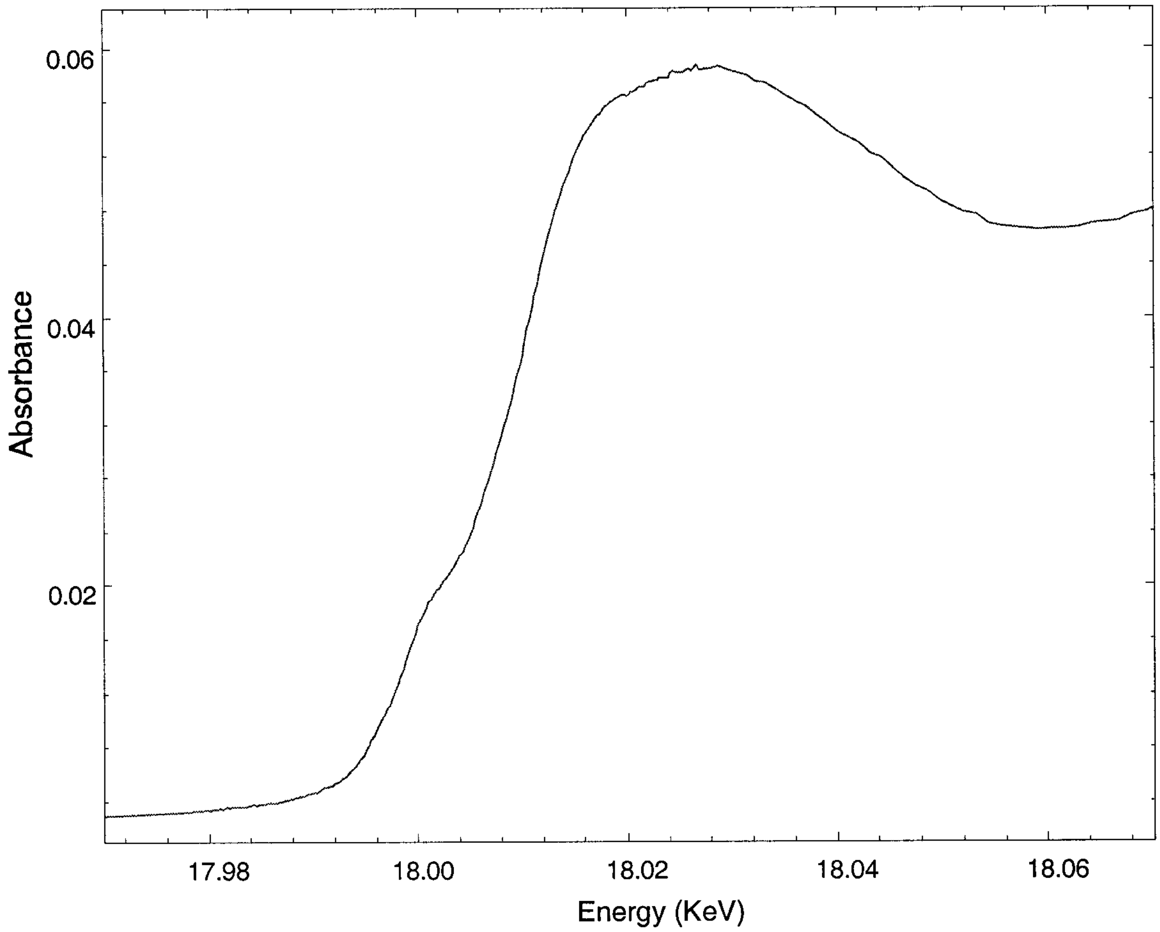

Figure 4.5: XANES spectrum of $(\equiv SiO)_2Zr{=}CHCMe_3$.

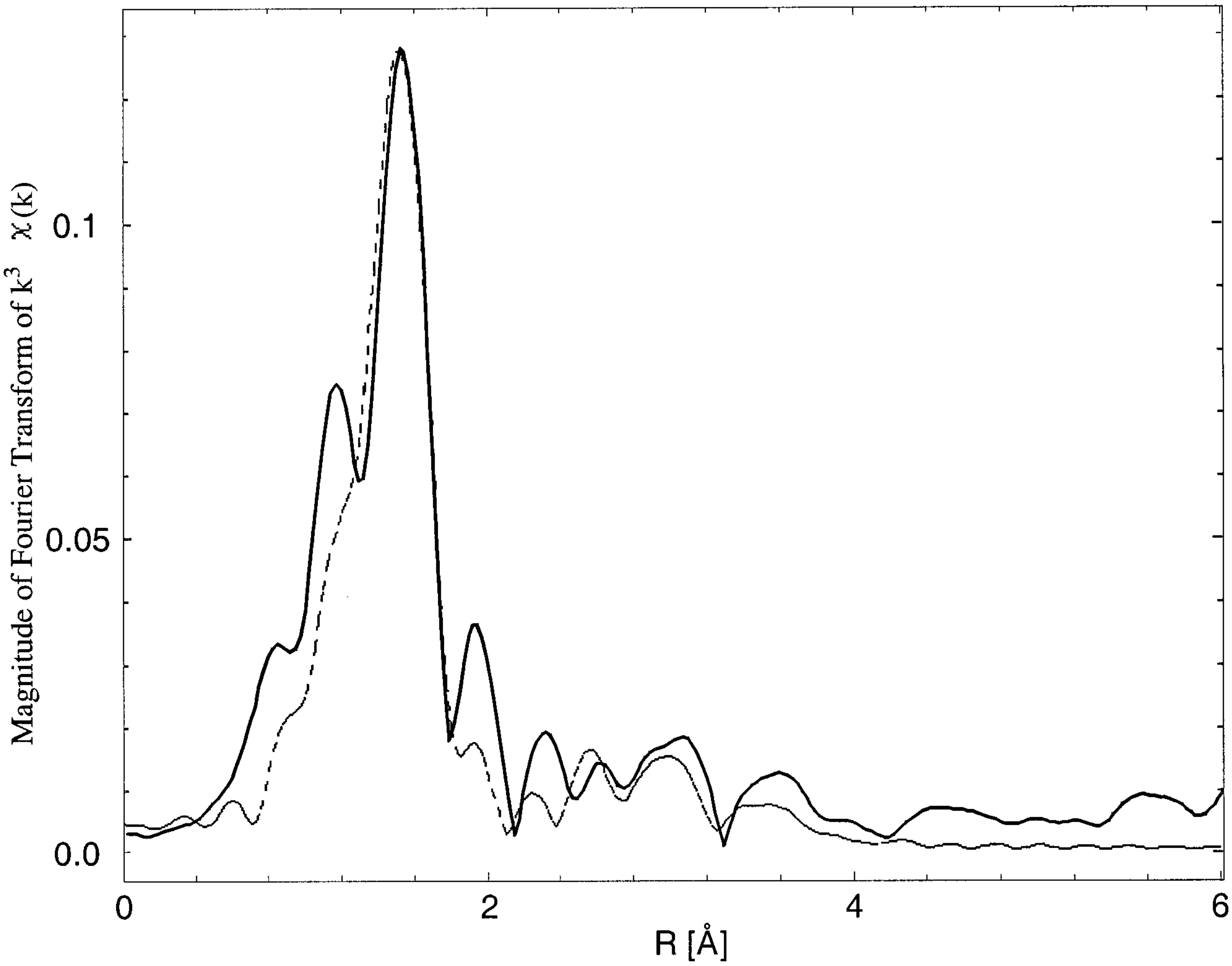

Figure 4.6: a) Fourier transformed EXAFS region of $(\equiv SiO)_2Zr{=}CHC(CH_3)_3$ (solid line), simulated EXAFS spectrum of $(\equiv SiO)_2Zr{=}CHC(CH_3)_3$ (dashed line).

Table 4.2: Structural parameters of $(\equiv SiO)_2(ZrCH_2C(CH_3)_3)_2$ from EXAFS fit

Shell	CN	R	σ^2
Zr-O	1	1.93	0.00500
Zr-O	1	1.94	0.000302
Zr-C	1	2.04	0.00454
Zr-Si	1	3.27	0.00213
Zr-Si	1	3.13	0.00498
Zr-O	1	3.63	0.00987
Zr-C	1	3.57	0.01
Zr-C	1	4.27	0.001
Zr-C	1	4.11	0.001

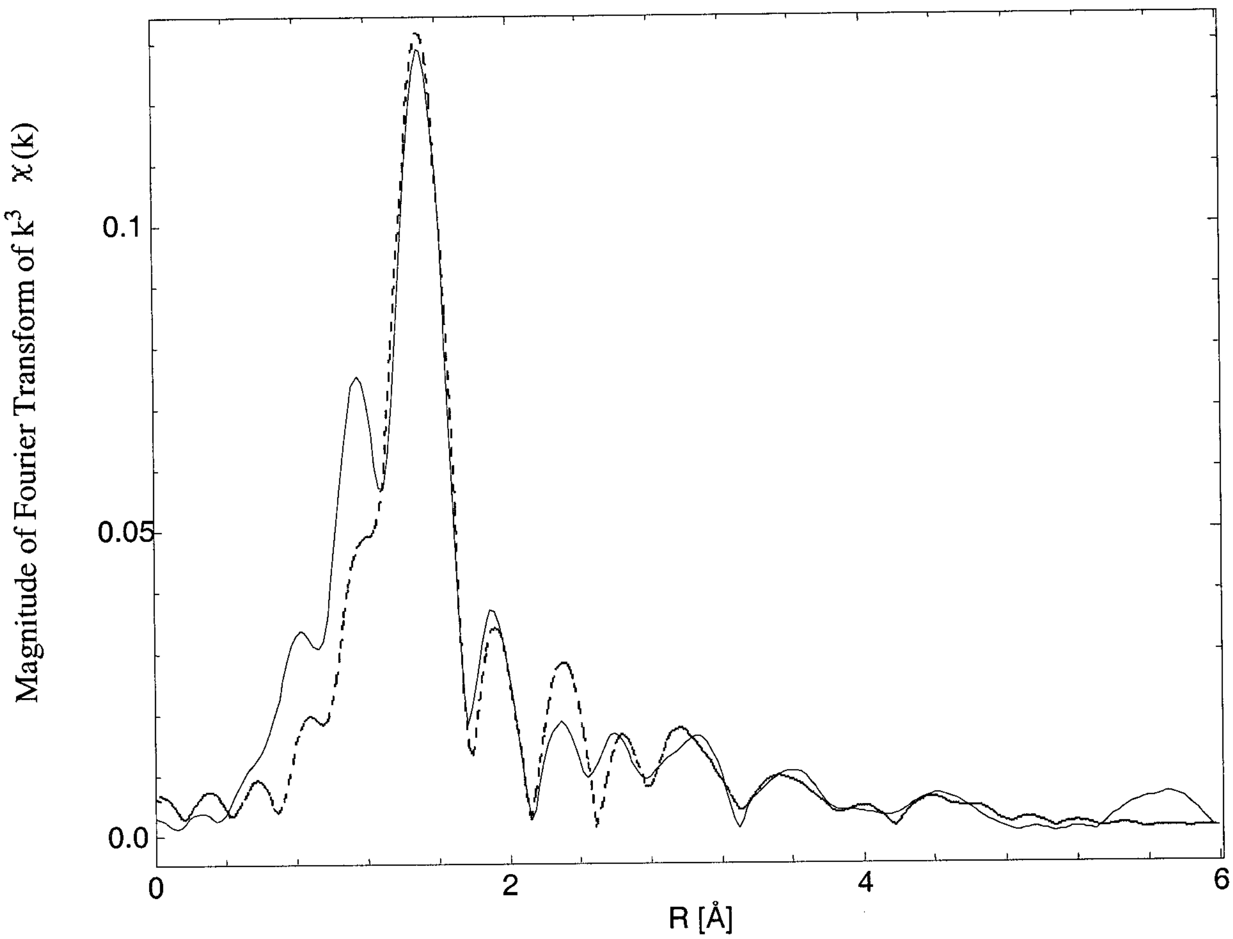

Figure 4.7: a) Fourier transformed EXAFS region of $(\equiv SiO)_2(\equiv Si_2O)Zr{=}CHC(CH_3)_3$ (solid line), simulated EXAFS spectrum of $(\equiv SiO)_2(\equiv Si_2O)Zr{=}CHC(CH_3)_3$ (dashed line).

Table 4.3: Structural parameters of $(\equiv SiO)_2(\equiv Si_2O)Zr{=}CHC(CH_3)_3$, with a coordinated siloxane oxygen, from EXAFS fit

Shell	CN	R	σ^2
Zr-O	1	1.93	0.00334
Zr-O	1	1.96	0.0001
Zr-O	1	2.14	0.00038
Zr-C	1	2.07	0.0011
Zr-Si	1	2.91	0.0053
Zr-Si	1	3.08	0.0002
Zr-C	1	3.24	0.0033
Zr-C	1	3.74	0.0097
Zr-C	1	3.86	0.0083
Zr-Si	1	3.50	0.01
Zr-C	1	4.80	0.01

The Zr-C bond distance was determined to be 2.07 Å (compared to 2.04 Å in the previous model). This model also agrees better with the XANES, since a coordinated siloxane makes the geometry at the zirconium centre pseudo-tetrahedral, similar to $(\equiv SiO)_2ZrNp_2$. This explains their similar pre-edge intensities.

4.5 Reaction with Olefins

When a sample of orange $(\equiv SiO)_2Zr{=}CHC(CH_3)_3$ was exposed to styrene vapor, there was an immediate change in color to white. GC analysis of the gas-phase revealed the presence of neohexene, as well as excess styrene and neopentane. No neohexene was detected when $(\equiv SiO)_2Zr{=}CHC(CH_3)_3$ was exposed to ethylene. Rather, polymerization was observed (to be discussed in Chapter 5).

4.6 Discussion

4.6.1 Stoichiometry of thermolysis

Comparison of the IR spectra of $(\equiv SiO)_2Zr(CH_2C(CH_3)_3)_2$ before and after its thermolysis showed a loss of half of the ν(C-H) intensity in the region 2800 to 3000 cm^{-1}. This is consistent with the loss of one of the two neopentyl ligands from the surface, equation 4.6.

$$(\equiv SiO)_2Zr(CH_2C(CH_3)_3)_2 \xrightarrow{\Delta} (\equiv SiO)_2Zr(C_5H_{10}) + C(CH_3)_4 \qquad (4.6)$$

The formation of one equivalent of neopentane was confirmed by its quantification in the gas phase; the amount of neopentane formed during thermolysis was precisely half of the amount formed during grafting. These results are very similar to the behavior observed during thermolysis of $(\equiv SiO)_2M(CH_2C(CH_3)_3)_2$ (M= Ti, Cr) and $(\equiv SiO)_2M(CH_2Si(CH_3)_3)_2$ (M= Cr, V).[11,15]

4.6.2 Kinetics of thermolysis

The kinetics of neopentane evolution from $(\equiv SiO)_2Zr(CH_2C(CH_3)_3)_2$ were found to be first order, as was the case for $Zr(CH_2C(CH_3)_3)_4$.[23] First-order kinetics were also observed in the thermolysis of $(\equiv SiO)_2Cr(CH_2C(CH_3)_3)_2$ to form the corresponding alkylidene and $[P_2Cp]ZrCl(CH_2Ph)_2$ to form $[P_2Cp]Zr{=}CHPh(Cl)$.[9,15]

From the Eyring plot, $\Delta H^{\ddagger}$ for neopentane extrusion from $(\equiv SiO)_2Zr(CH_2C(CH_3)_3)_2$ was found to be 24(5) kcal mol^{-1}. This value falls within the range reported for α-H abstraction, which is 20-30 kcal mol^{-1}.[9] Fryzuk reported $\Delta H^{\ddagger}$= 19(1) kcal mol^{-1} for $[P_2Cp]Zr(CH_2Ph)_2(Cl)$ while for $(TMS_2pda)W(NPhCH_2C(CH_3)_3)_2(PMe_3)$, $\Delta H^{\ddagger}$ was found to be 25.2(3) kcal mol^{-1}.[4]

$\Delta S^{\ddagger}$ was determined to be -19(7) cal mol^{-1} K^{-1}. This value is rather large compared to those found for other alkylidene systems (0 to -10 cal mol-1 K^{-1}).[9] However, there are other examples where large values of $\Delta S^{\ddagger}$ have been measured for the decomposition of a metal alkyl complex via an alkylidene intermediate. One such example is the α-H abstraction in $Ti(CH_2C(CH_3)_3)_4$ that is suggested to result in a transient neopentylidene intermediate.[18] $\Delta S^{\ddagger}$ for this reaction was measured to be -16 cal mol^{-1} K^{-1}. The formation of $[P_2Cp]Zr{=}CHPh(Cl)$ from $[P_2Cp]Zr(CH_2Ph)_2(Cl)$ had a similar value for $\Delta S^{\ddagger}$, -22 cal mol^{-1} K^{-1}.[9]

4.6.3 Characterization of neopentylidene complex

4.6.3.1 Reaction with styrene

The supported complex formed by the thermolysis of $(\equiv SiO)_2Zr(CH_2C(CH_3)_3)_2$ was confirmed to be the neopentylidene complex, $(\equiv SiO)_2Zr{=}CHC(CH_3)_3$ via its reaction with styrene. The formation of neohexene provides evidence for the presence of a Zr=C moiety, since this is the expected product of olefin metathesis, equation 4.7.

$$(\equiv SiO)_2Zr{=}CHC(CH_3)_3 + PhCH{=}CH_2 \rightarrow (\equiv SiO)_2Zr{=}CHPh + H_2C{=}CHC(CH_3)_3 \quad (4.7)$$

Isobutene, the expected deinsertion product of a zirconacyclobutane (equation 4.8) was not detected.

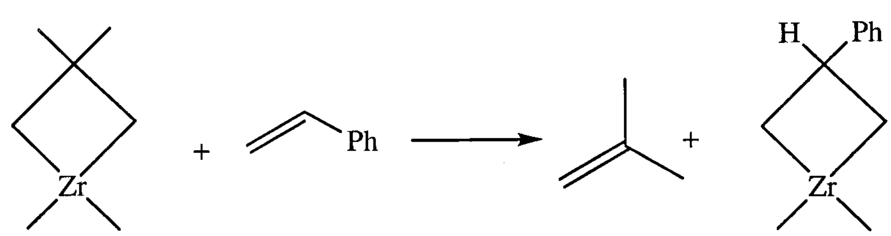

(4.8)

4.6.3.2 X-Ray absorption spectroscopy

The XANES region of the spectrum confirmed the presence of Zr(IV), based on comparison to the K-edge positions of other Zr(IV) complexes.[21,24] This is particularly important, since it rules out any possibility of reduction to Zr(III), which is known to happen at high temperatures.[25]

The Fourier transformed EXAFS region of the spectrum is consistent with the formulation $(\equiv SiO)_2(\equiv Si_2O)Zr{=}CHC(CH_3)_3$. The most salient bond length determined by the EXAFS is the Zr-C bond distance, at 2.07 Å. This value is slightly longer than Zr-C distances reported for molecular alkylidenes, including η^5-C_5H_5-1,3-$(SiMe_2CH_2PPr^i{}_2)_2]Zr{=}CHPh(Cl)$ (2.024 Å) and $[P_2Cp]_2Zr{=}CHSi(CH_3)_3$ (2.0159 Å)[9] but substantially shorter than typical Zr-C single bond lengths, at 2.20 Å.[26] Calculations predict a Zr-C bond distance of 1.983 Å in the neopentylidene formed by the thermolysis of tetra(neopentyl)zirconium.[18] Another important feature of the fit is that only one C atom is present in the first coordination sphere. Thus it is very unlikely that a zirconacyclobutane is present since a two-carbon shell would be expected with two Zr-C single bonds.

4.7 Conclusion

Thermolysis of $(\equiv SiO)_2Zr(CH_2C(CH_3)_3)_2$ at 120 °C resulted in the formation of $(\equiv SiO)_2Zr{=}CHC(CH_3)_3$ by α-H abstraction. The extrusion of one equivalent of neopentane gas was confirmed by in situ IR spectroscopy. The thermolysis exhibits first-order kinetic behavior, as expected of an intramolecular transformation. Rate constants were obtained by monitoring the formation of neopentane using IR spectroscopy at different temperatures, and these values were used to extract the activation parameters $\Delta H^{\ddagger}$ and $\Delta S^{\ddagger}$, 24(5) kcal mol^{-1} and -19(7) cal mol^{-1} K^{-1}, respectively. The presence of the alkylidene moiety was confirmed by its reaction with styrene which yielded the expected olefin metathesis product, neohexene. Further evidence was provided by EXAFS which is consistent with the formulation $(\equiv SiO)_2(\equiv Si_2O)Zr{=}CHC(CH_3)_3$, and from which a Zr-C bond distance of 2.07 Å was determined.

4.8 References

(1) Schrock, R. R. *Chem. Rev.* **2002**, *102*, 145.

(2) Schrock, R. R. *J. Am. Chem. Soc.* **1974**, *96*, 6796.

(3) Cundari, T. R.; Gordon, M. S. *J. Am. Chem. Soc.* **1991**, *113*, 5231.

(4) Vaughan, W. M.; Abboud, K. A.; Boncella, J. M. *J. Am. Chem. Soc.* **1995**, *117*, 11015.

(5) Feldman, J.; Schrock, R. R. *Prog. Inorg. Chem.* **1991**, *39*, 1.

(6) Fryzuk, M. D.; Mao, S. S. H. *J. Am. Chem. Soc.* **1993**, *115*, 5336-5337.

(7) Beckhaus, R. *Angew. Chem. Int. Ed. Engl.* **1997**, *36*, 686.

(8) Wengrovius, J. H.; Schrock, R. R. *J. Organomet. Chem.* **1980**, *205*, 319.

(9) Fryzuk, M. D.; Duval, P. B.; Mao, S. S. H.; Zaworotko, M. J.; MacGillivray, L. R. *J. Am. Chem. Soc.* **1999**, *121*, 2478-2487.

(10) Fryzuk, M. D.; Duval, P. B.; Mao, S. S. H.; Rettig, S. J.; Zaworotko, M. J.; MacGillivray, L. R. *J. Am. Chem. Soc.* **1999**, *121*, 1707.

(11) Beaudoin, M. C.; Womiloju, O.; Fu, A.; Amor Nait Ajjou, J.; Rice, G. L.; Scott, S. L. *J. Mol. Catal* **2002**, *190*, 159-169.

(12) Dufaud, V.; Niccolai, G. P.; Thivolle-Cazat, J.; Basset, J.-M. *J. Am. Chem. Soc.* **1995**, *117*, 4288.

(13) Lefort, L.; Chabanas, M.; Maury, O.; Meunier, D.; Coperet, C.; Thivolle-Cazat, J.; Basset, J.-M. *J. Organomet. chem.* **2000**, *593-594*, 96.

(14) Marks, T. J.; Ahn, H. *J. Am. Chem. Soc.* **2002**, *124*, 7103.

(15) Amor Nait Ajjou, J.; Rice, G. L.; Scott, S. L. *J. Am. Chem. Soc.* **1998**, *120*, 13436.

(16) Smith, D. C.; Rubiano, R. R.; Healy, M. D.; Springer, R. W. In *Proc.11th In. Conf. Chemical Vapor Deposition*; 5 ed.; Jensen, K. F., Cullin, G. W., Eds.: NJ, 1993, p 417.

(17) Parmeter, J. E.; Smith, D. C.; Healy, M. D. *J. Vac. Sci. Technol. A* **1994**, *12*, 2107.

(18) Cheon, J.; Dubois, L. H.; Girolami, G. S. *J. Am. Chem. Soc.* **1997**, *119*, 6814.

(19) Cheon, J.; Rogers, D. M.; Girolami, G. S. *J. Am. Chem. Soc.* **1997**, *119*, 6804.

(20) Wu, Y.-D.; Peng, Z.-H.; Chan, K. W. K.; Liu, X.; Tuinman, A. A.; Xue, Z. *Organometallics* **1999**, *18*, 2081.

(21) Greegor, R. B.; Blohowiak, K. Y.; Osborne, J. H.; Krienke, K. A.; Cherian, J. T. *J. Sol-Gel Sci. and Tech* **2001**, *20*, 35-50.

(22) Espelid, Ø.; Børve, K. J. *J. Catal.* **2000**, *195*, 125-139.

(23) Davidson, P. J.; Lappert, M. F.; Pearce, R. *J. Organomet. Chem.* **1973**, *57*, 269-277.

(24) Gavin, M.; Pickup, D.; Anderson, R.; Wallidge, G. W.; Holland, M. A.; Newport, R. J.; Smith, M. E. *Phys. Chem. Chem. Phys* **2000**, *2*, 2455-2460.

(25) Cotton, F. A.; Wilkinson, G. *Advanced Inorganic Chemistry*; 5 ed.; Wiley: New York, 1988.

(26) McAlexander, L. H.; Li, L.; Yang, Y.; Pollitte, J. L.; Xue, Z. *Inorg. Chem.* **1998**, *37*, 1423.

Chapter 5

Ethylene polymerization by silica-supported Zr(IV) neopentyl and neopentylidene complexes

5.1 Introduction

Polyethylene was discovered in the 1930s at ICI, but it was only in the 1950s, with the invention of new cpolymerization catalysts (Ziegler-Natta and Phillips processes) that extensive commercial exploitation of polyethylene was triggered.[1] Since then, its physical properties have been found to suit many applications in modern life. Different classes of polyethylene include high density, low density, linear low density, very low density and crosslinked. These are shown in Figure 5.1. High density polyethylene is semicrystalline with three phases: crystalline, interfacial and non-crystalline.

In 1973, various groups reported that tetra(neopentyl)zirconium catalyzes the polymerization of olefins and dienes.[2,3] However, the catalytic activity of oxide-supported neopentyl Zr(IV) in the polymerization of olefins has not been extensively studied. Most investigations have focused on its use as a precursor for the synthesis of supported hydrides or alkoxides.[4,5]

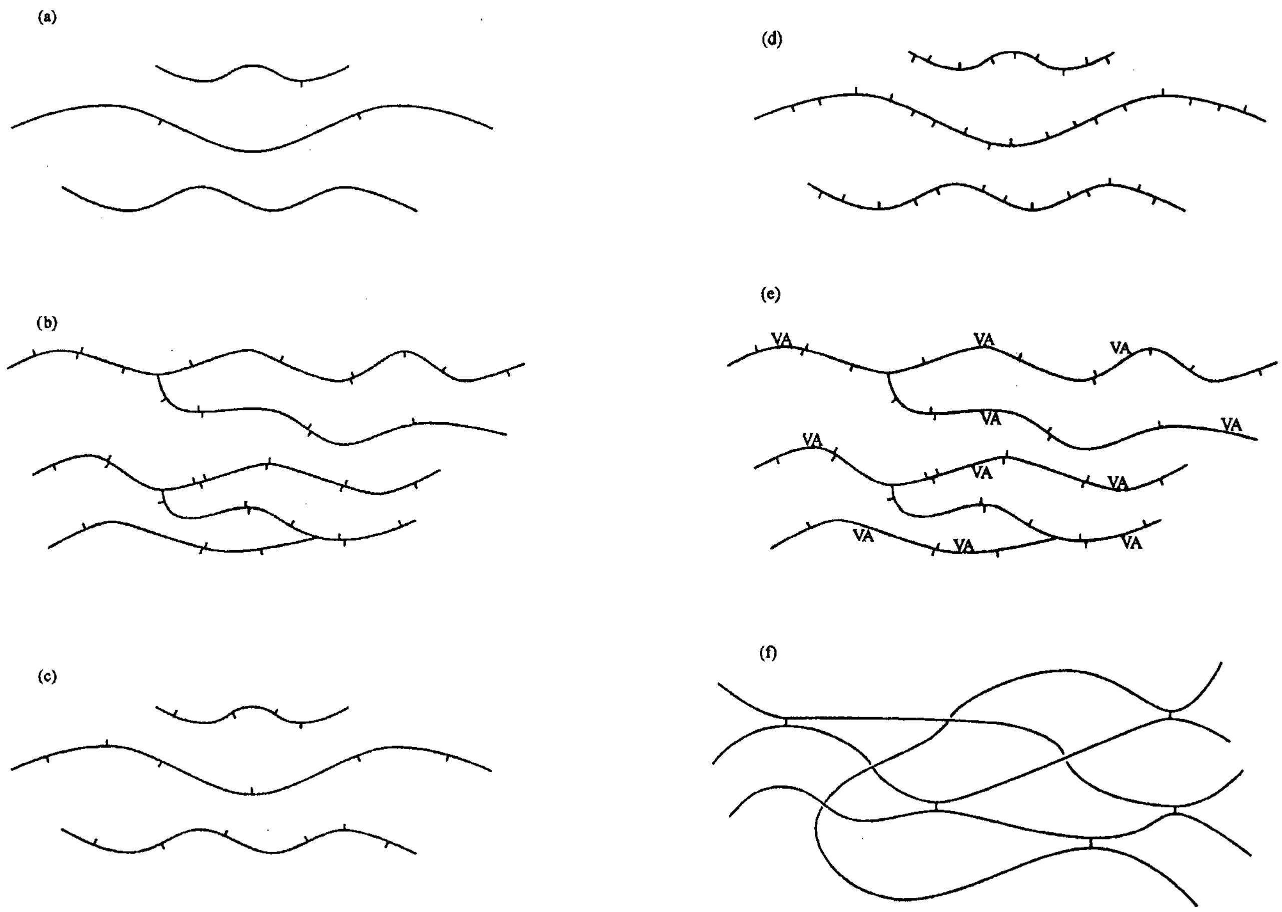

Figure 5.1: Schematic representations of the different classes of polyethylene (PE). (a) High density PE; (b) low density PE; (c) linear low density PE; (d) very low density PE; (e) ethylene-vinyl acetate copolymer; (f) cross-linked PE.

On silica pretreated at 500 °C, insertion of ethylene in the Zr-C bond was reported, equation 5.1.[6]

$$\equiv Si\text{-}O\text{-}ZrNp_3 + n\,C_2H_4 \rightarrow \equiv Si\text{-}O\text{-}ZrNp_x[(C_2H_4)_nNp]_{3-x} \tag{5.1}$$

No further details were provided. However, Marks *et al.* studied the polymerization of ethylene and propylene catalyzed by $Zr(CH_2C(CH_3)_3)_4$ supported on zirconia.[1] The polyethylene formed was of very high molecular weight and the polypropylene was found to be mostly atactic.

Terminal alkylidene complexes have mainly been studied as catalysts for olefin metathesis and ring-opening metathesis reaction.[7] A few studies have focused on these complexes as olefin polymerization catalysts. A homogeneous catalyst, $Ta{=}CHCMe_3(H)PMe_3)_3I_2$, was found to effect ethylene polymerization via a mechanism of alternating alkylidene and metallacyclobutane intermediates.[8] Amor Nait Ajjou *et al.* reported the catalytic activities of two silica-supported Cr(IV) alkylidenes, $(\equiv SiO)_2Cr{=}CHC(CH_3)_3$ and $(\equiv SiO)_2Cr{=}CHSi(CH_3)_3$.[9] Both complexes were found to catalyze the polymerization of ethylene at room temperature, resulting in the formation of polyethylene as well as volatile olefins. $(\equiv SiO)_2Cr{=}CHC(CH_3)_3$ also catalyzed the polymerization of propylene and 1-hexene to formed polypropylene and poly-1-hexene, respectively. However, a Cossee mechanism of migratory insertion was proposed, and it was suggested that the alkylidene ligand evolved to an alkyl during the initiation stage of the reaction.

In this chapter, we report the polymerization of ethylene catalysed by silica-supported neopentyl and neopentylidene complexes of Zr(IV).

5.2 Ethylene Polymerization by Silica-supported Bis(neopentyl)zirconium(IV)

When C_2H_4 (80 Torr) was added to silica (50 mg) modified with tetraneopentylzirconium, a slow uptake of ethylene was observed as the silica was stirred. A thin white film was seen to be formed on the powder. The temperature was maintained at 23.0°C by immersing the glass sidearm containing $(\equiv SiO)_2Zr(CH_2C(CH_3)_3)_2$ in a beaker of water at room temperature. The course of the reaction was followed by monitoring the disappearance of ethylene from the gas phase, by integrating the IR intensity in the ν(CH) region of the ethylene spectrum. The kinetic curve is shown in Figure 5.2a. The data was fitted to the first-order rate equation, with k_{obs} = (0.0053 ±0.0001) min^{-1}. We note that only a small fraction (ca. 20%) of the ethylene present was consumed before the reaction terminated.

At the end of the reaction, GC/MS analysis of the gas phase revealed the presence of unreacted C_2H_4 and a mixture of butene isomers. The amount of solid in the reactor increased by ca. 16 mg.

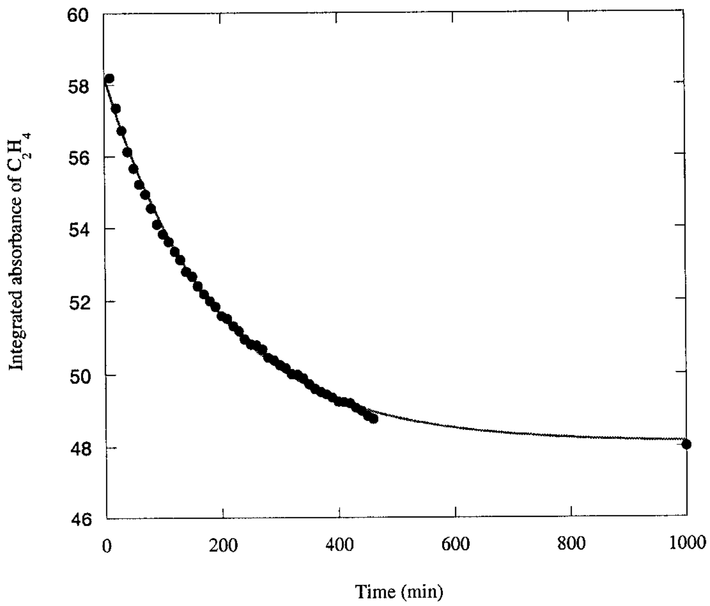

a

$A = A_\infty + (A_0-A_\infty)\exp(-k_{app}t)$		
	Value	Error
A_∞	48.10	0.09
A_0	58.19	0.08
k_{app}	0.0053	0.00013
R	0.999	NA

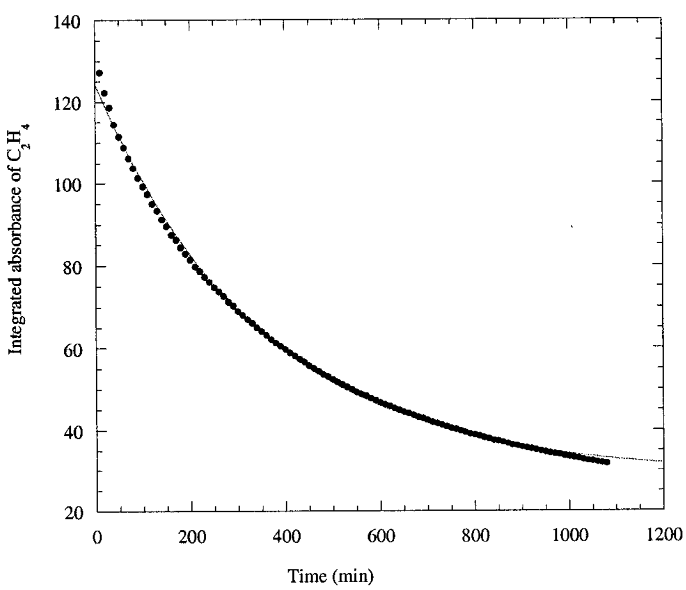

b

$A = A_\infty + (A_0-A_\infty)\exp(-k_{app}t)$		
	Value	Error
A_∞	28.78	0.35
A_0	124.23	0.42
k_{app}	0.0028	.00004
R	0.999	NA

Figure 5.2: Time-resolved consumption of (a) 80 Torr C_2H_4; and (b) 150 Torr C_2H_4 during polymerization over $(\equiv SiO)_2Zr(CH_2C(CH_3)_3)_2$ at (23.0 ± 0.2) °C.

The polymerization reaction was repeated with 150 Torr of C_2H_4 and a fresh sample (50 mg) of $(\equiv SiO)_2Zr(CH_2C(CH_3)_3)_2$. The kinetics were again pseudo-first-order, Figure 5.2b, but slower, with k = (0.00285 ± 0.00004) min^{-1}. However, a much greater fraction of the ethylene was consumed (ca. 80%). At the end of the experiment, a significant increase in mass of the powder, to about 150 mg, was noted. Furthermore, isomers of butene, hexene and octene as well as excess C_2H_4 were detected in the gas phase, Figure 5.3.

5.3 Ethylene Polymerization by Silica-supported Neopentylidenezirconium(IV)

When a 35 mg pellet of $(\equiv SiO)_2Zr{=}CHC(CH_3)_3$ was exposed to C_2H_4 (50 Torr), there was no immediate change in the orange color of the pellet. However, after 12 hours, there was a visually detectable white coating on its surface. Its IR spectrum, Figure 5.4, is consistent with the presence of polyethylene. The plastic-like material was easily pulled off the silica pellet and was found to weigh 9.4 mg. It was insoluble in chloroform, as expected.

The polymerization reaction was repeated with a 50 mg powdered sample of the catalyst and 100 Torr C_2H_4 at 23.0 °C. Figure 5.5 shows the first-order fit to the data, with k =(0.00606 ± 0.00005) min^{-1} . There was an obvious change of color from orange to white, and an increase in mass from 50 to 80 mg. GC/MS analysis of the gas phase showed the presence of butenes, pentenes, hexenes and heptenes, in addition to unreacted C_2H_4, Figure 5.6.

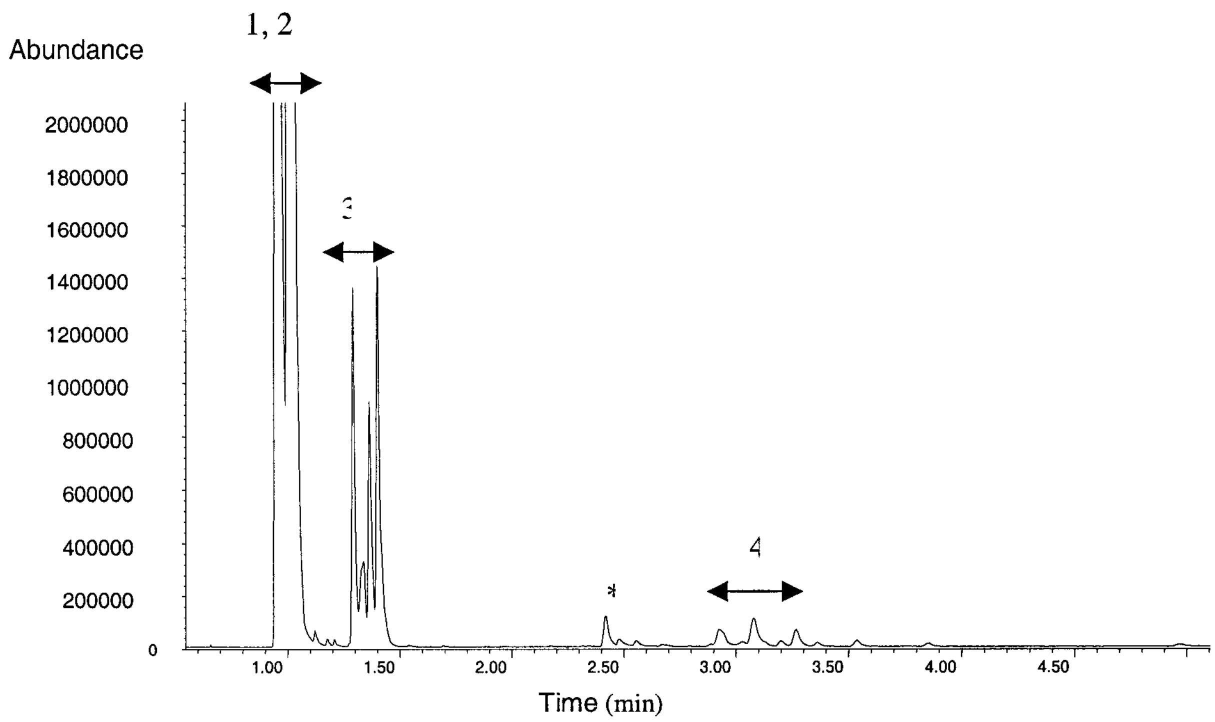

Figure 5.3: GC/MS of volatiles remaining after polymerization of C_2H_4 by $(\equiv SiO)_2Zr(CH_2C(CH_3)_3)_2$. (1) C_2H_4; (2) butenes; (3) hexenes; (4) octenes (*: contaminants).

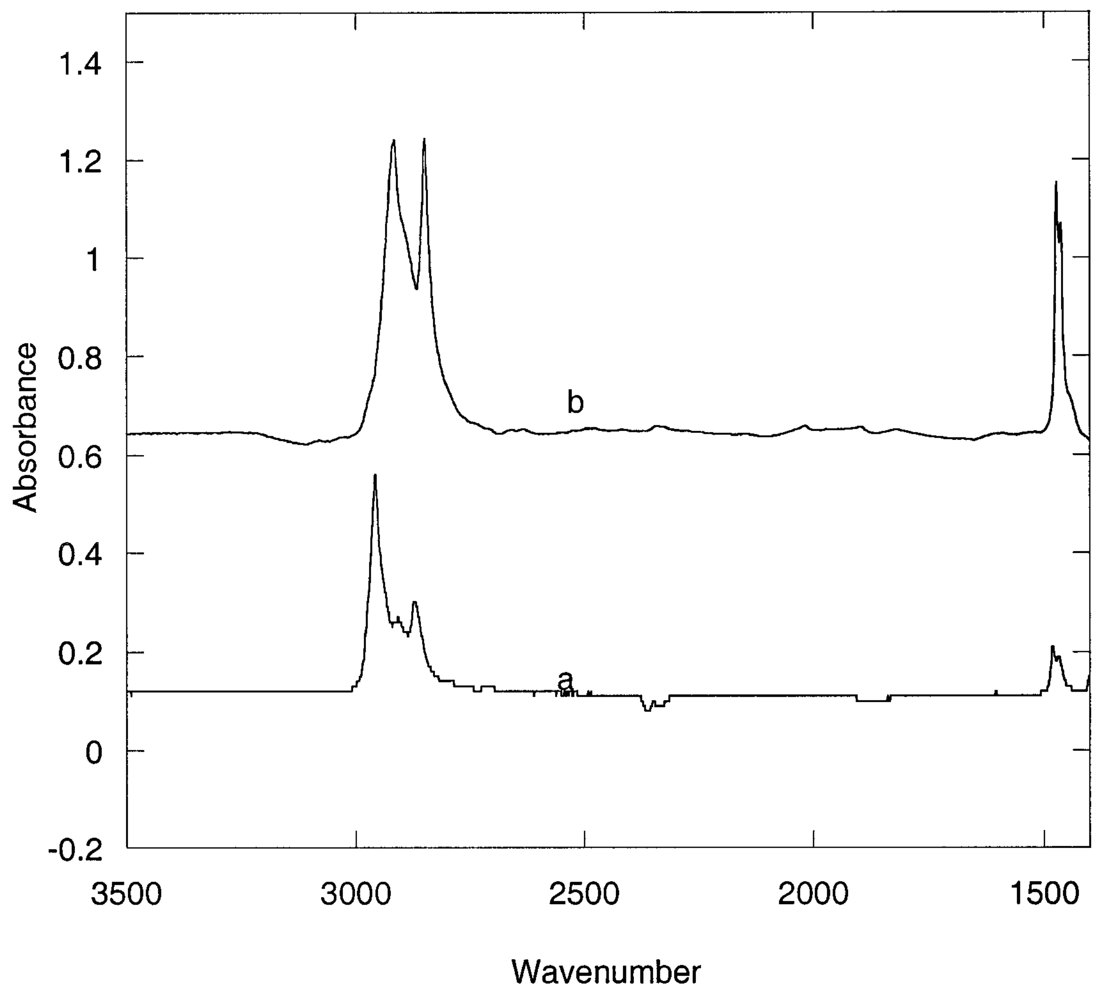

Figure 5.4: In situ IR spectra of (a) $(\equiv SiO)_2Zr{=}CHC(CH_3)_3$; (b) after reaction with 50 Torr of ethylene, followed by evacuation of volatiles.

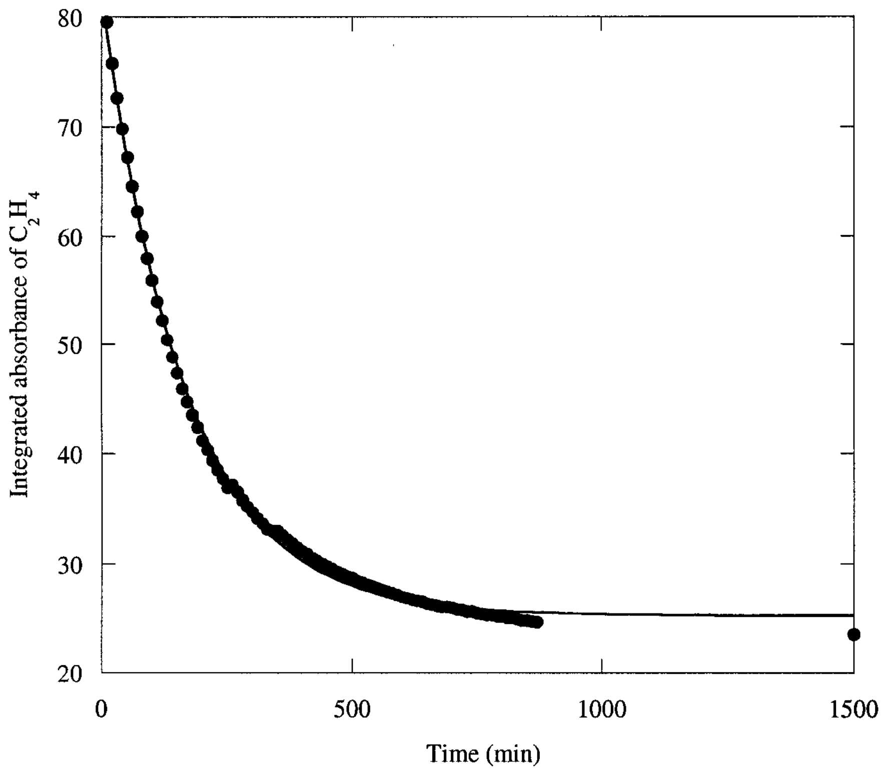

$A = A_\infty + (A_0 - A_\infty)\exp(-k_{app}t)$		
	Value	Error
A_∞	25.26	0.12
A_0	81.73	034
k_{app}	0.0061	0.00007
R	0.999	NA

Figure 5.5: Time resolved consumption of 100 Torr of C_2H_4 during polymerization over $(\equiv SiO)_2Zr{=}CHC(CH_3)_3)_2$ at (23.0 ± 0.2) °C.

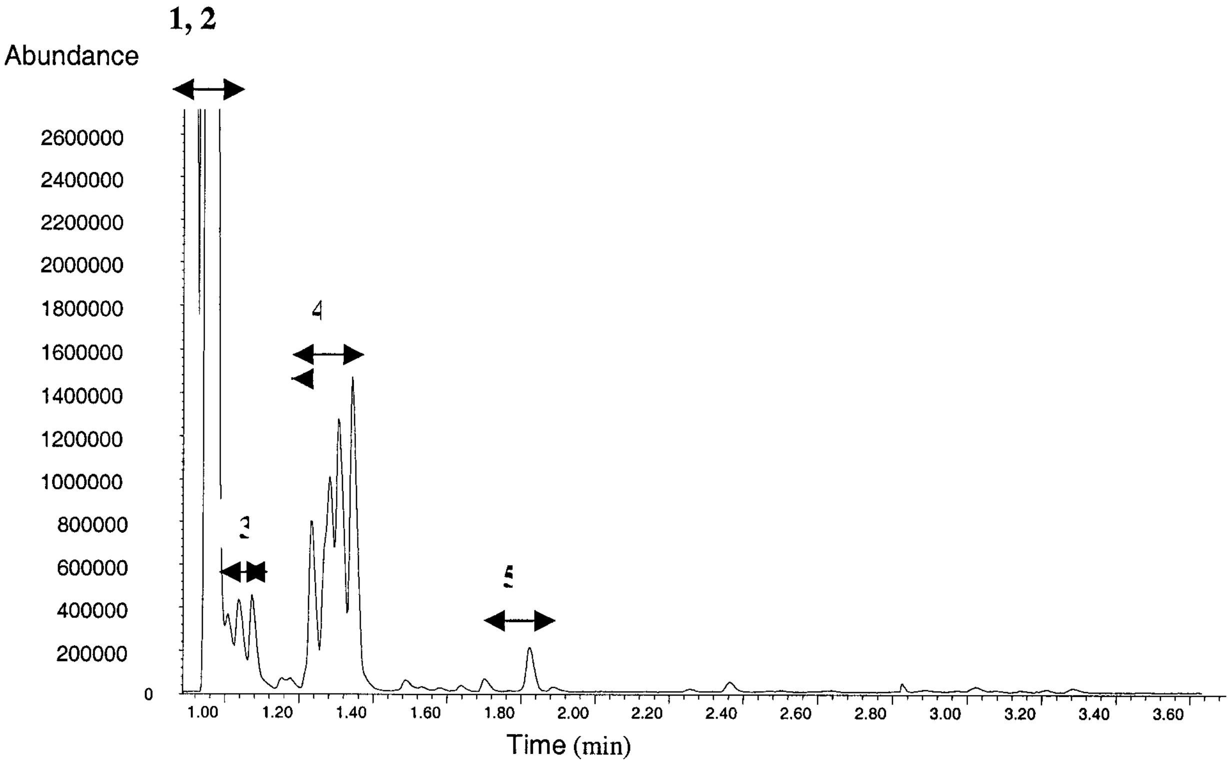

Figure 5.6: GC/MS analysis of volatile products of the reaction between $(\equiv SiO)_2Zr{=}CHC(CH_3)_3)_2$ and C_2H_4. (1) ethylene; (2) butenes; (3) pentenes; (4) hexenes; (5) heptenes.

5.4 Discussion

Ballard speculated that an olefin complex forms during the polymerization of ethylene catalyzed by Zr(IV) alkyls and their supported analogues, equation 5.2. However, the concentration of such complexes is very small.[2]

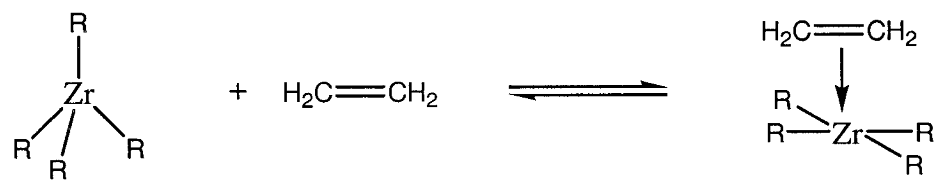

(5.2)

Insertion of ethylene in the Zr-C bond is then postulated, equation 5.3.[10]

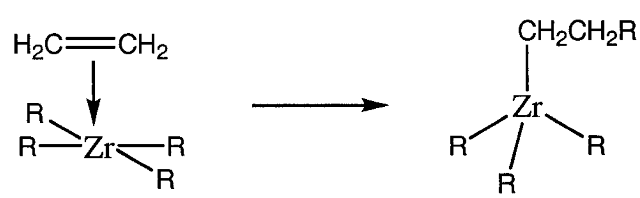

(5.3)

Other studies have argued against the formation of ethylene-metal complexes, and instead have proposed the direct insertion of the olefin into the Zr-C bond as the first step.[11]

In this chapter, it has been demonstrated that indeed, $(\equiv SiO)_2Zr(CH_2C(CH_3)_3)_2$ catalyses the oligomerization and polymerization of ethylene, since both polyethylene and isomers of even-numbered olefins were detected. It is important to point out here that when 80 Torr of C_2H_4 was used, only butenes and hexenes were detected, whereas 150 Torr of C_2H_4 also gave octenes. The presence of these olefins implies termination after insertion of two or three ethylene molecules. The presence of many isomers of each C_{2n} oligomer suggests that the catalyst also causes olefin isomerization. This is consistent with other reports of silica-supported Zr as an isomerization catalyst.[1] The kinetics of the reaction are first order, indicating the absence of slow initiation.[12]

Fryzuk and co-workers studied the reaction between the molecular alkylidene [η^5-C_3H_5-1,3-($SiMe_2CH_2P^iPr_2)_2$]Zr=CHR(Cl) (R= Ph, $SiMe_3$) and C_2H_4.[13] Scheme 5.1 shows the mechanism proposed for the reaction. In the first step of the reaction, ethylene binds to the Zr centre after the dissociation of one of the labile sidearm phosphines. Formation of a zirconacyclobutane complex occurs by [2+2] cycloaddition between the Zr=C of the alkylidene and the ethylene molecule, followed by β-H elimination to form the Zr(IV) hydride complex. An intermediate four-membered metallacycle has been trapped in other such experiments.[14] Upon addition of another ethylene molecule, reductive elimination of CH_2=$CHCH_2R$ results in the formation of a zirconacyclopropane complex.

Studies on the catalytic activity of (≡SiO)$_2$Cr=CHC(CH_3)$_3$ showed that the latter very effectively catalyzed the formation of polyethylene as well as the formation of oligomers such butenes, hexenes.[9,15] Some oligomers contained the neopentylidene moiety so it was concluded that the alkylidene ligand is eliminated during initiation from the supported catalyst. Although no neohexene was detected, the presence of 2,3,3-trimethylbutene prompted the authors to propose that de-insertion of neohexene was followed by rapid rotation of the coordinated olefin and subsequent re-addition to (≡SiO)$_2$Cr=CH_2 to form the chromacyclobutane with the *tert*-butyl substituent in the β-position, Scheme 5.2.

Scheme 5.1: Proposed mechanism for the reaction of [η^5-C_3H_5-1,3-($SiMe_2CH_2P^iPr_2)_2$]Zr=CHR(Cl) with C_2H_4

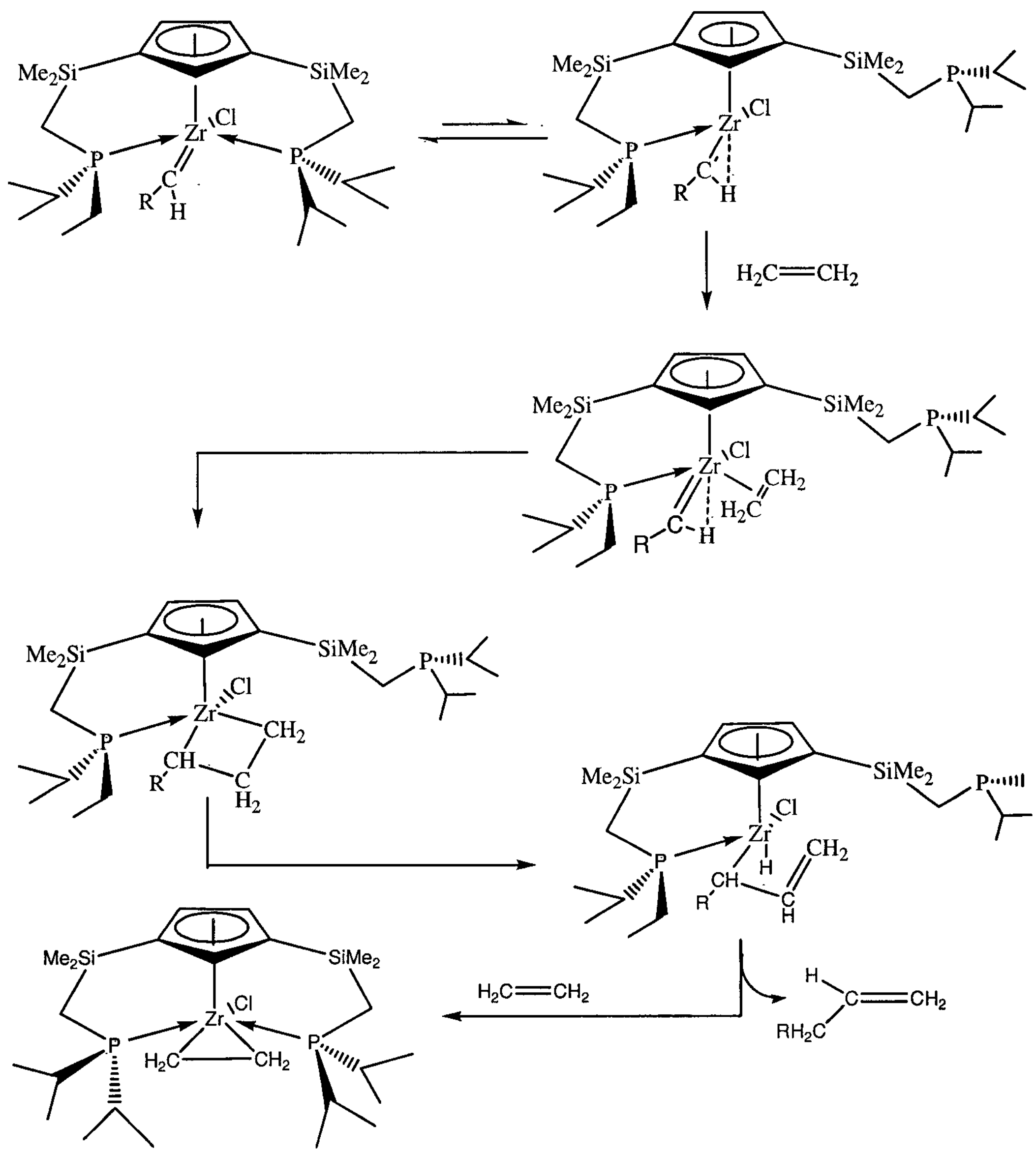

Scheme 5.2: Proposed mechanism for the reaction $(\equiv SiO)_2Cr=CHC(CH_3)_3$ with C_2H_4

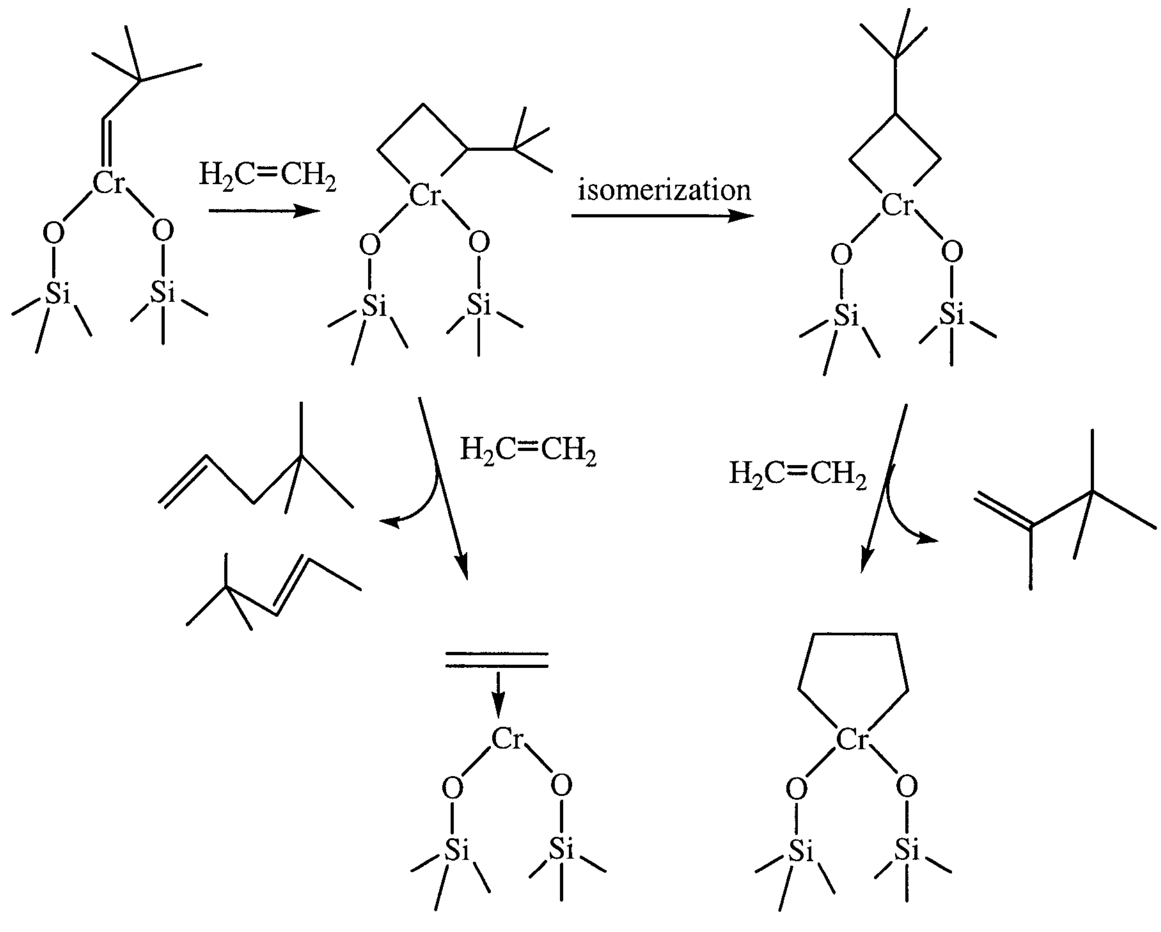

In the case of reaction of $(\equiv SiO)_2Zr=CHC(CH_3)_3$ with ethylene, the consumption of ethylene was found to be first order and both polyethylene and ethylene oligomers (butenes and hexenes) were formed. However, no neohexene was detected, indicating that olefin metathesis does not take place when the neopentylidene is exposed to C_2H_4.

Interestingly, olefins with odd numbers of carbon were also detected. The formation of these odd oligomers could be rationalized by the mechanism shown in Scheme 5.3, which is analogous to Fryzuk's and Amor Nait Ajjou's mechanisms (Scheme 5.2 and 5.3).[13,16]

Scheme 5.3: Proposed mechanism for the formation of odd oligomers in the reaction of $(\equiv SiO)_2Zr{=}CHC(CH_3)_3$ with C_2H_4

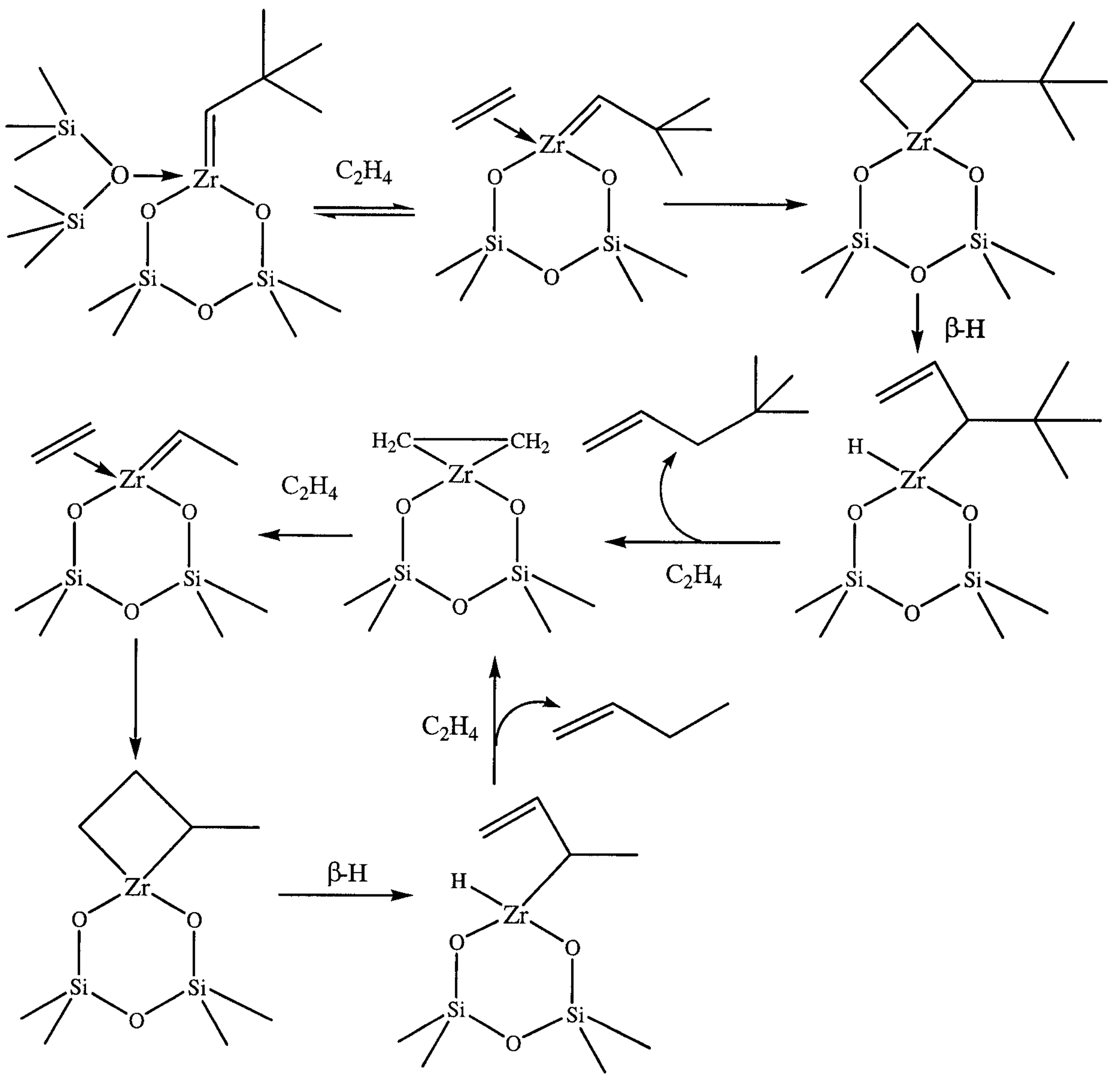

5.5 Conclusion

Both $(\equiv SiO)_2Zr(CH_2C(CH_3)_3)_2$ and $(\equiv SiO)_2Zr{=}CHC(CH_3)_3$ catalyze the polymerization of ethylene at room temperature, and the reactions are pseudo-first order. Oligomerization of ethylene to form isomers of butenes, hexenes and octenes also occurred in both cases. Moreover, with $(\equiv SiO)_2Zr{=}CHC(CH_3)_3$, olefins with odd numbers of carbon atoms, namely pentenes and hexenes were formed. However, more experiments are needed to quantify activity and mechanism of ethylene polymerization catalyzed by $(\equiv SiO)_2Zr(CH_2C(CH_3)_3)_2$ and $(\equiv SiO)_2Zr{=}CHC(CH_3)_3$.

5.6 References

(1) Marks, T. J.; Ahn, H. *J. Am. Chem. Soc.* **2002**, *124*, 7103.

(2) Ballard, D. G. H. *Adv. Catal.* **1973**, *23*, 263-325.

(3) Davidson, P. J.; Lappert, M. F.; Pearce, R. *J. Organomet. Chem.* **1973**, *57*, 269-277.

(4) King, S. A.; Schwatz, J. *Inorg. Chem.* **1991**, *30*, 3771-3774.

(5) Quignard, F.; Graziani, O.; A., C. *Appl. Cat.* **1999**, *182*, 29-40.

(6) Quignard, F.; Lecuyer, C.; Choplin, A.; Olivier, D.; Basset, J.-M. *J. Mol. Catal.* **1992**, *74*, 353-363.

(7) Feldman, J.; Schrock, R. R. *Prog. Inorg. Chem.* **1991**, *39*, 1-69.

(8) Turner, H. W.; Schrock, R. R.; Fellman, J. D.; Holmes, S. J. *J. Am. Chem. Soc.* **1983**, *105*, 4942.

(9) Amor Nait Ajjou, J.; Scott, S. L. *J. Am. Chem. Soc.* **2000**, *122*, 8968-8976.

(10) Zakharov, V. A.; Yermakov, Y. I. *Catal. Rev.-Sci. Eng* **1979**, *19*, 67-103.

(11) Ballard, D. G. H.; Burnham, D. R.; Twose, D. L. *J. Catal.* **1976**, *44*, 116.

(12) Yermakov, Y.; Zakharov, V. *Adv. Catal.* **1975**, *24*, 173-243.

(13) Fryzuk, M. D.; Duval, P. B.; Mao, S. S. H.; Rettig, S. J.; Zaworotko, M. J.; MacGillivray, L. R. *J. Am. Chem. Soc.* **1999**, *121*, 1707.

(14) Wallace, K. C.; Dewan, J. C.; Schrock, R. R. *Organometallics* **1986**, *5*, 2162.

(15) Beaudoin, M. C.; Womiloju, O.; Fu, A.; Amor Nait Ajjou, J.; Rice, G. L.; Scott, S. L. *J. Mol. Catal.* **2002**, *190*, 159-169.

(16) Amor Nait Ajjou, J.; Scott, S. L. *J. Am. Chem. Soc.* **2000**, *122*, 8968-8976.

Chapter 6

General Conclusions

A. Grafting reaction: The grafting of $Zr(CH_2C(CH_3)_3)_4$, both from solution and by sublimation, on Aerosil 200 treated thermally at 200 °C results in the formation of $(\equiv SiO)_2Zr(CH_2C(CH_3)_3)_2$, accompanied by the evolution of two equiv. neopentane. The nature of the surface organometallic fragment was investigated by IR, ^{13}C CP/MAS NMR and, most definitively, by XAS. The K-edge shift in the XANES spectrum establishes the oxidation state of Zr as IV, while the EXAFS confirms the presence of two Zr-C single bonds of length 2.24 Å and two Zr-O single bonds of length 1.94 Å. A second coordination sphere analysis is consistent with two C neighbors at 2.24 Å and two Si neighbors at 3.12 Å.

B. Thermolysis of $(\equiv SiO)_2Zr(CH_2C(CH_3)_3)_2$: When $(\equiv SiO)_2Zr(CH_2C(CH_3)_3)_2$ is heated in vacuum at 125 °C, the material extrudes one equiv. neopentane, while the IR spectrum of the silica shows a loss of (50.9 ± 1.1)% of its integrated ν(C-H) intensity. The reaction is first order, with $k = (0.00191 \pm 0.00004)\ min^{-1}$. Analysis of the temperature variation of the rate constant resulted in values for $\Delta H^\ddagger$ and $\Delta S^\ddagger$ of 24(5) kcal mol^{-1} and -19(7) cal mol^{-1} K^{-1}, respectively. Both are within the range of previously reported values for α-H abstraction. Further evidence for the formation of $(\equiv SiO)_2Zr{=}CHC(CH_3)_3$ was provided by its metathesis with styrene to yield neohexene. The K-edge energy confirms retention of Zr in oxidation state IV, while the EXAFS is consistent with the formulation $(\equiv SiO)_2(\equiv Si_2O)Zr{=}CHC(CH_3)_3$ in which the Zr=C distance of 2.07 Å is 0.17 Å shorter than in the bis(neopentyl) complex and demonstrates double bond character. Curve fitting suggests coordination of an additional siloxane oxygen to the zirconium centre.

C. Polymerization of ethylene: Both $(\equiv SiO)_2Zr(CH_2C(CH_3)_3)_2$ and $(\equiv SiO)_2Zr{=}CHC(CH_3)_3$ catalyze the polymerization of ethylene at room temperature in the absence of cocatalyst. The reactions are pseudo-first-order. In addition to excess ethylene, $(\equiv SiO)_2Zr(CH_2C(CH_3)_3)_2$ generated isomers of butenes, hexenes and octenes while $(\equiv SiO)_2Zr{=}CHC(CH_3)_3$ gave, in addition, pentenes and heptenes suggesting a role for the neopentylidene ligand in initiation.